

# The Role of Chemical Mechanisms in Neural Computation and Learning

by

Martha Jean Hiller

S.B., Massachusetts Institute of Technology (1987)

S.M., Massachusetts Institute of Technology (1987)

Submitted to the Department of Electrical Engineering and  
Computer Science

in partial fulfillment of the requirements for the degree of

Doctor of Philosophy

at the

MASSACHUSETTS INSTITUTE OF TECHNOLOGY

May 1993

© Massachusetts Institute of Technology 1993

Signature of Author .....  
Department of Electrical Engineering and Computer Science  
May 13, 1993

Certified by .....  
Rodney A. Brooks  
Associate Professor, EECS  
Thesis Supervisor

Accepted by .....  
Campbell L. Searle  
Chairman, Departmental Committee on Graduate Students

# **The Role of Chemical Mechanisms in Neural Computation and Learning**

by  
Martha Jean Hiller

Submitted to the Department of Electrical Engineering and Computer Science  
on May 13, 1993, in partial fulfillment of the  
requirements for the degree of  
Doctor of Philosophy

## **Abstract**

Most computational models of neurons assume that their electrical characteristics are of paramount importance. Because the speed of electrical transmission and the binary nature of action potentials is so similar to modern computer technology, other aspects of the neural substrate have been regarded as irrelevant. However, electrical properties of neurons are modulated in important ways by chemical mechanisms. In addition to mediating all long-term changes, chemical mechanisms can have short-term effects that change the cell's response properties. They also play important roles in the creation of the brain's anatomical structure during development.

The topic of this dissertation is the interaction between electrical and chemical mechanisms in neural learning and development. Plasticity is prevalent at all levels in the brain, and it plays a central role in the establishment of the brain's structure and function. My central thesis is that chemical mechanisms must be taken into account if we are to build accurate models of neural computation.

To demonstrate their role, two neural systems are modelled in some detail. The first is the gill withdrawal reflex circuit in *Aplysia*, a marine snail. The mechanisms underlying habituation, sensitization, and associative learning in this circuit have been extensively studied. These mechanisms display an intricate interaction between electrical conductances and chemical processes inside the synaptic terminals.

The second system modelled is the early visual pathway. The initial connections formed between structures in this pathway are highly disordered. A detailed map topography is produced using a combination of chemical and electrical mechanisms to sort the axonal projections. A simplified model of individual neurons is used in this simulation so that network interactions can be studied. However, some care is taken to remain compatible with experimental results.

Thesis Supervisor: Rodney A. Brooks  
Title: Associate Professor, EECS

## Acknowledgments

This work, like all theses, would probably never have been completed without the support and encouragement of many friends and advisors (not to mention the motivation of a very hard deadline).

Rod Brooks has been a wonderful advisor. He has been consistently available to talk to, even while “away” on sabbatical, and has continued to support me and take an interest in my work even after I drifted away from robotics, and despite my insecurity and ambivalence about the whole business of doing research. I almost feel guilty for wishing he knew more neuroscience.

I’m also grateful to Ken Miller for taking the time to make many detailed comments on my thesis draft. His interest in my work and technical support have been invaluable.

Marvin Minsky is an eternal source of mystery; I never know what he’s going to do next. His offer to sit on my committee came as a complete surprise, and our conversation about quartz crystals before my defense was a great way to defuse my nerves. Patrick Winston has been a source of much information on how to present myself to the outside world (now if only I could convince myself to make use of it.)

Other people at school have also been very important. Without Tom Knight’s encouragement, I might never have entered graduate school, and he has continued to be available for occasional pep talks. And And Marilyn Pierce is one of the most amazing unofficial department heads ever. Without her help, dealing with the administration would have been a much more forbidding obstacle.

I’m not sure I would have survived without the loving attention of my friends, who have provided hours of assistance keeping my life together, and been very tolerant of my eternal requests for backrubs. It’s been wonderful having Barb Moore and Karen Sarachek to share the ups and downs of being a graduate student with. Barb in particular has been provided a lot of support over the past two months.

Don Ross deserves my love and gratitude for giving me something pleasant to daydream about while I work, for hugs and backrubs, and for many hours of help keeping my life together and my room clean, and scanning in all those figures for me.

Jay Sekora has helped keep me fed, done my laundry, and provided me with many hugs and backrubs. Laura Bagnall has also done laundry duty, and provided me with recycled archival bond. David Wald has provided invaluable technical support in the form of latex hacking, along with an occasional backrub. And Jennifer Lee has been a source of spiritual support and grounding, and I am eternally grateful to her for teaching me the Brigid poems.

Then there’s David Chapman... I’ve had a love-hate relationship with David for years, but he has consistently expressed a high opinion of my ability, which has been an important source of confidence. And I owe him a long-overdue thank you for his support and thorough comments on paper drafts and on my (\*ahem\*) master’s thesis.

And, of course, there’s me. I’ve done an incredible amount of work to get this

finished, and have continued to love and take care of myself throughout. I am continually amazed by my ability to learn and grow, and by the strength of my motivation to do the best I can for myself.

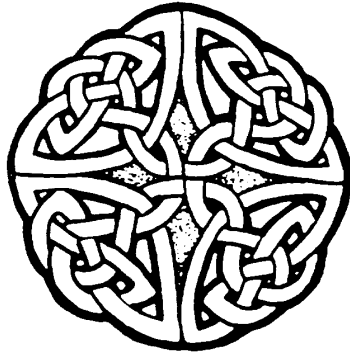
### *The Genealogy of Brigid*

Brigid of the mantles,  
Brigid of the peat heap,  
Brigid of the twining hair,  
Brigid of the augury,  
Brigid of the white feet,  
Brigid of calmness,  
Brigid of the kine,  
Brigid, daughter of the Dagdah:  
I am under the shielding  
of Good Brigid each day,  
I am under the shielding  
of Good Brigid each night.  
Brigid is my companion,  
Brigid is my maker of song,  
Brigid is my helping Goddess,  
my sustenance,  
my guide.

Every day and every night  
that I recite the genealogy of Brigid,  
I shall not be killed,  
I shall not be harried,  
I shall not be put into a cell,  
I shall not be wounded,  
I shall not be anguished,  
I shall not be ravaged,  
I shall not be blinded,  
I shall not be left bare  
or forgotten.  
No fire shall burn me,  
Nor sun shall burn me,  
Nor moon shall blanch me,  
Nor lake shall drown me,  
Nor flood shall drown me,  
Nor briny sea shall drown me,  
Nor dart of faerie sting me,  
Nor seed of faerie lift me,  
Nor earthly being destroy me.

For I am the child of Poetry,  
Poetry, child of Reflection,  
Reflection, child of Meditation,  
Meditation, child of Lore,

Lore, child of Research,  
Research, child of Great Knowledge,  
Great Knowledge, child of Intelligence,  
Intelligence, child of Comprehension,  
Comprehension, child of Wisdom,  
Wisdom, child of Brigid.



# Contents

<b>1</b>	<b>Introduction</b>	<b>15</b>
1.1	Goals . . . . .	15
1.2	Chapter Organization . . . . .	16
<b>2</b>	<b>Modelling in Neuroscience</b>	<b>17</b>
2.1	The Value of Models . . . . .	18
2.2	Is it Real or is it Artifact? . . . . .	18
2.3	Selecting a System for Modelling . . . . .	20
<b>I</b>	<b>Classical Conditioning in Aplysia</b>	<b>21</b>
<b>3</b>	<b>Synaptic Plasticity in Aplysia</b>	<b>23</b>
3.1	The Nature of the Beast . . . . .	23
3.1.1	What Does <i>Aplysia</i> Learn? . . . . .	25
3.1.2	Why Does <i>Aplysia</i> Learn? . . . . .	26
3.1.3	How Does <i>Aplysia</i> Learn? . . . . .	28
3.2	A Simulation of the <i>Aplysia</i> Circuit . . . . .	34
3.2.1	Simulation Equations . . . . .	35
3.2.2	Results and Discussion . . . . .	39
3.2.3	Derivation of Chemical Interactions . . . . .	47
3.3	Summary . . . . .	56
<b>II</b>	<b>Topographic Map Formation in the Visual System</b>	<b>59</b>
<b>4</b>	<b>A Model of Topographic Map Formation</b>	<b>61</b>
4.1	Introduction . . . . .	62
4.2	Previous Models of Map Formation . . . . .	63
4.3	The Model . . . . .	63
4.3.1	The Simulation . . . . .	64
4.4	Results . . . . .	68
4.5	The Role of Target Activity . . . . .	71

4.5.1	Noise Reduction . . . . .	71
4.5.2	Convergence Properties . . . . .	73
4.6	Extensions to the Model . . . . .	74
4.6.1	Biological Mechanisms for Competition . . . . .	74
4.6.2	Map Expansion and Compression . . . . .	75
4.7	Discussion and Summary . . . . .	78
<b>5</b>	<b>Mathematical Analysis of Map Formation</b>	<b>81</b>
5.1	Description of Simulation . . . . .	81
5.1.1	Parameter Constraints . . . . .	84
5.2	Derivation of Activity-Dependent Decay . . . . .	86
5.3	Equilibrium Solutions and Stability . . . . .	92
5.3.1	Equilibrium Solution . . . . .	92
5.3.2	Stability of Equilibrium Solutions . . . . .	93
5.3.3	Equilibrium Solution with Uniform Input Activity . . . . .	93
5.3.4	Equilibrium Solution with No Lateral Connections . . . . .	96
<b>6</b>	<b>Summary and Conclusions</b>	<b>101</b>
<b>A</b>	<b>Modelling of Neurons</b>	<b>103</b>
A.1	Theme . . . . .	103
A.1.1	Basic Electrical Properties . . . . .	103
A.1.2	Anatomical and Functional Structure . . . . .	104
A.1.3	Mechanisms of Action Potential Generation . . . . .	106
A.2	Variations . . . . .	107
A.2.1	on the synapse . . . . .	107
A.2.2	on the inputs . . . . .	108
A.2.3	on the Outputs . . . . .	108
A.3	Recapitulation . . . . .	109
<b>B</b>	<b>Neurotransmitter Receptors</b>	<b>111</b>
B.1	Ionotropic Receptors . . . . .	111
B.2	Metabotropic Receptors . . . . .	111
B.3	The NMDA Receptor . . . . .	112
<b>C</b>	<b>The Importance of Calcium in Neurons</b>	<b>115</b>
C.1	Sources of Calcium . . . . .	115
C.1.1	Voltage-dependent Calcium Channels . . . . .	115
C.1.2	NMDA Receptors . . . . .	116
C.1.3	Calcium Release from Internal Stores . . . . .	116
C.2	Calcium Actions . . . . .	117
C.2.1	Electrical Effects . . . . .	117
C.2.2	The Role of Calcium in Neurotransmitter Release . . . . .	118

<b>D Protein Phosphorylation</b>	<b>119</b>
D.1 First and Second Messengers . . . . .	119
D.2 What is Protein Phosphorylation? . . . . .	120
D.3 What does it Do? . . . . .	120
D.4 How is it Controlled? . . . . .	121
<b>E Long-Term Potentiation</b>	<b>123</b>
E.1 Neural Plasticity and Learning . . . . .	123
E.2 Long-Term Potentiation . . . . .	123
E.2.1 Stages in LTP induction and maintenance . . . . .	124
E.2.2 Properties of LTP . . . . .	124
E.2.3 Induction of LTP . . . . .	124
E.2.4 Maintenance of LTP . . . . .	125
E.3 Summary . . . . .	125



# List of Figures

3-1	Aplysia’s “proud gait.” . . . . .	24
3-2	Aplysia’s body. . . . .	27
3-3	The gill withdrawal reflex. . . . .	28
3-4	Simplified Aplysia neural circuit. . . . .	29
3-5	Mechanisms for short-term learning. . . . .	32
3-6	The simulation model. . . . .	36
3-7	Results of recovery experiment. . . . .	40
3-8	Results of habituation experiments. . . . .	41
3-9	Results of sensitization experiments. . . . .	44
3-10	Results of associative learning experiment. . . . .	46
3-11	Effect of vesicle depletion on transmitter release. . . . .	47
3-12	The ISI effect. . . . .	53
3-13	Nonlinear distortion of ISI. . . . .	56
4-1	The early visual system. . . . .	62
4-2	Connections used in the simulation. . . . .	65
4-3	Typical target activity pattern. . . . .	67
4-4	Examples of initial and final projections. . . . .	69
4-5	Spacing error. . . . .	70
4-6	Arbor and receptive field strengths. . . . .	70
4-7	Map expansion and compression. . . . .	76
4-8	Map expansion after a source lesion. . . . .	79
4-9	Map compression after a target lesion. . . . .	80
5-1	Map formation with activity-dependent decay. . . . .	90
5-2	Variation in $K_i(t)$ with activity-dependent decay. . . . .	91
A-1	What a neuron looks like. . . . .	105



# List of Tables

4.1	Map Magnification and Receptive Field Properties. . . . .	77
-----	---	----



# Chapter 1

## Introduction

A study of the brain's architecture and learning mechanisms can be extremely useful in understanding the nature of intelligence and adaptive behavior. However, in the past, the usefulness of biological examples has been limited by the primitive state of our understanding of both computational systems and neuroscience, and by the limited interaction between computational modellers and experimentalists.

Research is progressing rapidly in both Computer Science and Neuroscience, and both fields benefit by maintaining communication between them. Computational modelling in neuroscience helps to understand and integrate experimental data and to test hypotheses about the function of neural circuits, and it provides a framework to focus the direction of future research. In artificial intelligence and connectionist research, the articulation of underlying principles of development in neural systems can provide important insights and design principles for the construction of intelligent systems.

This thesis describes mathematical and computational models of several known biological learning mechanisms. The methodology is to construct computer models of example systems utilizing two types of learning, classical conditioning in *Aplysia*, and long-term potentiation (LTP) in mammals. These circuits are studied in terms of both chemical interactions within and between neurons and overall network structure. Their capabilities and limitations are explored through simulation and analysis.

This work is, of necessity, speculative, and serves primarily to sketch out an area of study and identify some interesting problems, and to fill in a few details that point the way toward the kind of answers that are likely to be found as more work is done in this area.

### 1.1 Goals

The goal of this research is to better understand the relationship between structure and function in the nervous system: that is, between the biological mechanisms underlying different types of learning and their computational properties.

The questions I am interested in include:

1. What is the nature of the computational primitives in the brain, and what kinds of algorithms can be implemented efficiently with them?
2. What mechanisms underlie different forms of learning and memory?
3. What is the relative contribution of network properties and properties of individual neurons to the computational capabilities of the brain?
4. In what ways can learning be incorporated into structured networks?
5. How are biological learning mechanisms similar to or different from current computational learning models?

It is my hope that the neural systems described and modelled in this work provide some initial insights as to what the answers those questions may be.

## 1.2 Chapter Organization

The central chapters of this document take a detailed look at two neural systems which illustrate a variety of learning processes in neurobiology.

Chapter 2 discusses the process of modelling in neuroscience, at a philosophical level.

Chapter 3 describes a circuit controlling the gill withdrawal reflex in *Aplysia*, a marine snail, and presents a simulation and an analysis of the mechanisms underlying observed habituation, sensitization, and associative learning in the reflex. These mechanisms display an intricate interaction between electrical conductances and chemical processes inside the synaptic terminals.

The second simulation models the formation of ordered topographic connections between different structures in the early visual pathway. Chapter 4 describes a simulated model of topographic map formation in the visual system, and Chapter 5 presents a mathematical analysis of the system and the constraints necessary to ensure its success.

The final chapter draws the various parts of this research together and summarizes the insights into the particular brain systems studied. It discusses principles that are common to the different systems, and which may turn out to be more generally true of biological systems that mediate adaptive behavior.

## Chapter 2

# Modelling in Neuroscience

My primary reason for choosing this topic was a deep curiosity about the brain and how it works, particularly with regard to the nature of neural computation. One of the most interesting aspects of my undergraduate education was the explication of all the layers of abstraction in computers, from the internal electrical properties of a silicon transistor to a high-level programming language. I started this work with the goal (however unrealistic) of doing the same with the brain: understanding all the layers of neural processing from the underlying chemical processes to its higher-level functioning.

Just as the nature of the underlying hardware directs and constrains the character of computer languages, the nature of the neuronal substrate constrains the character of the computational primitives and “programming languages” used in the brain. For this reason, characterizing the behavior of neurons is crucial for developing an understanding of neural computation. Mechanisms involved in learning and development are emphasized throughout this work in recognition of the prevalence of plasticity at all levels in the brain, and its central role in the establishment of the brain’s structure and function.

Learning, in the context of traditional neural networks research, is conceptualized as permanent synaptic changes in response to information encoded in the neuron’s electrical activity. However, neurons and their synaptic connections change over time in a wide variety of ways, only a few of which fit this model. Although neural plasticity is often activity-dependent, many other processes in the cell, such as chemical and mechanical properties, also play important roles in the cell’s development over time.

Learning in the brain is thus a far richer and more complex phenomenon than is recognized by traditional models. A primary thesis of this work is that a recognition of the multiplicity of mechanisms for plasticity in the cell is essential to understanding the way the system functions as a whole. Because most previous models of the functional characteristics of neurons have concentrated exclusively on their electrical properties, the focus here is on chemical mechanisms.

## 2.1 The Value of Models

The field of neuroscience has progressed very rapidly in the past few years. A range of new experimental techniques allows researchers to probe the internal mechanisms of neurons in far more detail than was possible even five or ten years ago.

Even so, biological structures are so complex, and biochemical interactions are so intricate and difficult to isolate, that many aspects of the physical system must still be inferred from insufficient data. This is one of the major challenges of the field, and it limits the uses to which modelling can be put.

Until biological systems are understood far better than they are at present, a biological model, however rigorous it may be mathematically, is at best a working hypothesis. The question of whether a particular model is “correct” is therefore of far less interest than that of whether it is useful. How well does it reveal the gaps in our knowledge, and suggest questions to direct further experimentation?

At worst, a biological model is simply wrong. It can be difficult to keep track of the many many details of what is known about a neural system, and integrate them into a model that remains compatible with the current state of experimental research. The goal of biological modelling is to organize this information in a way that reveals some underlying structure or functional principle while maintaining a plausible correspondence between the mathematical properties of a simulation and its supposed biological substrate.

## 2.2 Is it Real or is it Artifact?

It can often be difficult to distinguish, when looking at a system in which everything interacts with everything else, whether a given effect is an integral part of the system’s functional design, or an artifact that is due to undesired but unavoidable constraints of the physical substrate. However, there are a number of properties which can be examined to help distinguish between these situations.

- One question we can ask is how many cellular resources participate in producing the effect, or would be necessary in order to avoid it. An effect which requires the coordination of many different processes is more likely to be significant than one which results from a single mechanism. Conversely, if a large number of cooperating processes would be necessary to prevent an effect from occurring, or if there is evidence for the presence of processes which minimize the effect, this would be a strong argument for classification of that effect as an unavoidable artifact.
- Another question is whether the behavior results from a cellular mechanism whose function in other systems is well established. Protein phosphorylation as a response to extracellular signals, for example, was first studied in the control

of glycogen metabolism, and has been established as an important mechanism for modulating a wide variety of metabolic processes in many different cell types [50]. This mechanism is therefore a likely candidate for mediating a neuron's metabolic responses to neurotransmitters.

- Given some parameter which activates and deactivates a particular process, a correspondence between the range of variability necessary to control the process and the observed range of variability of that parameter *in vivo*<sup>1</sup> may be an indication of functional significance.

Two examples involving the NMDA receptor, a protein involved in interneuronal communication, illustrate this point. The action of NMDA receptors is strongly potentiated in response to very small concentrations of glycine [23]. However, this effect reaches saturation even with trace amounts of glycine, comparable to the basal levels found in the extracellular fluid, so there is no evidence for a differential response to a controlled variation in the glycine concentration *in vivo*. This does not, however, rule out the possible significance of glycine potentiation, as there may be controlling processes which have not yet been discovered.

Basal levels of magnesium also affect the NMDA receptor, by blocking its activity in a voltage-dependent manner. The voltage at which magnesium ceases to act as an activity block falls well within the cell's normal operating range [34]. In this case, therefore, the evidence supports the hypothesized functional significance of the magnesium block.

- Another indication that may be useful in determining whether a mechanism is functionally important is its magnitude relative to other mechanisms that affect the same behavior. An example would be a comparison of synaptic depression to habituation. In synaptic depression, neurotransmitter release is reduced by only ten or fifteen percent following prolonged firing. In habituation in *Aplysia*, by contrast, synaptic transmission is reduced to thirty percent of its initial value by only a few training trials [30].

The absence of a large effect, however, does not necessarily rule out the functional significance of a candidate cellular mechanism. The lack of positive evidence could be due to limitations in the experiment. For example, localized effects may be lost in the noise if the measuring technique is not specific enough.

- A highly specific response to a particular chemical, and a lack of response to other similar chemicals, may also indicate functional significance.

Although none of these arguments is conclusive, and in many cases new experiments may provide evidence which counters our current intuitions, they nonetheless

---

<sup>1</sup>That is, in the living animal, as opposed to the petri dish.

can improve our ability to distinguish important effects from artifacts. The mechanisms discussed in this dissertation all satisfy at least one of these indications for a functionally significant effect.

## 2.3 Selecting a System for Modelling

There are a number of properties of neural systems which, if known, make it easier to model learning phenomena in that system. Some of these are:

1. A description of the input and output behavior of the circuit, both before and after learning.
2. A description of the internal and external connections in the circuit.
3. Information about the behavior of the synapses, for example, the strength of the connections, whether they are excitatory or inhibitory, and what forms of learning are present.
4. A high-level description of the function the system performs.
5. Evidence for the presence and importance of learning phenomena in the system.

Both the *Aplysia* gill withdrawal reflex and map formation in the early visual system have been extensively studied and are relatively well-understood. Because many of the mechanisms involved are widespread in other brain regions and across species, it is expected that the principles discovered here will generalize to other learning situations as well.

# Part I

## Classical Conditioning in Aplysia



# Chapter 3

## Synaptic Plasticity in *Aplysia*

This chapter presents a simulation and analysis of mechanisms underlying short-term learning in the marine snail *Aplysia*.

One purpose of this work is to test the conceptual models described by neurobiologists to discover whether the hypothesized mechanisms are adequate to explain the observed learning phenomena. The simulation demonstrates that the mechanisms described in the literature can produce some simple aspects of the experimental results, but there are many details which it cannot explain. For example, inconsistencies in learning and recovery rates when different training protocols are used require a more complex explanation.

Two specific mechanisms are analyzed in detail to explore the relationship between the macroscopic behavior of the system and the underlying mechanisms. These are the process governing the relationship between  $\text{Ca}^{++}$  influx and transmitter release and the chemical cascade which controls the effect of the inter-stimulus interval (ISI) on the strength of associative learning. The analysis predicts certain parameters of those processes, such as chemical reaction rates, which can be tested experimentally.

Studies of learning in *Aplysia* provide evidence for a specific biological implementation of classical conditioning phenomena, which makes use of both chemical and electrical properties of the synapses. Similar processes may be used to control a broad range of neural responses.

### 3.1 The Nature of the Beast

*Aplysia* is a marine gastropod mollusc, often (inaccurately) called a “sea slug”. Eric Kandel, one of the more prominent experimentalists working with *Aplysia*, describes the creature as follows:

As is readily appreciated from its proud gait, illustrated in Figure 3-1, *Aplysia californica* is a large, attractive, and obviously intelligent beast. It is just the sort of animal one would immediately select for studies of learning. [28, page 6]

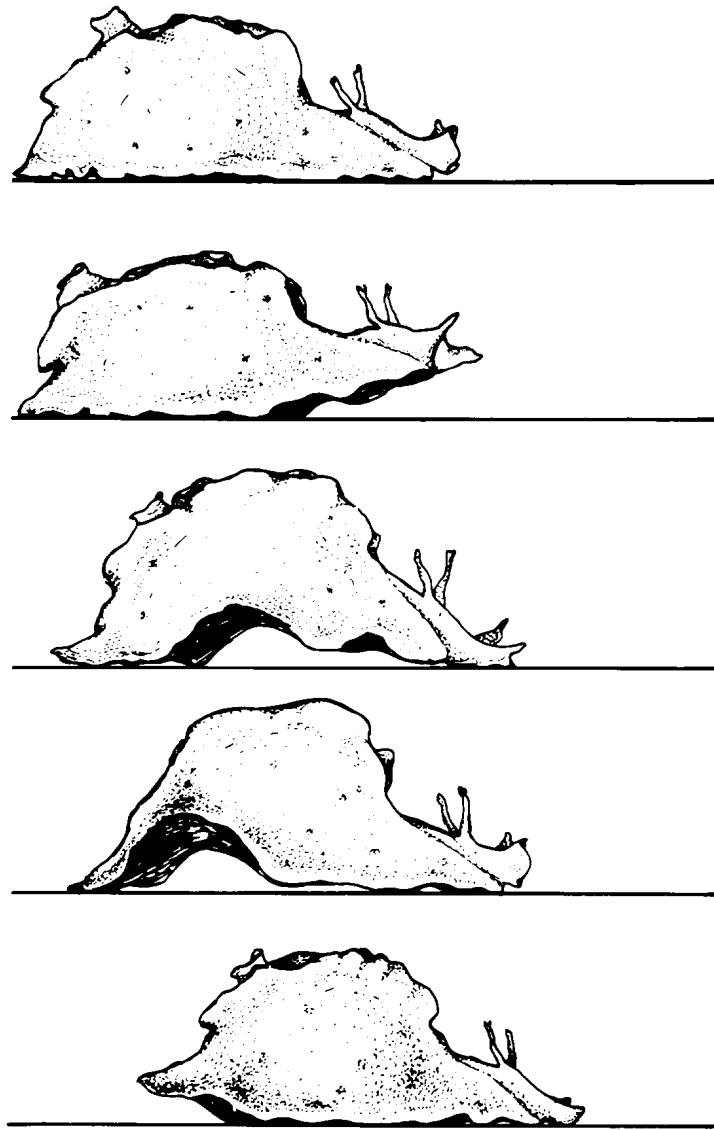


Figure 3-1: Aplysia's "proud gait" (from [28, page 7].)

*Aplysia* is currently in demand for studies in neuroscience for two major reasons.

The first is that its nervous system has a number of properties that make it easy to study [27]. Its neurons are relatively large, and the organization of its nervous system is consistent enough that individual neurons can be reliably identified from one animal to the next. Synapses are electrically close to the cell body, so intracellular recording of synaptic potentials is possible. This means that the interneuronal connections — the “wiring diagram” — of the animal can be determined through intracellular recording at the cell body.

The second reason is that it learns.

### 3.1.1 What Does *Aplysia* Learn?

The learning phenomena observed and studied in *Aplysia* and other gastropod molluscs fall under the category of classical conditioning responses. Classical conditioning builds on innate reflex responses, which are modified in response to experience. A reflex consists of a sensory stimulus for which the animal exhibits a characteristic behavioral response.

#### The Phenomena of Classical Conditioning

First-order classical conditioning responses<sup>1</sup> include habituation, dishabituation, sensitization, associative learning, extinction and recovery [9]. In *habituation*, repeated application of a stimulus results in attenuation of the reflex response. This attenuation can last for an extended period. *Dishabituation* and *sensitization* are very similar, as both involve an enhancement of the reflex response following a strong stimulus. This stimulus need not be the same as the one that normally elicits the reflex response. The difference between the two is that dishabituation acts on an already-habituated response, whereas sensitization can act regardless of whether the reflex is habituated.

*Associative learning* is the best-known phenomenon of classical conditioning. There are two stimuli involved in associative learning, called the unconditioned stimulus (US) and the conditioned stimulus (CS). The US naturally evokes the reflex response (UR). If the US and the CS are paired in a sequence of learning trials, the CS alone will begin to evoke the reflex response (CR).

In *extinction*, a CR gradually disappears following repeated application of the CS unpaired with the US. After a CR has been extinguished, it often reappears after a period of rest. This response is called *recovery*.

Higher-order classical conditioning phenomena include *second-order conditioning*, where a new stimulus is conditioned using an already conditioned stimulus-response pair in place of a primary reflex response, *generalization* to novel stimuli that are

---

<sup>1</sup>That is, responses which involve only a single conditioned stimulus.

similar to the CS, and *blocking*, where an already conditioned stimulus prevents conditioning of a new stimulus.

### The Gill Withdrawal Reflex

Classical conditioning in *Aplysia* is studied using the gill withdrawal reflex. One of the more prominent features of the molluscan body is the *mantle*, located on its back (see Figure 3-2). The mantle consists of a cluster of organs including a siphon and gill for breathing. Light tactile stimulation of the siphon induces a protective reflex, in which the siphon and gill are contracted and withdrawn into the parapodium (see Figure 3-3.)

This reflex has been shown to exhibit several forms of first-order conditioning [30, 21]. The reflex habituates after repeated tactile stimulation of the siphon, and sensitization occurs following an electrical shock to the tail [28]. Simple associative learning has also been found [1]. The tail shock is used as the unconditioned stimulus (US), and the conditioned stimulus (CS) is tactile stimulation of the siphon. The response to associative learning is stronger and lasts longer than with sensitization alone.

Some types of higher-order conditioning have also been found in *Aplysia* or its close relatives [21, 56]. All of these effects have a short-term form, lasting a few hours, and a long-term form which can last for at least several weeks.

#### 3.1.2 Why Does *Aplysia* Learn?

One might wonder just what it is that a sea slug has to learn about, being a simple grazing animal with no natural predators. As the marine neurobiologist is a relatively recent arrival on the scene, it can hardly be expected to have evolved these abilities for the sole purpose of showing off in a petri dish.

However, even the life of such a gentle beast is fraught with circumstance. Many of these creatures live in the littoral, or intertidal, zone of the ocean. In Kandel's words,

Animals living in the littoral zone are often exposed to the air for several hours a day and are buffeted about by the tides. These animals must withstand wide and rapid changes in temperature, humidity, salinity, pressure, mechanical stimulation, and wind, and survive repeated exposure to air and immersion in the sea. [27, page 74]

It is easy to see why a creature living in such an environment might evolve the capacity to learn. If a gentle tactile stimulus, such as might be caused by the beginnings of an undertow, is a reliable predictor that *Aplysia* is about to be torn from its footing and smashed against a rock by an incoming wave, it will clearly benefit by recognizing this contingency and tucking its more delicate organs safely out of the way.

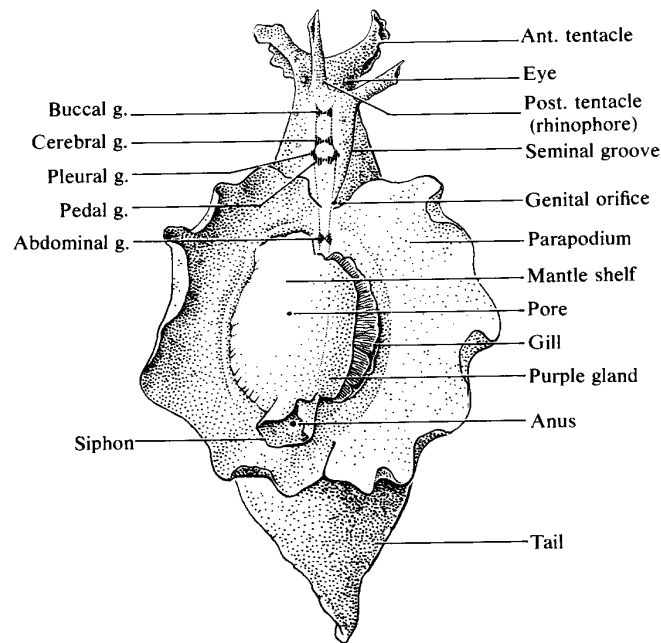
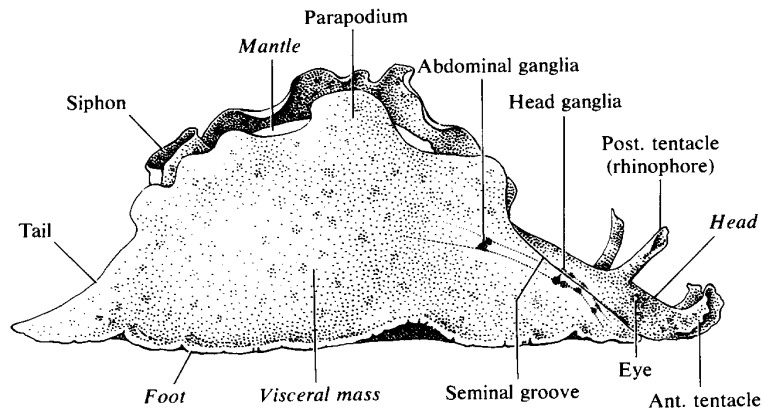
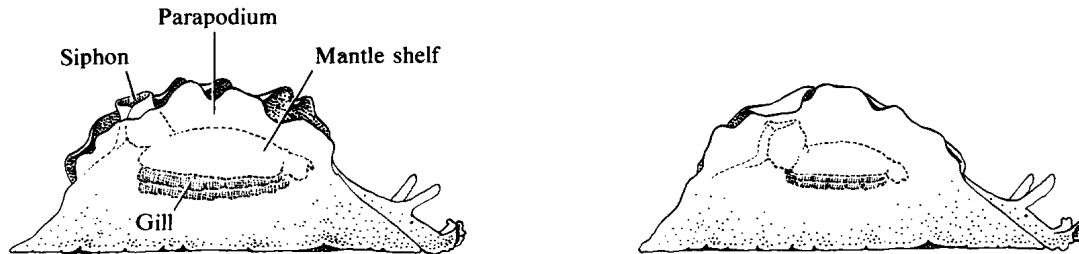


Figure 3-2: *Aplysia*'s body (from [27, page 76].)



**Figure 3-3:** The gill withdrawal reflex (from [27, page 85].)

Other members of the species live deeper in the sea, in the sublittoral zone, where they are rarely exposed to air. Life is a lot calmer in the sublittoral zone.

### 3.1.3 How Does *Aplysia* Learn?

*Aplysia's* nervous system contains about 20,000 central neurons [28]. These are grouped into nine ganglia, each of which contains about 2000 neurons. An important part of the circuitry for the gill withdrawal reflex resides in its abdominal ganglion. The complete circuit is comprised of some fifty or so neurons, including a large number of interneurons [19]. The circuit can be reduced to a simplified form containing only the primary monosynaptic connections and a few interneurons. The result is shown in Figure 3-4.

The basic reflex is implemented by direct connections from sensory neurons that respond to tactile stimulation of the siphon to motor neurons that contract the gill.

Tactile stimulation at a point on the siphon activates about 8 sensory neurons, each of which fires 1 to 2 spikes [28].

Sensory neurons from the tail connect indirectly, via facilitatory interneurons, to the presynaptic terminals of the siphon sensory neurons. These presynaptic terminals are the primary locus for the identified mechanisms underlying classical conditioning in *Aplysia*.<sup>2</sup>

### Habituation

In habituation, the strength of the sensory-to-motor synapse is reduced by repeated firing of a sensory neuron. The cause of this change is hypothesized to involve voltage-

---

<sup>2</sup>Readers who are unfamiliar with neuroscience may wish to refer to Appendix A for background that will be helpful in following the material in this section.

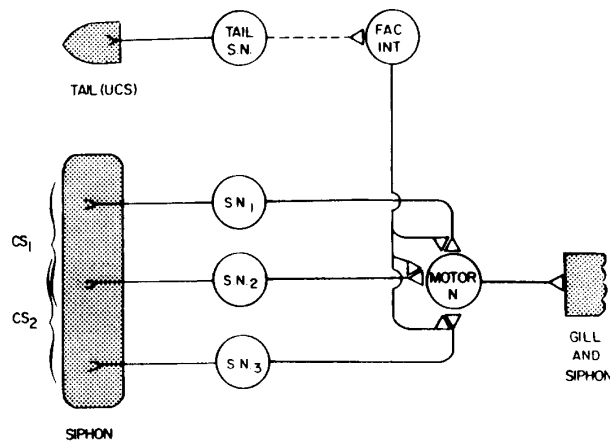


**Figure 3-4:** A diagram of the simplified *Aplysia* neural circuit. Sensory neurons from the siphon form direct reflex connections to the motor neurons controlling the gill withdrawal reflex. Tail sensory neurons act indirectly on the reflex via facilitator interneurons. The interneurons connect to the reflex pathway through synaptic contacts on the presynaptic terminals of the sensory outputs. The tail sensory neurons also make direct contacts with motor neurons (not shown). (from [21].)

sensitive calcium channels [28].<sup>3</sup> These channels are embedded in the cell membrane of the presynaptic terminal, and are closed when the cell is at rest. They open during action potentials to allow calcium ions ( $\text{Ca}^{++}$ ) to diffuse into the cell from the extracellular fluid.<sup>4</sup> The influx of  $\text{Ca}^{++}$  catalyzes neurotransmitter release [27].<sup>5</sup>

Habituation inactivates these channels, reducing the rate at which  $\text{Ca}^{++}$  diffuses into the synapse. This, in turn, reduces the amount of transmitter released in response to an action potential. This form of calcium channel inactivation only accounts for

<sup>3</sup>Although these experiments are relatively old, more recent work has concentrated on associative and/or long-term learning, so this explanation for the habituation response is still current.

<sup>4</sup>Ion channels can take on a number of distinct conformational states [46]. The probability of a state transition is determined by the relative energy and stability of the two states. This  $\text{Ca}^{++}$  channel, for example, has three identifiable states: open, closed, and inactivated. The closed state has the lowest energy under equilibrium conditions, and is therefore the channel's resting state. The state transition from closed to open is most probable when the membrane is depolarized, which changes the relative energy of the two states.

State transitions from the open to the inactive state appear to be common, causing a measurable number of channels to become inactivated over the millisecond time course of a single action potential. Transitions from the inactive state back to the resting (closed) state, in contrast, occur over a time period of minutes to hours, implying that the inactive state is relatively stable. This hypothesis corresponds to the observation that repeated depolarization results in a population shift toward the inactive state (that is, given a population of  $\text{Ca}^{++}$  channels, there is an increase in the percentage of channels that are inactive after habituation.)

<sup>5</sup>See Appendix C for information about cellular actions of  $\text{Ca}^{++}$ .

short-term habituation, as the channels decay back to their normal resting state within a few hours. The mechanism for long-term habituation is not known. It may act through a process that increases the duration of channel inactivation, or it may require some other mechanism.

### Sensitization

Sensitization apparently acts by a more complex mechanism, using the indirect connections between the sensitizing stimulus (the tail shock) and the presynaptic terminals of the siphon sensory neurons [30]. The neurotransmitter released by the intervening facilitator interneurons is believed to be serotonin. Serotonin receptors in the presynaptic terminal are metabotropic.<sup>6</sup> Unlike ionotropic receptors, which act through electrical conductance changes, the serotonin receptor is coupled to a G protein which stimulates adenylate cyclase activity. Adenylate cyclase synthesizes cyclic AMP (cAMP), a common cellular second messenger which controls a wide range of metabolic actions in different cell types [50]. cAMP has been hypothesized to act exclusively through a cAMP-dependent protein kinase. Protein kinases, when activated, modulate the cell's behavior by phosphorylating a specific set of proteins. Phosphorylation changes a protein's activity in a way that is dependent on the particular protein and phosphorylation site.<sup>7</sup>

The cAMP-dependent protein kinase in *Aplysia* apparently affects two types of potassium ( $K^+$ ) channels in the presynaptic terminal. These channels produce the end of an action potential by opening to repolarize the cell [22]. Phosphorylation inactivates the  $K^+$  channels, which slows repolarization and thereby prolongs the action potential.

The voltage-sensitive  $Ca^{++}$  channels remain open as long as the terminal is depolarized, so the  $Ca^{++}$  influx increases along with the action potential duration. This in turn increases transmitter release, resulting in a stronger motor response to the sensitized stimulus.

Again, these mechanisms explain short-term but not long-term sensitization. The increase in action potential duration lasts only as long as the increase in intracellular cAMP [28]. The cAMP concentration remains elevated for over an hour after a single brief pulse of serotonin, however, which is in sharp contrast to the millisecond time scale of the electrical effects of ionotropic receptors.

### Associative Learning

The hypothesized mechanism for associative learning [1] uses the same facilitator interneurons that are involved in sensitization.

---

<sup>6</sup>See Appendix B for background information on neurotransmitter receptors and their actions.

<sup>7</sup>Appendix D contains a brief introduction to protein phosphorylation.

Strong stimulation of the sensory neurons in the tail (the US) activates the gill withdrawal motor neurons directly (this is the unconditioned response, or UR), and it also activates the facilitator interneurons. This sensitizes the sensory synapses, increasing the likelihood that any tactile stimulus will elicit a withdrawal response. However, if another sensory neuron (the CS) fires shortly before the facilitator interneuron, the amplification of the withdrawal reflex for that stimulus is greatly enhanced, with an effect that may last several days.

The learned association between the US and the CS may occur as a result of a second function of  $\text{Ca}^{++}$ . Once it enters a cell,  $\text{Ca}^{++}$  is very quickly bound to calmodulin. Like cAMP, the  $\text{Ca}^{++}$ -calmodulin complex is a common cellular second messenger. One of the observed actions of  $\text{Ca}^{++}$ -calmodulin is increased activation of adenylate cyclase [1, 8].

The hypothesized effect of  $\text{Ca}^{++}$ -calmodulin on adenylate cyclase in the *Aplysia* synapse is modulatory. It does not directly activate cAMP production, but it enhances the effectiveness of serotonin activation. When  $\text{Ca}^{++}$ -calmodulin is active, therefore, a greater amount of cAMP will be produced in response to the same amount of serotonin.

The strength of associative learning depends strongly on the inter-stimulus interval (ISI), that is, the time delay between the CS and the US. The associative effect is transient, peaking and decaying within two seconds in the aftermath of an action potential [1]. Only if the facilitator interneuron fires within this time window is the sensitization effect enhanced, resulting in a differential response at that synapse.

In order for these mechanisms to produce associative learning, the US and the CS must each be capable of producing a withdrawal response alone, and there must be a facilitator interneuron connecting the US with the output terminal from the CS. The need for these pre-existing connections limits the organism's learning ability. Only stimulus-response pairings which are already in its behavioral repertoire can be learned. There are a huge number of facilitator interneurons in *Aplysia* [28], which is what we would expect if this hypothesis is correct: the more abundant these neural connections, the more versatile the animal will be in responding to its environment.

Another interesting property of these mechanisms is the parsimony of neural connections: the same connections that are necessary for sensitization, a general arousal mechanism, are also used to produce a selectively enhanced response to stimuli that consistently precede the US.

The mechanisms for these three forms of learning (habituation, sensitization, and associative learning) are summarized in Figure 3-5.

### Higher Order Learning Phenomena

Hawkins and Kandel, in response to these findings, speculate on the existence of a "cell-biological alphabet for learning" [21]. That is, they hypothesize the existence of a small set of primitive cellular mechanisms that can be combined to produce a wide

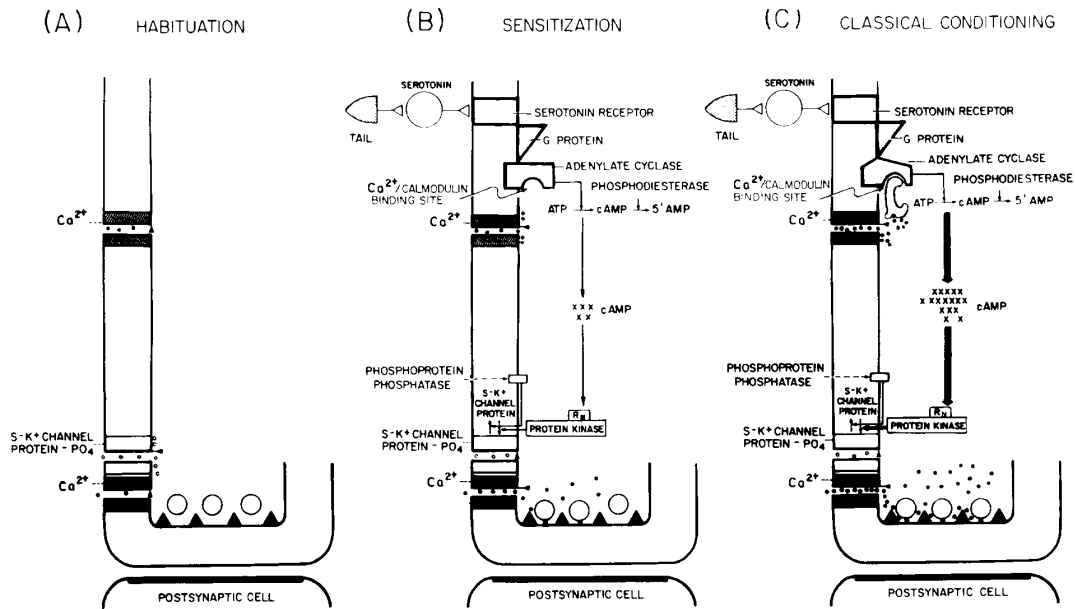


**Figure 3-5:** Summary of the mechanisms hypothesized to mediate (a) habituation, (b) sensitization, and (c) associative learning in Aplysia's gill withdrawal reflex. Each image shows the interior of a presynaptic terminal, and diagrams the chemical processes described in the text. (from [20, page 76].)

range of learning phenomena. They describe how mechanisms already found could, in principle, be combined to produce other learning phenomena that have not yet been studied.<sup>8</sup>

- Extinction and recovery were hypothesized to work via the same mechanism that mediates habituation.
- Second order conditioning is explained by introducing additional neural connections that cause a CS sensory neuron to excite the facilitator interneuron (IN). Synapses from the CS to the IN are also facilitated (their behavior is hypothesized to match a Hebbian learning model, unlike the CS-CR synapses). Thus, the ability of the CS to excite the IN is enhanced as it is conditioned. Once conditioning is complete, the CS can facilitate other stimuli through the IN in the same way the US did originally.
- Generalization across similar tactile stimuli was explained by the existence of overlapping receptive fields for many sensory stimuli, so that a similar stimulus would excite a subset of the sensory neurons that were conditioned.
- Additional properties of the facilitator IN were introduced to explain blocking. The IN fires only at the onset of a sustained input, so if a fully conditioned CS<sub>1</sub> fires before the US, it can block the facilitator from firing in response to the US neuron. This will in turn prevent facilitation of the new CS<sub>2</sub>. Because there is no time delay between firing of CS<sub>1</sub> and CS<sub>2</sub>, the response of the IN to CS<sub>1</sub> does not produce conditioning. If a response is only partly conditioned, the facilitator will be only partly blocked, and some conditioning of CS<sub>2</sub> will occur.
- Pre-exposure to the US may cause conditioning to the background environment, which in turn would block conditioning to a CS which is presented later.

Although these learning phenomena have not actually been observed in *Aplysia*, they are found in *Limax Maximus*, a close relative [16, 56].

### Mechanisms for Long-Term Learning

Following the training trials, as the short-term response decays, there is a progressive shift toward longer-term forms of learning. This shift occurs gradually over the course of several hours. Both the number of times a CS-US stimulus pair is presented and the time delay between successive presentations affect the degree to which the animal's long-term response changes.

---

<sup>8</sup>These phenomena are defined in Section 3.1.1.

Mechanisms for long-term learning have not yet been extensively explored, though it appears to involve both the production of new proteins [12, 65]<sup>9</sup> and new synapse formation [17].

One apparent mechanism for DNA transcription in long-term sensitization is cAMP-dependent phosphorylation of a substrate protein that acts as a DNA transcription factor [12]. This protein, when activated by cAMP, binds to a particular DNA sequence and activates (or, conversely, inhibits) transcription of the associated genes.

What, then, is the function of the proteins encoded by these up- or down-regulated genes? One answer is that they may lead to long-term changes in phosphorylation of the same set of substrate proteins that is phosphorylated in a short-term manner by the presence of cAMP in the presynaptic terminal [65]. In this case, long-term facilitation would be mediated by long-term spike broadening, via the long-term inactivation of  $K^+$  channels.

One set of proteins which are down-regulated during long-term sensitization has been identified as an NCAM-related class of cell adhesion molecules, which attach to the external surface of sensory neurons [29]. NCAMs are important in regulating cell growth during development, and may be part of the mechanism for new synapse formation.

## 3.2 A Simulation of the *Aplysia* Circuit

This section describes a simulation of the *Aplysia* gill withdrawal circuit. Individual synapses are the primary site of learning in this network, so the model concentrates on the electrical and chemical mechanisms within a single synapse.

There are at least six distinct learning mechanisms in the circuit, which result in short and long term forms of habituation, sensitization, and associative learning, and which allow for the possibility of higher-order forms of learning such as differential conditioning and blocking. Only the short-term forms of learning are modelled here.

Some of these mechanisms have previously been modelled elsewhere. Byrne and Gingrich [8] model the effects of chemical diffusion and synaptic vesicle transport within the synapse, which captures the effect of synaptic depression due to vesicle depletion. The model presented by Hawkins [20] demonstrates his hypotheses about higher-order learning phenomena, as described in [21].

The computational model presented here is a straightforward instantiation of the conceptual models used in biology, and a major purpose of the simulation is to test the adequacy of current conceptual models for short-term learning. For this rea-

---

<sup>9</sup>There are two major processes which can be blocked to test for the involvement of protein production in a cellular process. The first is DNA transcription, which produces new strands of messenger RNA (mRNA). The second is translation of mRNA into amino acid sequences during protein synthesis.

son, certain aspects of the experimental data are considered more rigorously than in other models. Parameter selection is based directly on experimental data, and tested against experiments which use different protocols, rather than selected to maximize the desired result [20] or left unspecified [8]. The model derived here for the dependency of transmitter release on  $\text{Ca}^{++}$  influx explains aspects of the experimental data that cannot be explained using the simpler models used in [8] and [20]. The process underlying associative learning is also modelled in a novel manner that better predicts the observed effect of the ISI on the strength of learning.

### 3.2.1 Simulation Equations

Individual action potentials are treated as atomic events which can occur at 10 msec intervals.<sup>10</sup> However, state variables, such as concentrations of chemicals in the presynaptic terminal, are updated only when their values are needed to model the cell's response to new events. The short-term dynamics of individual learning trials can be modelled in this way without the need to step the system through large numbers of small time steps during extended periods (e.g. between learning trials) when nothing interesting is going on.

Four state variables are used to model the environment inside the presynaptic terminal of a sensory neuron. These variables track the factors hypothesized to mediate conditioning in the synapse. A diagram of the simulated system is shown in Figure 3-6.

When a  $\text{Ca}^{++}$  channel is inactivated during habituation, it ceases to be available for influx of calcium during an action potential.  $[N](t)$ , the concentration of available  $\text{Ca}^{++}$  channels, is used to track this effect.

The sensitization effect involves a cascade of several chemical events, but it is rate-limited by the concentration of cAMP [30].<sup>11</sup> It is modelled here with a single variable,  $[\text{cAMP}](t)$ , representing the cAMP concentration. The dynamics of protein kinase activation, protein phosphorylation, and  $\text{K}^+$  channel inactivation are assumed to follow cAMP changes closely, and are not modelled separately.

The factors mediating associative learning are more complex. Again a chemical cascade is involved, but here the dynamics of the interaction between  $\text{Ca}^{++}$ , calmodulin, and adenylate cyclase are modelled to capture the effect of the ISI on associative learning. Two state variables are used,  $[C](t)$  and  $[B](t)$ .  $[C](t)$  is the concentration of free  $\text{Ca}^{++}$ -calmodulin, and  $[B](t)$  is the concentration of  $\text{Ca}^{++}$ -calmodulin bound to adenylate cyclase.

---

<sup>10</sup>The duration of an individual action potential is on the order of 3-4 msec, which is much shorter than this 10 msec time scale.

<sup>11</sup>That is, the change in action potential duration appears to be primarily controlled by an ongoing elevation of the cAMP concentration, rather than by some other step in the chemical cascade.

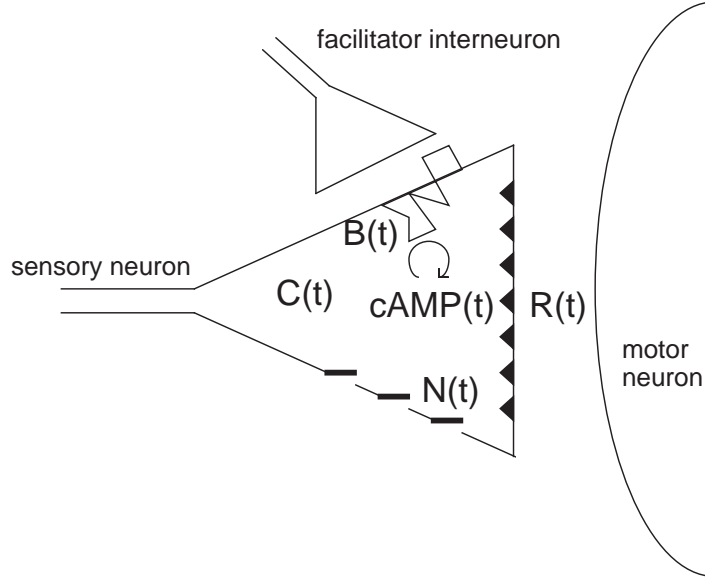


**Figure 3-6:** A diagram showing the state variables used in the simulation model.  $[N](t)$  is the concentration of active calcium channels;  $[cAMP](t)$  is the cAMP concentration;  $[C](t)$  is the concentration of  $Ca^{++}$ -calmodulin, and  $[B](t)$  is the concentration of  $Ca^{++}$ -calmodulin bonds with adenylate cyclase.  $[R](t)$  represents transmitter released into the synaptic cleft.

### Behavior in the Absence of Activity

When there is no activity in the sensory neuron or the facilitator, state variables decay to their equilibrium values according to the following equations:<sup>12</sup>

$$[N](t) = N_0 - (N_0 - [N](t_0)) \cdot e^{(t-t_0)/\tau_N} \quad (3.1)$$

$$[cAMP](t) = [cAMP](t_0) \cdot e^{(t-t_0)/\tau_{cAMP}} \quad (3.2)$$

$$[C](t) = c_1 e^{m_1(t-t_0)} + c_2 e^{m_2(t-t_0)} \quad (3.3)$$

$$[B](t) = c_1 a_1 e^{m_1(t-t_0)} + c_2 a_2 e^{m_2(t-t_0)} \quad (3.4)$$

where  $t_0$  is the time of the most recent event,  $[N]_{\max}$  is the total concentration of  $Ca^{++}$  channels,  $\tau_N$  is the time constant for  $Ca^{++}$  channel recovery,  $\tau_{cAMP}$  is the time constant for the cAMP concentration decay, and  $m_1$ ,  $m_2$ ,  $c_1$ ,  $c_2$ ,  $a_1$ , and  $a_2$  are determined by the reaction rates between  $Ca^{++}$ -calmodulin and adenylate cyclase and

<sup>12</sup>These equations are derived from standard rate equations for chemical reactions (see [25] for an introduction to this topic). Linear kinetics are assumed for simplicity, except where otherwise indicated.

the initial conditions at time  $t_0$  (see Section 3.2.3 for a derivation of these parameters.)

### Response to Events

There are two kinds of events that cause step changes in the internal state of the presynaptic terminal. The first is an incoming action potential from the sensory neuron; the second is an action potential in the facilitator interneuron.

**Sensory Action Potentials** The concentration of cAMP is used to determine the duration of an action potential in the sensory neuron.

$$D(t) = D_0(1 + K_D \cdot [\text{cAMP}](t)) \quad (3.5)$$

where  $D_0$  is the initial duration in the absence of any learning effects, and  $K_D$  is the magnitude of cAMP's effect on action potential duration.

The action potential has a primary effect on the rate of  $\text{Ca}^{++}$  influx ( $[\text{I}_{\text{Ca}}](t)$ ), which determines both the amount of transmitter released ( $[\text{R}]$ ) and the concentration of  $\text{Ca}^{++}$ -calmodulin. It also changes the concentration of inactivated  $\text{Ca}^{++}$  channels, which changes the rate of  $\text{Ca}^{++}$  influx for future action potentials. The effect of an action potential is modelled as follows:

$$[\text{I}_{\text{Ca}}](t) = I_{\text{Ca}0}[\text{N}](t) \quad (3.6)$$

$$\Delta[\text{C}](t) = [\text{I}_{\text{Ca}}](t) \cdot D(t) \quad (3.7)$$

$$\Delta[\text{N}](t) = -[\text{N}](t)(1 - K_N) \quad (3.8)$$

$$[\text{R}](t) = R_0 \left( \frac{[\text{I}_{\text{Ca}}](t)}{I_{\text{Ca}0}} \right)^4 \left( \frac{D(t)}{D_0} \right)^5 \quad (3.9)$$

$I_{\text{Ca}0}$  is the  $\text{Ca}^{++}$  influx per  $\text{Ca}^{++}$  channel per unit time,  $R_0$  is the transmitter released by a single sensory action potential in the absence of learning, and  $K_N$  is the percentage of  $\text{Ca}^{++}$  channels still active after an action potential.

The magnitude of the gill withdrawal response is assumed to be proportional to transmitter release.<sup>13</sup> Equation 3.9 is derived in Section 3.2.3.

**Facilitator Action Potentials** The other type of event is an action potential in the facilitator interneuron. The primary effect of this is a change in the cAMP level,

---

<sup>13</sup>In biological experiments, this response has been measured in terms of the magnitude of the excitatory post-synaptic potential (EPSP) in the motor neuron, the number of motor neuron spikes generated by the EPSP, the magnitude of the withdrawal response (that is, how far the gill is retracted), or the duration of the withdrawal response. The relationship between number of motor neuron spikes and the magnitude of the withdrawal response is approximately linear [27, page 551].

which is modelled as instantaneous.<sup>14</sup>

$$\Delta[\text{cAMP}](t) = [\text{cAMP}]_0(1 + K_{\text{cAMP}} \cdot [\text{B}](t)) \quad (3.10)$$

$[\text{cAMP}]_0$  is the cAMP released per facilitator action potential in the absence of  $\text{Ca}^{++}$ -calmodulin, and  $K_{\text{cAMP}}$  is the percentage increase in cAMP production in response to a unit concentration of  $\text{Ca}^{++}$ -calmodulin bonds with adenylate cyclase.

### Parameter Selection

The parameters in the model correspond to specific physical quantities whose value can be determined from the experimental data.

For simplicity in interpreting the results, the parameters describing the initial state of the synapse (in the absence of learning) were normalized, so that all results are shown in proportion to the initial state.

$$N_0 = D_0 = I_{Ca0} = R_0 = \text{cAMP}_0 = 1.0$$

The “weak tactile stimuli” used in intact animals are assumed to consist of a single action potential in the sensory neuron, in accordance with the response described in [28] (one to two spikes per sensory neuron in response to a tactile stimulus).

Parameters for the calcium channels are set to match the experimental results of habituation Experiments 1 and 2 (described in Section 3.2.2 below.) The habituation coefficient  $K_N$  is set to produce habituation to 30% of the initial response after 15 trials at an inter-trial interval of 1.5 minutes, and the recovery rate is set to give 75% recovery 10 minutes later.

$$\begin{aligned} K_N &= 0.896 \\ \tau_N &= 350.0 \text{ seconds} \end{aligned}$$

Parameters controlling the sensitization response were set to match the experimental results for the calibration test described in sensitization Experiment 1 (described in Section 3.2.2.) The value for  $\tau_{\text{cAMP}}$  was estimated from the graph shown in Figure 3-9(a), and  $K_D$  was set to produce a maximum response of 450% of the pre-test level.

---

<sup>14</sup>Again, this is a simplification, since the dynamics of the chemical cascade resulting from the G protein activation of adenylate cyclase must take some time; the assumption here is that the cAMP concentration will have reached its final value before the next event which depends on it. The discrepancy between the behavior of this model and sensitization Experiment 2 (described below) can be explained if the experimental protocol used in that experiment violates this assumption.

$$K_D = 0.0045$$

$$\tau_{cAMP} = 1000.0 \text{ seconds}$$

There were a number of sensitization and associative learning experiments where the strength of the US was not specified. The value used in the simulation was chosen to match the strength of the initial response in sensitization Experiment 3. The tail shock (and every other noxious stimulus used in experiments other than the calibration test) is assumed to consist of 30 facilitator action potentials at 30 Hz.<sup>15</sup>

The parameter  $K_{cAMP}$ , which controls the strength of the associative response, is set using associative learning Experiment 1 (described in Section 3.2.2.) The serotonin puff, like other noxious stimuli, was assumed to produce the equivalent of 30 spikes over its 1 second duration.

$$K_{cAMP} = 13.5$$

The parameters which determine the effect of the ISI on learning are discussed in Section 3.2.3.

### 3.2.2 Results and Discussion

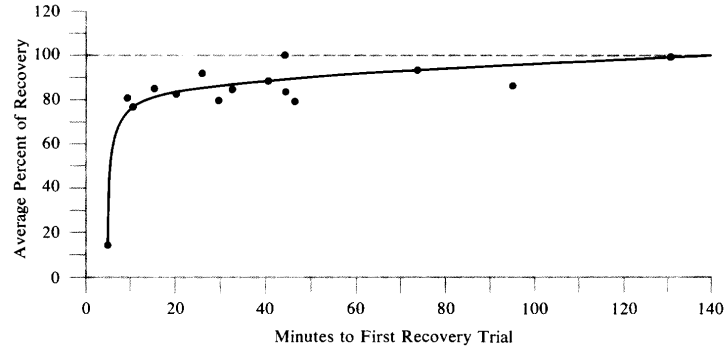
#### Habituation and Recovery

The habituation response in the model was tested against experimental results which illustrate the character of the response in *Aplysia*. These results are:

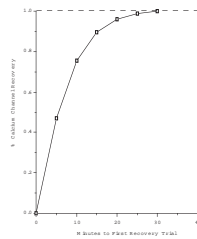
1. In [30], light tactile stimulation of the siphon at 1.5 minute intervals caused habituation to 30% of the initial response within 10-15 stimuli.
2. The habituation reflex shows 75% recovery 10 minutes after a single training session [27, page 544] (see Figure 3-7(a).)
3. Stimulating every 30 seconds, the withdrawal reflex is reduced to 20% of the maximum response after 10 stimuli. After a 10 minute rest, the reflex recovers to over 90% of the maximum. The reflex habituates more quickly during rehabituation after resting [27, page 544] (see Figure 3-8(a).)
4. Habituation to 50% of the maximum response occurs with an intertrial interval of half an hour [30] (see Figure 3-9(c).)

---

<sup>15</sup>The simulation assumes that the amount of serotonin released by a single facilitator action potential does not change with repeated activity, and that the relationship between the amount of serotonin released, the amount of cAMP produced, and the increase in sensory action potential duration is linear.



(a)



(b)

**Figure 3-7:** Results of recovery experiment. (a) Percent recovery of Aplysia’s habituation reflex, tested at different recovery intervals following a single habituation session. (from [27, page 544].) (b) Recovery in the model using same experimental protocol, with a training session consisting of 15 trials at 1.5 minute intervals.

5. Less habituation is observed when stronger tactile stimuli are used [27, page 545] (see Figure 3-8(d).)<sup>16</sup>

The recovery time constant  $\tau_N$  for the habituation tests was calculated using the data from Experiment 2, and the habituation coefficient  $K_N$  was then set to match the habituation data for Experiment 1. These parameters were then tested using the experimental protocols for Experiments 3 and 4.<sup>17</sup> Test results are shown in Figures 3-7 and 3-8.

<sup>16</sup>The strength of the tactile stimulus is measured in terms of the force of water emitted from a water jet, which is used to apply the stimulus.

<sup>17</sup>Experiment 5 was not tested, as it was clear from the start that no mechanism is present in the model that can produce this result.

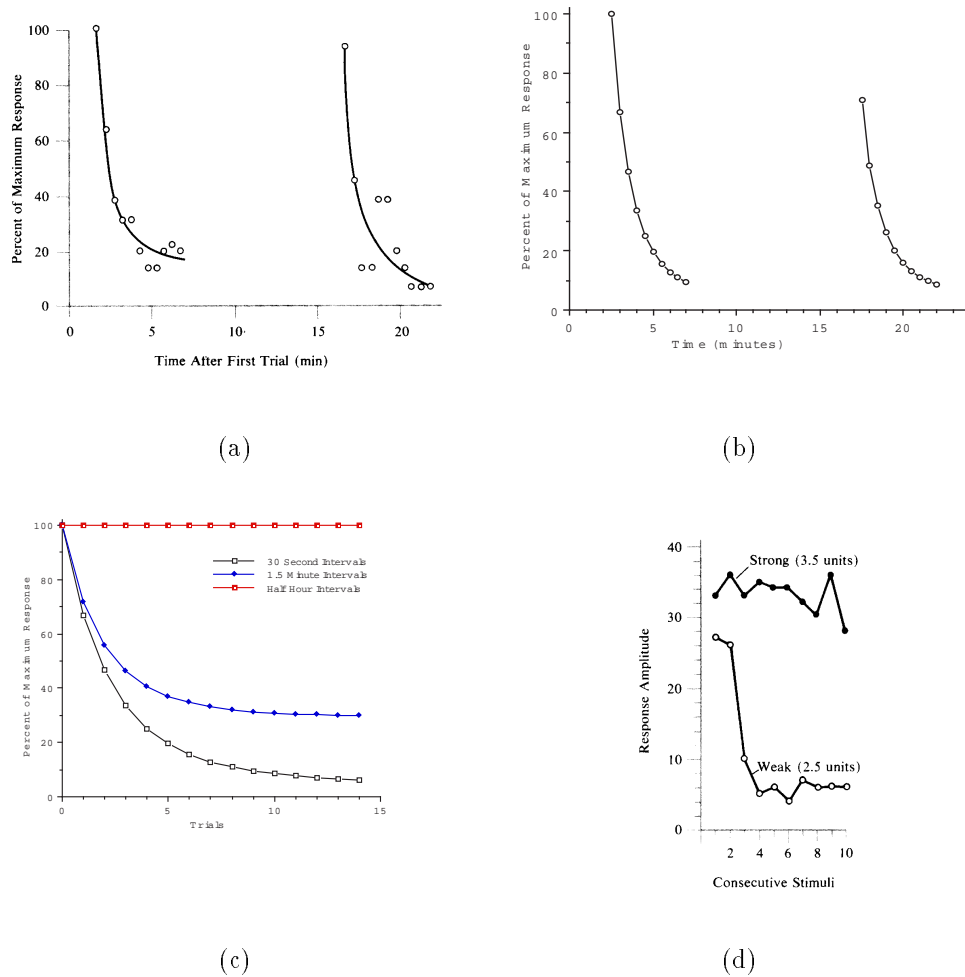


**Figure 3-8:** Results of habituation experiments. (a) Habituation, recovery, and rehabituation in Aplysia, using a 30 second intertrial interval and a 10 minute rest after the 10th trial (from [27, page 544]). (b) Habituation in the model using the same experimental protocol. (c) Habituation in the model with three different inter-trial intervals. (d) Degree of habituation found in Aplysia with different stimulus strengths (from [27, page 545].)

**Discussion** The conceptual model used by neuroscientists is unable to explain the experimental data on habituation without hypothesizing a more complex set of  $\text{Ca}^{++}$  channel states.

The time course of habituation and recovery in this model is determined by  $K_N$  and  $\tau_N$ . These parameters were selected so that the model would match the time course of a single habituation experiment well. However, the results of experiments using different inter-trial intervals produce different estimates of the parameter values. In particular, longer inter-trial intervals result in larger estimates of the recovery time constant. Also, the observed time course of recovery follows a roughly exponential curve, but the tail of the curve is much longer than would be obtained if the recovery rate were constant (as can be seen in Figure 3-7).

In addition to the complexities in the recovery time, the model is unable to reproduce the experimentally observed enhancement of the habituation response during rehabituation after a recovery period.

These observations may indicate the presence of a multi-stage recovery process, where the channel is more susceptible to long-term inactivation in some later recovery stage.

One way to model this would be to use a more complex model of the  $\text{Ca}^{++}$  channels. A channel that has two or more inactive states with different recovery time constants, for example, could explain both the observed recovery curve and the enhancement of channel inactivation during rehabituation.

An increased susceptibility to long-term inactivation during the late phase of recovery could then be used to explain the presence of habituation with a half-hour inter-trial interval. Long-term inactivation would reduce the pool of  $\text{Ca}^{++}$  channels participating in rapid recovery, which would shift the entire habituation curve downward.

The decrease in habituation observed with strong stimuli also cannot be reproduced with this simple habituation mechanism. In fact, the model predicts greater habituation for strong stimuli, not less. The biological effect may be the result of unmodelled connections from the sensory neurons onto the facilitator neuron. When strong stimuli are used, these connections could produce indirect sensitization of the synapse from the sensory to the motor neuron.

### Sensitization

The following experiments, taken from the *Aplysia* literature, were used to evaluate the model's sensitization response.

1. In a fully habituated synapse receiving sensory stimulation at 10 second intervals, a facilitating stimulus was presented at 6 Hz. for 10 seconds. This resulted in facilitation to 450% of the habituated response strength, which decayed over the course of an hour to about 150% of the habituated response. The time course closely matched the decay in cAMP over the first hour following

incubation with serotonin [28] (see Figure 3-9(a).)

2. A sequence of 13 stimuli was presented at 1.5 minute intervals, followed by a strong sensitizing stimulus,<sup>18</sup> followed by another 12 trials [27, page 551]. Sensitization following habituation caused a gradual increase in the response over the first 3 stimuli presented after the sensitizing stimulus before reaching a maximum.
3. Stimulus presentations at half hour intervals following sensitization shows a response that is initially almost double the baseline response. Sensitization decays over the course of four hours to match the level of habituation that would be found if sensitization had not occurred [30].

The sensitization parameters  $K_D$  and  $\tau_{cAMP}$  were determined using Experiment 1, and then tested with the protocols used in Experiments 2 and 3. Test results are shown in Figure 3-9.

**Discussion** The matching time course of decay of sensitization and of the cAMP concentration is cited as evidence for a correspondence between the two. However, because of the assumed nonlinear dependency between action potential duration and strength of the withdrawal response, the time course of the two would not necessarily be expected to match closely.

The observed EPSP shown in Figure 3-9(a) does not return to the baseline level, but instead stabilizes at approximately 150% of baseline. This may be evidence for the presence of long-term sensitization in this response.

The gradual increase in the strength of sensitization over the course of the first 5 minutes (see Figure 3-9) does not appear in the model. This observation may indicate that the dynamics of the cAMP-dependent cascade do, in fact, produce a significant delay. A more accurate model would include two or more stages in the chemical cascade from the serotonin receptor to the  $K^+$  channel.

As is the case with habituation, there is some disagreement between experiments on the duration of the period over which the cAMP concentration is elevated, and the corresponding duration of the sensitization response.

### Associative Learning

The following *Aplysia* experiments were used to evaluate associative learning in the model.

1. A train of 6 spikes at 10 Hz. (the CS) was immediately followed by a puff of serotonin (the US) one second in duration. cAMP levels were measured at four

---

<sup>18</sup>The exact magnitude of the sensitizing stimulus is not specified.

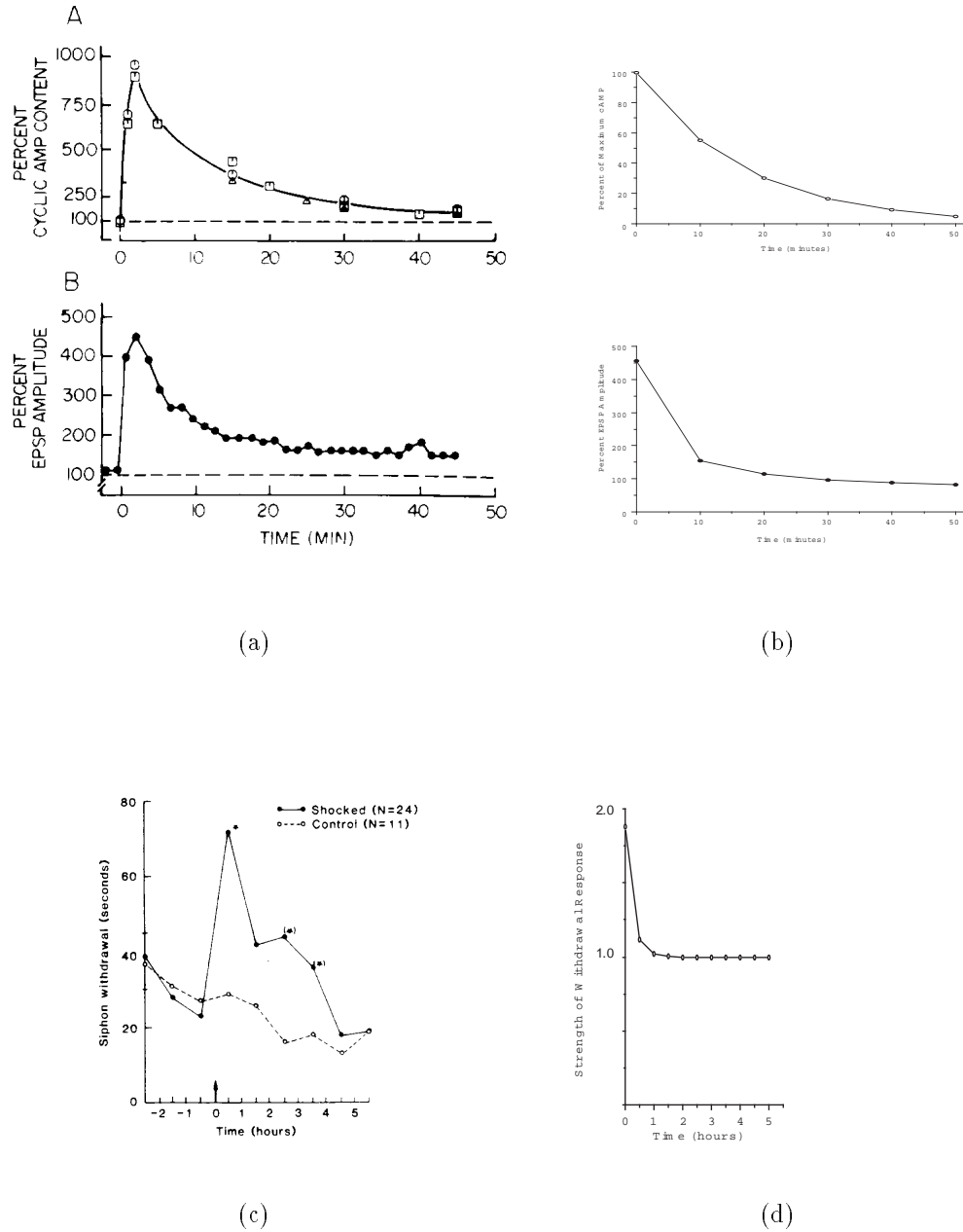


**Figure 3-9:** Results of sensitization experiments. (a) Time course of cAMP concentration decay and strength of motor neuron EPSP using 10 second inter-trial intervals (from [28, page 51].) (b) Model behavior using same experimental protocol as in (a). (c) Decay of sensitization of gill withdrawal reflex following the protocol described in Experiment 3 (from [30, page 435].) (d) Model behavior using same experimental protocol as in (c).

times the concentration found when an unpaired serotonin puff was used [1, page 228].

2. A weak tactile stimulus in the intact animal was followed immediately by a strong unconditioned stimulus, in 15 training trials at a 5-minute inter-trial interval, followed by a 30 minute rest period. The strength of the withdrawal response was compared to a control group in which the conditioned stimulus was presented 2.5 minutes after the unconditioned stimulus. The strength of the unpaired response was approximately 1.7 times the pre-test response, whereas the associative response was over 4 times the pre-test response (measured in terms of duration of gill withdrawal) [1, page 217].
3. In *Aplysia*, with a sequence of 5 training trials at 5 minute intervals, the strength of associative learning stabilized at 300% of the initial response [8]. Response strength was measured at 5 minute intervals, offset from the training trials by 2.5 minutes. Results of this experiment in CS+ (paired stimuli at 600 msec ISI), CS- (CS follows US by 2 minutes), and sensitization only conditions is shown in Figure 3-10(a).
4. In five training trials at 5 minute intervals, a train of 6 spikes at 10 Hz. was administered to a sensory neuron, immediately followed by a strong tail shock. Again, a control neuron was stimulated 2.5 minutes after the tail shock. An hour after the training trials, the motor neuron EPSP in response to the associated sensory stimulus was nearly double its pre-test amplitude, whereas the response to the control neuron showed no facilitation [1, page 221].

The value of the parameter  $K_{cAMP}$  was set to match the difference in cAMP levels observed in Experiment 1. The resulting value was  $K_{cAMP} = 13.5$ . The model behavior was then tested using the other experiments listed.

The values for the reflex strength obtained using the protocol described in Experiment 2 were 1.4 and 1.8, respectively. Results of Experiment 3 are shown in Figure 3-10(b). Experiment 4 was not run, because the strength of the associative response after half an hour in Experiment 3 was already well below the value observed after one hour in Experiment 4.

**Discussion** Most of the inaccuracies in the modelling of associative learning could be resolved by increasing the time constant for the cAMP concentration decay. The experimentally observed value of this parameter is reported as anywhere from about twenty minutes to an hour in different experiments. A time constant of an hour or more would be necessary to match data on the persistence of associative learning, whereas the time constant measured in sensitization experiments is around ten to twenty minutes. Part of this difference may be explained by the slow onset of long-term learning over the time period in which the short-term response decays. However,

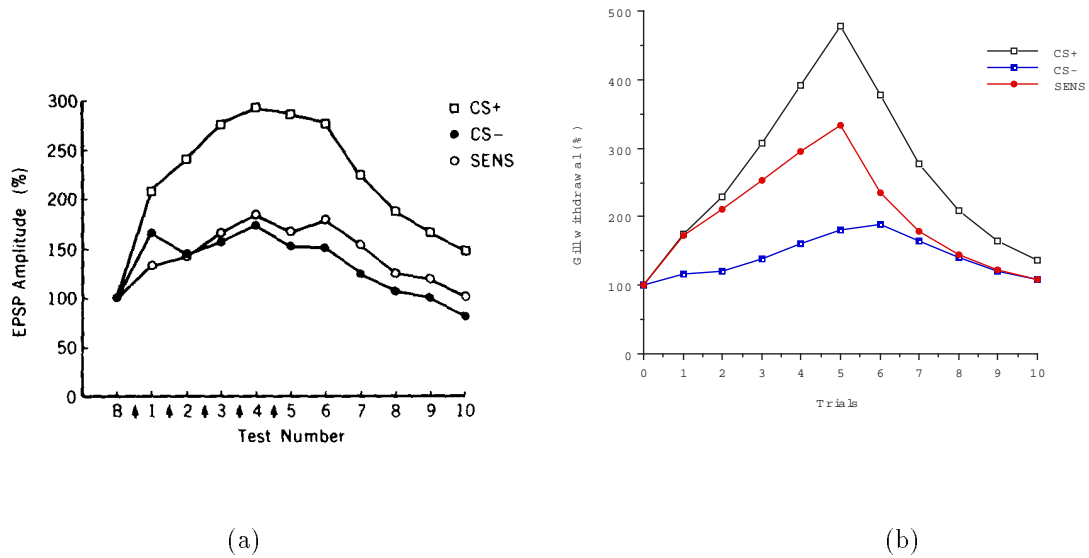


**Figure 3-10:** Results of associative learning experiment, showing 5 training trials followed by a sequence of test trials. (a) Strength of gill withdrawal (as percent of initial strength) in Aplysia in CS+, CS-, and sensitization only test conditions (from [8, page 66].) (b) Model behavior using same experimental protocol.

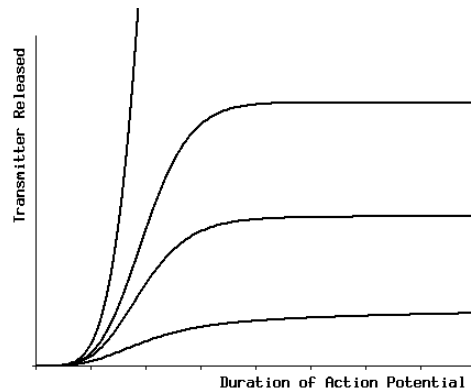


**Figure 3-11:** Effect of vesicle depletion on transmitter release. Each curve is for a different value of  $[V](t_0)$ ; the value of  $k_1[V](t_0)$  is kept constant.

if the presence of a  $\text{Ca}^{++}$ -calmodulin bond increases the duration of adenylate cyclase activity as well as its amplitude, this could also explain the increased time constant observed with associative learning.

In Experiment 3, the strength of associative learning appears to stabilize at around 300% of the baseline reflex strength. The model presented in [8] matches this result. They hypothesize that this is because a steady-state concentration of cAMP is reached. This would result if the decay in cAMP concentration between trials matches the influx during a trial.

The parameters used in this model for cAMP production and decay, which are based directly on experimental data, will saturate at a point where the action potential duration is approximately three times as long as the baseline duration. This would produce saturation of the motor response at 300% *only if* a first-order relationship between  $\text{Ca}^{++}$  influx and transmitter release is used. However, as explained in Section 3.2.3, experimental evidence suggests that this relationship is higher order.

As the duration increases, the relationship between it and transmitter release will gradually become linear; however, a 200% increase in transmitter release occurs with about a 25% increase in action potential duration, which is far from saturating either this reaction or the cAMP production process.

Another obvious candidate for explaining the saturation of the associative response is depletion of the available pool of vesicles. In this model, the vesicle pool is assumed to be of constant size, so this effect is not modelled. Figure 3-11 shows the effect of vesicle depletion on transmitter release, for different initial concentrations of vesicles.

### 3.2.3 Derivation of Chemical Interactions

The details of the chemical reactions involved in classical conditioning in *Aplysia* have a significant effect on the observed macroscopic behavior. Two of these reactions are

analyzed below.

### Calcium Influx and Transmitter Release

The dependency of transmitter release on  $\text{Ca}^{++}$  influx believed to be fourth order [27].<sup>19</sup> This makes the synapse highly sensitive to small changes in the  $\text{Ca}^{++}$  concentration during an action potential. The resulting dependency between transmitter release and action potential duration can be as high as fifth-order, as derived below. In experimental observations, a 20% increase in the duration of the action potential can double the size of the EPSP [1, page 224].

Other models [8, 20] assume a first-order dependency of transmitter release on action potential duration, which is incompatible with this experimental result. With a fifth order dependency, the maximum EPSP amplitude in the experiment shown in Figure 3-9(a) requires only a 35% increase in action potential duration to obtain, whereas with a first-order dependency a more than fourfold increase would be required.

To establish the relationship between action potential duration,  $\text{Ca}^{++}$  influx, and transmitter release, we must make certain assumptions about the dynamics of the underlying chemical reactions. The simplest form for modelling a fourth-order chemical reaction is:



where V is one vesicle of transmitter, and R is one vesicle of transmitter released into the synaptic cleft. The corresponding differential equation is

$$\frac{d[\text{R}](\tau)}{d\tau} = k \cdot [\text{V}](\tau) \cdot ([\text{Ca}](\tau))^4 \quad (3.12)$$

The variable  $\tau$  is used to represent the (continuous) time period over which an action potential occurs, as distinct from the discrete time  $t$  at which it appears in the simulation.

As vesicles are released into the synaptic cleft, the vesicle concentration  $[\text{V}](\tau)$  will decrease, but we assume here that it remains relatively constant over the course of a single action potential.<sup>20</sup>

Because  $\text{Ca}^{++}$  calmodulin bonds form so quickly, it is assumed that the free  $\text{Ca}^{++}$  concentration during an action potential is proportional to the rate of  $\text{Ca}^{++}$  influx, and does not build up over time.<sup>21</sup>

---

<sup>19</sup>That is, four  $\text{Ca}^{++}$  ions must bond with each vesicle of transmitter in order to release it into the synaptic cleft.

<sup>20</sup>The reduction in  $[\text{V}](t)$  does, however, play a role in synaptic depression after extended activity [8], and may explain part of the mismatch between the behavior of this model and the experimental results shown in Figure 3-10.

<sup>21</sup>This assumption is also made by both [8] and [20].

$$[I_{Ca}](\tau) = \begin{cases} [I_{Ca}](t) & 0 < \tau < D(t) \\ 0 & \text{otherwise} \end{cases} \quad (3.13)$$

and the solution for transmitter release is therefore:

$$\begin{aligned} [R](t) &= \int_0^{D(t)} k[V] \cdot ([I_{Ca}](t))^4 d\tau \\ &= k[V] \cdot ([I_{Ca}](t))^4 \cdot D(t) \end{aligned} \quad (3.14)$$

This equation, though it is fourth order with respect to the  $Ca^{++}$  concentration, is first-order with respect to the action potential duration: this result does not give us the observed sensitivity to small changes in action potential duration.

This apparent contradiction can be resolved, however, by modelling the chemical reaction in greater detail. The hypothesized mechanism for transmitter release involves four bonding sites between  $Ca^{++}$  and each vesicle of transmitter. Transmitter will be released when a single vesicle has all four bonding sites filled. This reaction has several intermediate forms, with vesicles forming 1, 2, or 3  $Ca^{++}$  bonds. If we assume that the bonds form independently, then the probability of transmitter release from a vesicle  $V$ , with four binding sites  $\{V_1..V_4\}$ , is

$$\mathbf{P}[V_i \text{ filled}] = \frac{[V_f]}{[V_f] + [V_o]} = \frac{[V_f]}{4[V]} \quad (3.15)$$

$$\begin{aligned} \mathbf{P}[R] &= \mathbf{P}[V_1 \text{ filled}] \wedge \mathbf{P}[V_2 \text{ filled}] \wedge \mathbf{P}[V_3 \text{ filled}] \wedge \mathbf{P}[V_4 \text{ filled}] \\ &= \left( \frac{[V_f]}{4[V]} \right)^4 \end{aligned} \quad (3.16)$$

where  $[V_o]$  is the concentration of open bonding sites, and  $[V_f]$  is the concentration of filled bonding sites.

Averaging over the population of vesicles, we get the following equation for transmitter release:

$$\frac{d[R](\tau)}{d\tau} = \left( \frac{[V_f](\tau)}{4[V]} \right)^4 \quad (3.17)$$

$$[R](t) = \int_0^{D(t)} \left( \frac{[V_f](\tau)}{4[V]} \right)^4 d\tau \quad (3.18)$$

The bonding reaction can be described by the following equation:



where  $\text{V}_o$  is one open bonding site, and  $\text{V}_f$  is one filled site. The differential equations for this reaction are

$$\frac{d}{d\tau}[\text{V}_f](\tau) = k_1[\text{I}_{\text{Ca}}](t) \cdot [\text{V}_o](\tau) - k_2 \cdot [\text{V}_f](\tau) \quad (3.20)$$

$$\frac{d}{d\tau}[\text{V}_o](\tau) = -[\text{V}_f](\tau) \quad (3.21)$$

If we assume that all bonds  $\text{V}_f$  decay between one action potential and the next, then  $[\text{V}_f](0) = 0$ ,  $[\text{V}_o](0) = 4[\text{V}]$ , and  $[\text{V}_o](\tau) = 4[\text{V}] - [\text{V}_f](\tau)$ . In this case, the equation for  $[\text{V}_f](\tau)$  becomes

$$\frac{d}{d\tau}[\text{V}_f](\tau) = 4k_1[\text{V}][\text{I}_{\text{Ca}}](t) - (k_1[\text{I}_{\text{Ca}}](t) + k_2)[\text{V}_f](\tau) \quad (3.22)$$

$$[\text{V}_f](\tau) = \frac{4k_1[\text{V}][\text{I}_{\text{Ca}}](t)}{k_1[\text{I}_{\text{Ca}}](t) + k_2} (1 - e^{-(k_1[\text{I}_{\text{Ca}}](t) + k_2)\tau}) \quad (3.23)$$

and the transmitter released during an action potential is

$$\begin{aligned} [\text{R}](t) &= \int_0^{\text{D}(t)} \left( \frac{[\text{V}_f](\tau)}{4[\text{V}]} \right)^4 d\tau \\ &= \left( \frac{k_1[\text{I}_{\text{Ca}}](t)}{k_1[\text{I}_{\text{Ca}}](t) + k_2} \right)^4 \int_0^{\text{D}(t)} (1 - e^{-(k_1[\text{I}_{\text{Ca}}](t) + k_2)\tau})^4 d\tau \end{aligned} \quad (3.24)$$

Although it is possible to solve this equation exactly, it is more informative to look at the two limiting cases, when the time constant  $(k_1[\text{I}_{\text{Ca}}](t) + k_2)^{-1} \ll \text{D}(t)$  and when  $(k_1[\text{I}_{\text{Ca}}](t) + k_2)^{-1} \gg \text{D}(t)$ . In the former case,  $[\text{V}_f](\tau)$  will saturate very quickly relative to the duration of the action potential, and can be approximated as constant. Equation 3.24 then becomes:

$$\begin{aligned} [\text{R}](t) &\approx \left( \frac{k_1[\text{I}_{\text{Ca}}](t)}{k_1[\text{I}_{\text{Ca}}](t) + k_2} \right)^4 \int_0^{\text{D}(t)} d\tau \\ &= \left( \frac{k_1[\text{I}_{\text{Ca}}](t)}{k_1[\text{I}_{\text{Ca}}](t) + k_2} \right)^4 \cdot \text{D}(t) \end{aligned} \quad (3.25)$$

This corresponds to the case where bonds either form or decay very quickly. Note that the dependence of transmitter release on  $[I_{Ca}](t)$  in this case depends on the relative speed of the two reactions; if  $[I_{Ca}] \ll k_2/k_1$ , then transmitter release is fourth order relative to  $[I_{Ca}]$  (this corresponds to the solution given in Equation 3.14), whereas if  $[I_{Ca}] \gg k_2/k_1$ , transmitter release is independent of small changes in the calcium concentration and depends only on action potential duration.

In the other limiting case, where both reaction rates are slow, we can do a linear approximation to the exponential, and Equation 3.24 simplifies to:

$$\begin{aligned} [R](t) &\approx \left( \frac{k_1[I_{Ca}](t)}{k_1[I_{Ca}](t) + k_2} \right)^4 \int_0^{D(t)} ((k_1[I_{Ca}](t) + k_2)\tau)^4 d\tau \\ &= \frac{(k_1[I_{Ca}](t))^4}{5} (D(t))^5 \end{aligned} \quad (3.26)$$

In this case, we have a fifth order relationship between  $[R](t)$  and the action potential duration, as well as a fourth order relationship with the  $Ca^{++}$  concentration.

The experimental data in *Aplysia*, where a very small percent increase in action potential duration produces a large percent increase in the motor neuron EPSP (which presumably results from a large percent increase in transmitter released) provides evidence supporting the claim that vesicle bonds both form and decay slowly relative to the duration of an action potential. This also implies that the proportion of vesicles released in a single action potential is small relative to the total number of vesicles available.

One consequence of a fifth order dependence of transmitter release on action potential duration, assuming that the relationship between cAMP and action potential duration is linear (which it may well not be), is that the learning rate<sup>22</sup> remains nearly constant even with large changes in synaptic strength.

### Determining the ISI Effect

In studies of associative learning in *Aplysia*, the measured effect of the inter-stimulus interval on learning reaches a maximum at 0.5 seconds, and decays to about 25% of its maximum value after 2 seconds [1].

A possible functional reason for the delayed onset of the associative response could be to prevent the sensory neuron from learning that it is a predictor of itself. This could occur if the sensory neuron stimulates a facilitator interneuron that, in turn, makes contacts with the sensory neuron's presynaptic terminals. Facilitator

---

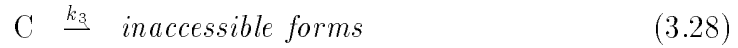
<sup>22</sup>The learning rate is defined as the percent increase in synaptic strength resulting from a single paired stimulus presentation. In the model, this increase is proportional to the total  $Ca^{++}$  influx during a sensory neuron action potential. With a higher-order dependency on action potential duration, only a small increase in  $Ca^{++}$  influx is necessary to potentiate the synapse.

interneurons exhibit recurrent inhibition [21], firing only at the onset of a sustained input. If interneuron firing ceases within a fraction of a second, the delay in the ISI effect will be sufficient to prevent auto-association.

Hawkins's model [20] uses a 10 second time step, which is sufficient to model the learning phenomena at a very rough scale, but prevents accurate modelling of ISI effects. In Byrne's model [8], where the associative response is directly proportional to the  $\text{Ca}^{++}$  concentration, the maximum response is reached almost immediately after an action potential and decays exponentially thereafter.

In the model presented here, the strength of the associative learning response is proportional to the increase in cAMP caused by bonds between  $\text{Ca}^{++}$ -calmodulin and adenylate cyclase. Its time course is determined by the dynamics of the interactions between  $\text{Ca}^{++}$ , calmodulin, and adenylate cyclase. Bonding between  $\text{Ca}^{++}$  and calmodulin is assumed to be essentially instantaneous, so that the dynamics of formation and dissolution of the  $\text{Ca}^{++}$ -calmodulin-adenylate cyclase bonds and the decay of the  $\text{Ca}^{++}$ -calmodulin concentration are the primary factors involved in determining the ISI.

The bonding reaction is



where A is adenylate cyclase, C is  $\text{Ca}^{++}$ -calmodulin, B is the  $\text{Ca}^{++}$ -calmodulin-adenylate cyclase complex, and  $k_1$ ,  $k_2$  and  $k_3$  are the rate constants for the various reactions. The second equation represents the removal of  $\text{Ca}^{++}$ -calmodulin from the synapse, through a combination of diffusion, uptake into intracellular structures, and expulsion of  $\text{Ca}^{++}$  from the cell through an ion pump.<sup>23</sup>

The resulting equations for the dynamics of the reactions are

$$\frac{d[B](t)}{dt} = k_1[C](t) \cdot [A](t) - k_2[B](t) \quad (3.29)$$

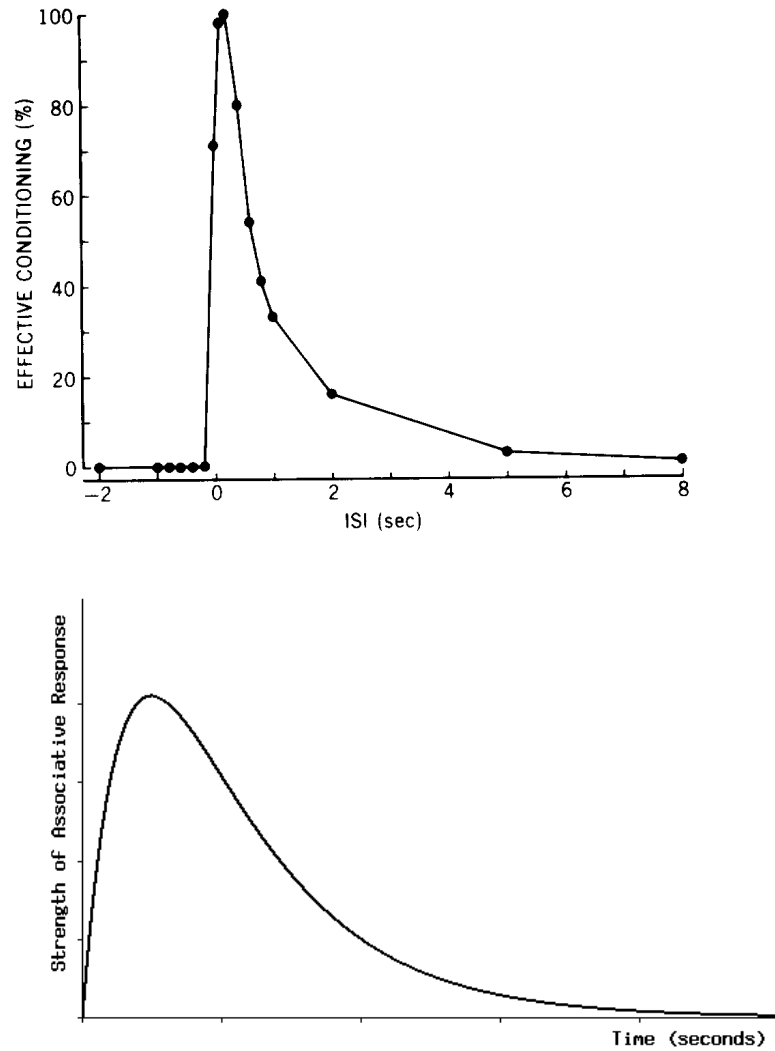
$$\frac{d[A](t)}{dt} = -k_1[C](t) \cdot [A](t) + k_2[B](t) \quad (3.30)$$

$$\frac{d[C](t)}{dt} = -k_1[C](t) \cdot [A](t) + k_2[B](t) - k_3[C](t) \quad (3.31)$$

If we assume that there is an excess of adenylate cyclase in the system, so that only

---

<sup>23</sup>These mechanisms for  $\text{Ca}^{++}$  uptake may have different time constants, but it is assumed here that one rate dominates.



(b)

**Figure 3-12:** The ISI effect resulting from a simple  $\text{Ca}^{++}$  concentration dependency decays exponentially as the delay between the CS and the US increases. Two alternative models are shown here. a) ISI effect seen in Byrne's model, which has a simple dependency on the  $\text{Ca}^{++}$  concentration, but achieves a slight delay (170 msec.) in the peak response by modelling  $\text{Ca}^{++}$  diffusion within the synapse (from [8, page 69].) (b) ISI effect obtained with the two-stage reaction used in my model.

a small amount is bound by  $\text{Ca}^{++}$ -calmodulin at any given time, we can approximate this nonlinear system with the following linear one:

$$\frac{d[\text{B}](t)}{dt} = k_1[\text{A}] \cdot [\text{C}](t) - k_2[\text{B}](t) \quad (3.32)$$

$$\frac{d[\text{C}](t)}{dt} = -(k_1[\text{A}] + k_3)[\text{C}](t) + k_2[\text{B}](t) \quad (3.33)$$

The general solution to these equations is given in Equations 3.3 and 3.4, with parameter values of:

$$c_1 = \frac{[\text{B}](t_0) - a_2[\text{C}](t_0)}{(a_1 - a_2)} \quad (3.34)$$

$$c_2 = \frac{[\text{B}](t_0) - a_1[\text{C}](t_0)}{(a_2 - a_1)} \quad (3.35)$$

and, defining  $a = (k_1[\text{A}] + k_2)/2$ ,

$$m_1 = -a + \sqrt{a^2 - k_2 k_3} \quad (3.36)$$

$$m_2 = -a - \sqrt{a^2 - k_2 k_3} \quad (3.37)$$

$$a_1 = \frac{m_1 + k_1[\text{A}] + k_3}{k_2} \quad (3.38)$$

$$a_2 = \frac{m_2 + k_1[\text{A}] + k_3}{k_2} \quad (3.39)$$

In the case encountered in the learning trials,  $[\text{B}](t_0) = 0$ , so

$$[\text{B}](t) = K (e^{m_1(t-t_0)} - e^{m_2(t-t_0)}) \quad (3.40)$$

$$K = [\text{C}](t_0) \frac{a_1 a_2}{a_2 - a_1} \quad (3.41)$$

This function reaches its maximum at

$$\frac{d[\text{B}](t_{max})}{dt} = 0$$

$$\begin{aligned}
0 &= K (m_1 e^{m_1(t_{max}-t_0)} - m_2 e^{m_2(t_{max}-t_0)}) \\
t_{max} - t_0 &= \frac{\ln |m_1| - \ln |m_2|}{m_2 - m_1}
\end{aligned} \tag{3.42}$$

To get a maximum at 0.5 seconds, and a decay to 25% of its maximum at 2 seconds, we must set  $m_1$  and  $m_2$  according to the following equations:

$$\begin{aligned}
[B](t_0 + 2) &= 0.25 [B](t_0 + 0.5) \\
e^{2m_1} - e^{2m_2} &= 0.25 (e^{0.5m_1} - e^{0.5m_2})
\end{aligned} \tag{3.43}$$

and

$$\frac{\ln |m_1| - \ln |m_2|}{m_2 - m_1} = 0.5 \tag{3.44}$$

Solving these equations gives us the following parameter values, which are used in the simulation:

$$\begin{aligned}
m_1 &= -2.93 \\
m_2 &= -1.28 \\
a_1 &= -0.34 \\
a_2 &= 0.52 \\
k_2 k_3 &= 3.76 \\
k_1[A] &= 4.22 - \frac{3.76 + k_2^2}{k_2}
\end{aligned}$$

For the value of  $k_1[A]$  to be positive,  $k_2 k_3$  must fall within a fairly narrow range.

$$\begin{aligned}
1.28 &< k_2 < 2.93 \\
1.28 &< k_3 < 2.93
\end{aligned}$$

The maximum value for  $k_1[A]$  that matches the experimental results is 0.34, at  $k_2 = k_3 = 1.94$ . Using this value for  $k_1[A]$ , and starting with  $[B](t_0) = 0$ , the maximum concentration of bonds (at an inter-stimulus interval of 0.5) is  $[B]_{max} = 0.06[C](t_0)$ , which means we must have  $[A] \gg 0.06[C](t_0)$ , and  $k_1 \ll 5.7[C](t_0)^{-1}$ , for our first-order approximation to be valid.

If  $[A]$  is not sufficiently high, the system will saturate, and much of the available adenylate cyclase will be used up. The effect on the strength of the associative response is shown in Figure 3-13.

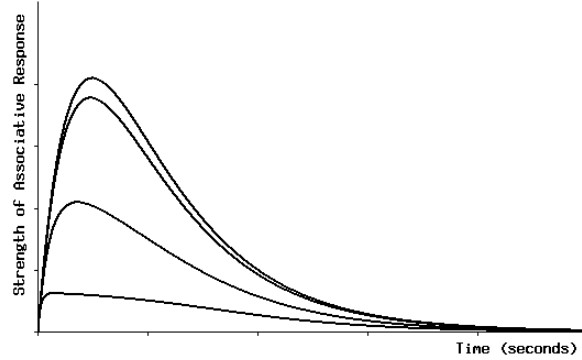


**Figure 3-13:** Nonlinear distortion of ISI when adenylate cyclase concentration is low. The value of  $k_1[A](t_0)$  is kept constant. The uppermost curve is without saturation; the saturated curves are (in descending order) for  $[A](t_0) = .5[C](t_0)$ ,  $[A](t_0) = .05[C](t_0)$ , and  $[A](t_0) = .01[C](t_0)$ .

The numeric parameters used here are specific to the mechanism which determines the strength of the associative learning response. However, the general form of the equations is common to many processes that involve chemical second messengers. For these equations to apply, two conditions must hold: the activation of the protein complex must be dependent on the continued presence of the second messenger, and the concentration of the second messenger must decay at a regular rate.

### 3.3 Summary

Traditional computational models of neurons consider only two time scales: the very fast time scale of the cell's electrical responses, and the "permanent" changes which result from long-term learning. A few exceptions can be found in real-time models of reinforcement learning (e.g. [2, 62, 63]), where an exponentially decaying internal memory trace is used to model the effect of the ISI on the learning response. The mechanisms found in *Aplysia's* synapses, however, demonstrate the presence of an wide range of processes acting at different time scales which have a significant impact on the synaptic strength, and therefore on the computational properties, of the reflex circuit.

These mechanisms can be broken down into distinct categories based on their time course. Electrical responses and the dynamics of transmitter release are very fast, taking place on a millisecond time scale. The chemical processes which determine the ISI effect take place on a time scale of a few seconds, while short-term learning operates on a time scale of minutes to hours. Long-term learning in *Aplysia*, which is not modelled here, occurs over the course of several hours and lasts for at least several

weeks. Processes operating at similar time scales can have complex interactions, whereas a large difference in time scales leads to a decoupling of effects.

Both calcium ions ( $\text{Ca}^{++}$ ) and cyclic AMP are important mediators of *Aplysia*'s learning responses. These chemicals are used throughout the animal kingdom as cellular *second messengers*, controlling many different metabolic processes [50]. Processes similar to those modelled here may therefore play a role in many different aspects of neural computation.

The model presented in this chapter reveals the importance of understanding the underlying chemical dynamics in *Aplysia*'s synapses in order to model the macroscopic behavior of the circuit for the gill withdrawal reflex. Two specific processes, which control the dynamics of transmitter release and of the ISI effect, are examined in detail.

The results of testing the model against data from biological experiments reveal enough similarity to support the claim that these mechanisms play an important role in conditioning of the reflex, but they also differ in many details. The differences may be due to as yet undetected complexity in the underlying chemistry or to the contribution of parts of the reflex circuit that are not modelled.



## **Part II**

# **Topographic Map Formation in the Visual System**



## Chapter 4

# A Model of Topographic Map Formation

Topographically ordered projections from one region to another are a prominent feature in the brain. The presence of such maps has been known since the 1920's [31], when the spatial locations of electrical responses to sensory stimulation in the somatosensory cortex were discovered to lie in an orderly arrangement relative to the location of the stimulated body part. These maps have since been found throughout the brain.

The process of map formation in embryonic and early childhood development has been most extensively studied in the visual system, in projections from the retina to the thalamus and superior colliculus, and in projections from the thalamus to the primary visual cortex [66]. These connections form over long distances, and initially they are highly disordered. After the initial axonal projections form, they sort themselves over time to produce a detailed topographic correspondence between the retinal image and the image in the target structure. This map formation process makes use of a variety of chemical and electrical mechanisms.

A simulated model of the effects of chemical and activity-dependent mechanisms in topographic map formation is presented in this chapter. These mechanisms work together to allow rapid and robust development of detailed maps. This model resolves a number of difficulties found in previous modelling attempts. These difficulties include controlling the final map orientation, attaining rapid convergence without loss of map continuity, and demonstrating a biologically plausible mechanism that produces the necessary coactivation pattern between source and target structures during activity-dependent map formation.

Experimental results on the ability to form rough, but not refined, maps in the absence of electrical activity, expansion of heavily stimulated areas, and map expansion and contraction following lesions are matched by this model. Although a highly simplified neural model is used, the goal is to explore organizational principles of biological development, so some care is taken to remain compatible with experimental

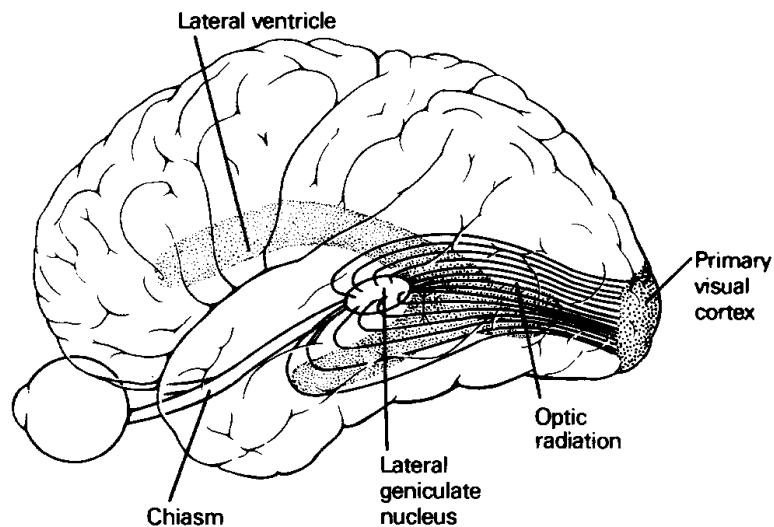


**Figure 4-1:** Axonal projections between brain structures in the early visual system. During development, these projections sort themselves to produce topographic mappings between the retina, the lateral geniculate nucleus of the thalamus, the superior colliculus (not shown), and the primary visual cortex (from [31, page 363].)

results and with what is known about the underlying biological mechanisms.

## 4.1 Introduction

The motivation for this work comes from recent experimental findings about biological mechanisms that give rise to topographic map formation. A variety of such mechanisms have been studied in the early visual system, including the maintenance of axonal order within the optic tract, positional labelling via chemical markers, and activity-dependent synaptic plasticity [66].

The presence of chemical markers guiding map formation has been demonstrated in a variety of experimental preparations [66, 59]. Although some early researchers believed these markers might be sufficient to fully specify the final mapping, in practice this does not seem to be true. Evidence for the presence of other mechanisms comes partly from studies of expansion and compression of maps following changes in input activity or after lesions. Experiments described in [60] point to electrical activity in particular as an important contributor to map formation. In this study, blocking activity during development prevents the formation of a refined topographic map, although rough maps still appear.

The bulk of experimental evidence, therefore, points to cooperation among a va-

riety of mechanisms, physical, chemical, and activity-dependent, for the formation and maintenance of topographic maps. Previous computational models, however, have attempted to find a single unified map formation process, and fail to exploit the advantages of combining multiple mechanisms.

## 4.2 Previous Models of Map Formation

There are four major problems to be overcome by any functional model of biological map formation. These are specifying the orientation of the map, maintaining global as well as local continuity, attaining a rapid convergence rate, and specifying a biologically plausible implementation.

Willshaw and von der Malsburg [68] simulated an early activity-based model. It solves the problems of map orientation and continuity, but requires the presence of a nucleation region in which the initial axonal connections are fully specified. Because of the need for a nucleation region, the process converges very slowly. There is no biological evidence for such a region. Their marker-based model [67] solves most of these problems, but does not match recent experiments establishing the dependence of the process on electrical activity.

Other activity-based models have been based on Kohonen's mapping algorithm [36, 37]. This model is mathematically successful, but is not well grounded in biology. The input to his algorithm is a vector specification of a single point in the input space, rather than a pattern of activity<sup>1</sup> over that space (which corresponds to the input cell layer), as is found in biology. The final map orientation is random, and the algorithm assumes a specific activity pattern in the target map without considering how that pattern could result from a biological process.

More recent modelling efforts have concentrated on the formation of ocular dominance and orientation columns, but some have included map formation as well. Obermayer [51] uses a variant of the Kohonen algorithm which demonstrates map formation using a biological input representation. Miller's model [47] displays activity-dependent map refinement, but the initial topography is fully specified, and axonal arbors narrow over time around a fixed location.

## 4.3 The Model

The model described in this paper is based on the following (biologically motivated) description of the developmental process: initial synaptic contacts from the source (presynaptic) cell layer are formed over a broad region in the target (postsynaptic) layer. Varying concentrations of chemical markers across the surface of the maps

---

<sup>1</sup>An activity pattern is the strength of activation of the neurons, as a function of their location in the map.

determine the affinity of synapses between particular source and target regions. This chemoaffinity provides a rough initial mapping.

Although some form of chemoaffinity has been found in all biological systems studied, the details vary considerably from one system to another. Instead of modelling the details of a particular chemical mechanism, therefore, an attempt is made to determine what constraints all chemical mechanisms must satisfy to ensure a correct and detailed final map when combined with an activity-based refinement process. The chemical mechanisms are assumed to produce a rough map topography (possibly by the mechanism described in [67]), which is used to determine the initial connections between source and target layers. Chemical markers do not, in this model, play a role in the dynamics of the refinement process.

Activity-dependent mechanisms then act to refine the initial connections that result from chemoaffinity. Synapses are strengthened via a Hebbian mechanism that is patterned after long-term potentiation [34].<sup>2</sup>

The coactivation pattern driving these changes results from correlations in the activity of near neighbors in the source map, combined with short-range lateral activation in the target to increase the activity of near neighbors that receive strong source inputs. Correlated activity of neighboring neurons in the developing retina, prior to the maturation of photoreceptors, has been observed in rat [15, 41], and in cat and ferret [42]. The observed activity patterns consist of short correlated bursts of activity (lasting a few seconds) separated by relatively long periods of silence.

Synaptic growth is limited by competition between synapses projecting to the same target neuron. Competitive effects cause map expansion under heavy stimulation, and also cause the breaks in multiple uncorrelated source maps that result in ocular dominance column formation.

### 4.3.1 The Simulation

The simulation uses one-dimensional source and target layers to reduce computational complexity so that longer-range interactions can be studied. The algorithm does, however, generalize to two or more dimensions. Two types of synaptic connections are included, as shown in Figure 4-2: modifiable excitatory projections from the source layer to the target layer, and unmodifiable excitatory lateral connections within the target layer.

Chemical markers are assumed to be present in source and target maps in a linear concentration gradient over the surface of the map. The chemical concentration is assumed to be detectable by the growing axons with some finite error. These assumptions are used to determine the initial connectivity of the map, before the activity-dependent process begins. However, the simulation results are valid not only for this particular hypothesized mechanism but also for any other mechanism which

---

<sup>2</sup>See Appendix E for background on long-term potentiation.

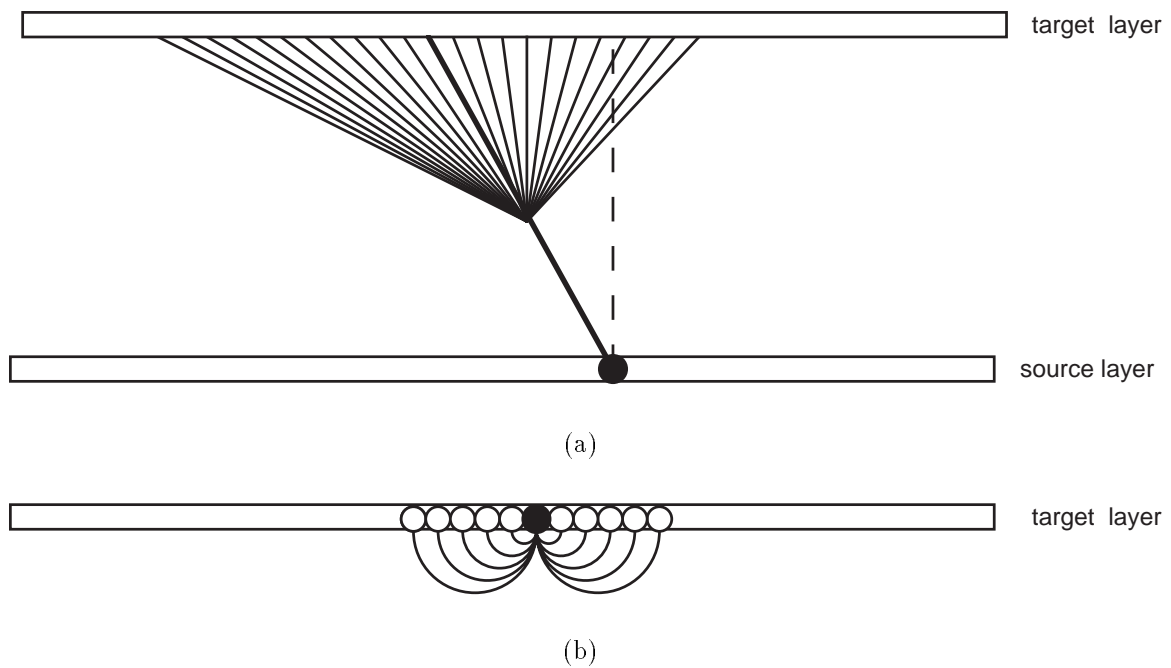


**Figure 4-2:** Connections used in the simulation. a) Modifiable projections from source (filled circles) to target (open circles) layers. The axonal arbor for a single source neuron is shown. b) Fixed-strength lateral connections within the target layer.

produces a similar pattern of connections. Initial connections from each source neuron cover a broad but finite region in the target, close to (and including) the desired final location.

Lateral connections are localized to a neighborhood around each cell, and their strength decreases as the distance between neurons increases.

Input activity is assumed to occur in spatially and temporally localized clusters of neurons. Each input activity cluster occurs at a random location within the source layer. For simplicity, all neurons within a cluster are given the same level of activity.

Each input activity cluster is simulated as a single “trial” of the learning algorithm. Within a trial, the source is activated, activation is spread through the target layer, and connection strengths are updated according to a learning rule which combines Hebbian learning (in the numerator) with input normalization as a competitive mechanism (in the denominator).

$$w_{ij}(T+1) = \frac{w_{ij}(T) + \alpha A_{ij}(T) o_i(T) a_j(T)}{\frac{1}{K} \sum_{j=0}^{m-1} (w_{ij}(T) + \alpha A_{ij}(T) o_i(T) a_j(T))} \quad (4.1)$$

$w_{ij}(T)$  is the connection strength between source neuron  $j$  and target neuron  $i$ ,  $\alpha$  is the learning rate,  $a_j$  and  $o_i$  are the source and target activity,  $A_{ij} = 1$  if there is a synapse between source  $j$  and target  $i$ , and 0 otherwise, and  $K$  is the “competition limit”, that is, the total synaptic strength over all inputs to a given target neuron.

The Hebbian component is assumed to arise from long term potentiation (LTP). The biological underpinnings of competition are not well understood, though some kind of competitive mechanism is necessary to explain experimental results such as expansion of a heavily stimulated map region [66].

### High-level Modelling of LTP

When using such a highly simplified neural model, some care is necessary to ensure that the model maintains some correspondence with its known biological underpinnings.

Other computational models ignore the transient response to an input stimulus, and instead use a hypothetical steady-state frequency response as the target activity. However, LTP, the best candidate for a biological form of Hebbian learning, operates at a very fast time scale, on the order of 100 msec.<sup>3</sup> The dynamics of the transient response is therefore critical, as the system does not have time to settle into steady-state within that time window.<sup>4</sup>

---

<sup>3</sup>For example, in the model of LTP described in [7], the strength of the LTP response is assumed proportional to the peak  $Ca^{++}$  concentration; their simulation shows this concentration peaking and subsiding within 100-200 msec. after presentation of the input stimulus.

<sup>4</sup>The LTP response assumed by this model is proportional to  $\int_0^\tau o_i(t)dt$ , for a time window of length  $\tau$ . Even if the response does reach steady state near the end of the time window, therefore,

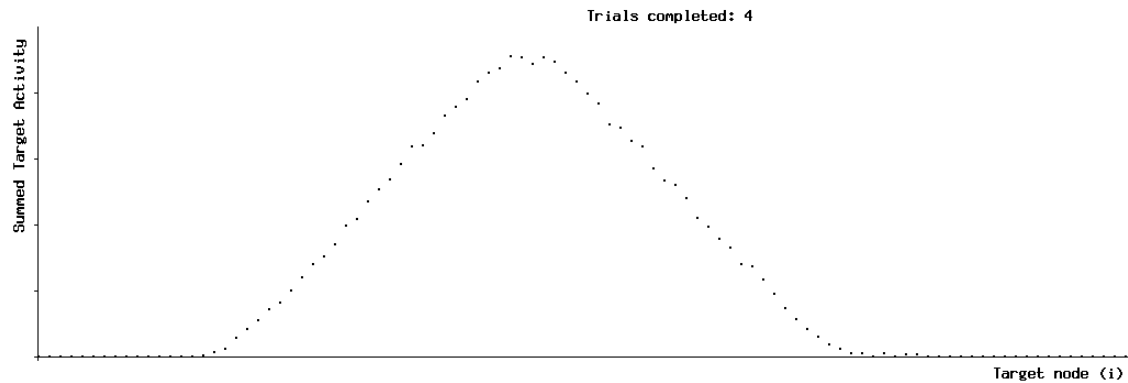


**Figure 4-3:** Typical target activity pattern in response to an input activity cluster.

In this model, the dynamics of the target response are simulated as follows:

1. Individual target neurons are modelled as simple thresholded elements. Their activation is a weighted sum of their inputs, and if it is above threshold they fire.
2. Each “trial” is divided into time steps. In each time step neurons whose input is above threshold fire a single action potential.
3. Inputs from the source layer arrive at the target neurons at the first time step of each trial, and initiate firing in neurons over some region.
4. Firing in the source layer ceases after the first time step, but activation continues to spread laterally in the target map. At each time step, inputs arrive through lateral connections from target neurons that fired in the previous time step. Lateral synaptic strengths are set in such a way that the active region in the target shrinks over time.
5. Activation is summed over the duration of the target response to get the activity  $o_i$  for learning.

If most of the cells within some region in the target layer are activated, the activity will die out in a wave moving inward from the edges of that region. Neurons in its center therefore remain active longest. The reasons for assuming this pattern of target activity are discussed in Section 4.5.

Parameters in this simulation were set to give maximum burst lengths of about 10-20 spikes. At 100 Hz., this response would last no more than 200 msec., which

---

the transient response will still dominate.

is of the same order of magnitude as the LTP time window. This gives us a rough approximation of the actual target activity that would result from this pattern of lateral connections. Mathematical details and parameter constraints are given in Section 5.1.

## 4.4 Results

Tests were run on one-dimensional source and target layers, with 100 neurons in each layer. The ends were wrapped around to reduce edge effects. The location of the input activity cluster for each trial was chosen at random in a uniform distribution over the input map. Each test ran for 10,000 trials.

In all cases, the final map orientation is correct, and the map is continuous at a global level. Convergence to the correct location is extremely fast, being essentially complete within 1000 trials (an average of ten presentations of each input cluster).

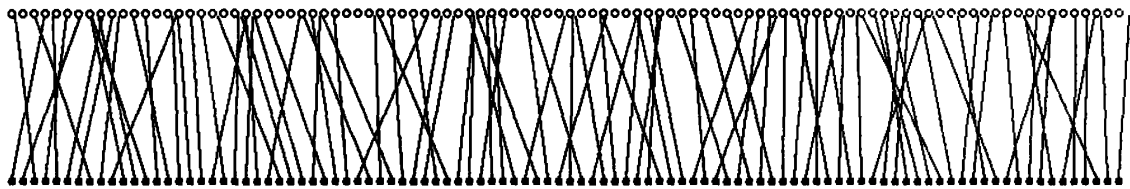
The centroid of the axonal projection from each source neuron, weighted by connection strength, is used as a measure of its “location” in the target layer; the maximum strength connection is generally very close to the centroid. Examples of initial and final maps are shown in Figure 4-4.

The average “spacing error”, the variance in distance between centroid locations of neighboring source cells, is used to evaluate the accuracy of the local ordering in the map. If these locations are equally spaced in the target, the spacing error will be zero. At large variances, projections may be “crossed”; that is, their centroid locations may be ordered differently in the target than the neurons are in the source.

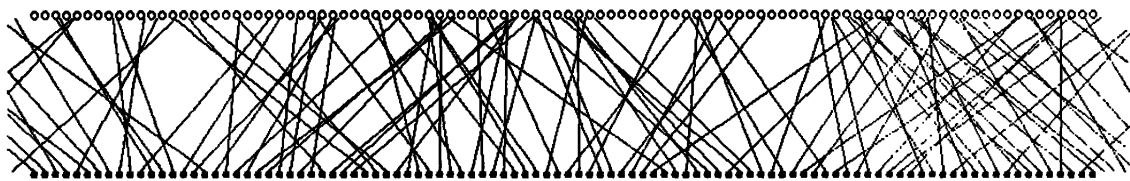
Figure 4-5 shows the results of two sets of tests. In one, the source activity cluster size is set at a constant, while the initial maximum position error of the projections is varied. The accuracy of the resulting map was found to be nearly independent of the position error, for values up to  $\pm 20$  neurons. Follow-on tests (results not shown) were done by doubling the size of the target layer (to 200 neurons) and using position errors of  $\pm 30$  and  $\pm 40$ . Again, the final result is near perfect, though it takes slightly longer to converge.

The second set of tests uses a fixed position error, and looks at the effect of the source activity cluster size. Larger cluster sizes converged more rapidly, and with the smallest cluster size (number of simultaneously active neurons = 2), the final map was somewhat disordered. Reasons for this are discussed in Section 4.5.1.

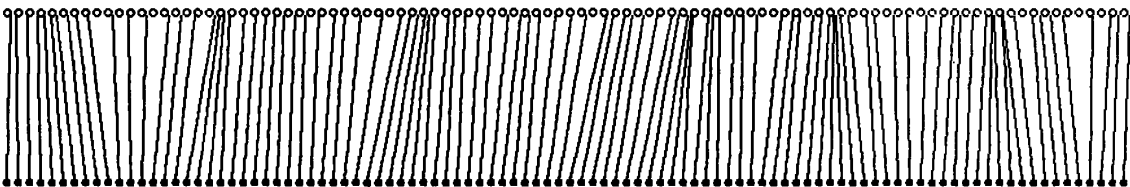
Another important question in map formation is the shape of the axonal arbors (in terms of their connection strengths), and of the receptive fields in the target layer. These features are functionally important, and they are easily measured experimentally. Figure 4-6 shows the initial and final shape of a typical axonal arbor, and the strength of a typical receptive field of a target neuron to activity at different locations in the source. The receptive field is the combined response to the source and to secondary lateral stimulation, so it corresponds to what would be seen in a biological experiment.



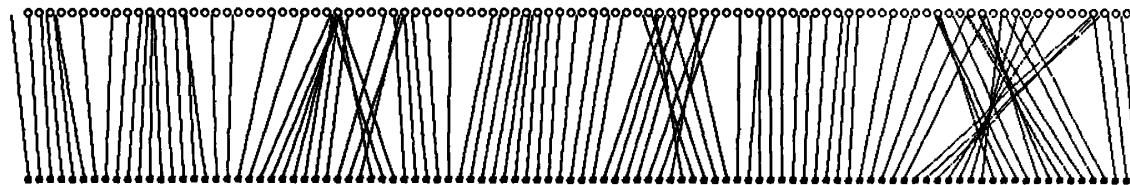
(a)



(b)



(c)



(d)

**Figure 4-4:** Examples of initial and final projections. Filled circles are source neurons, open circles are target neurons. Lines are drawn from each source neuron to the centroid of its axonal projection. (a–b) initial state, with position errors of  $\pm 5$  and  $\pm 20$ . (c) typical result after 10,000 input stimulus presentations. Results from 15 of 16 tests were very similar. (d) worst case result (1 test out of 16), with an initial position error of  $\pm 20$ , cluster size = 2 (discussed in text).

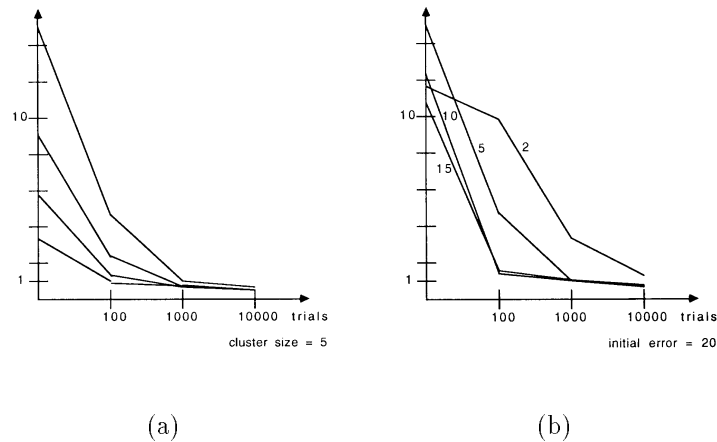


**Figure 4-5:** Spacing error. (a) fixed cluster size of 5, with several position errors. (b) fixed position error of  $\pm 20$ , with several cluster sizes.

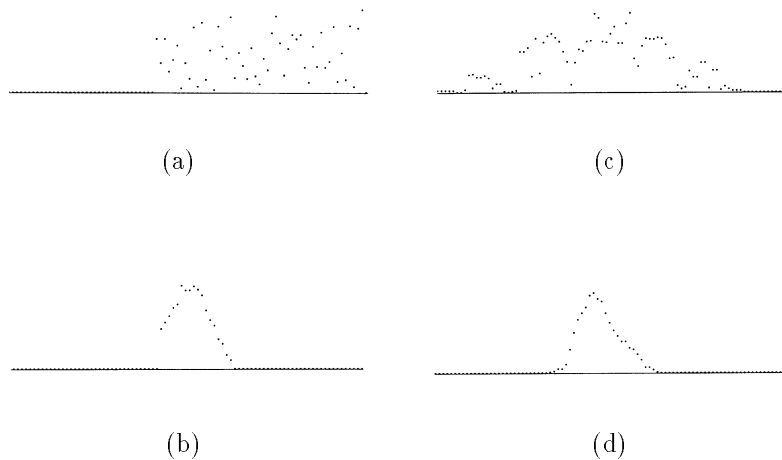


**Figure 4-6:** Typical arbor and receptive field strengths. (a–b) initial and final connection strengths across the target for a given source neuron. (c–d) initial and final receptive field strengths of a given target neuron, in response to activity in different locations across the source. A source activity cluster size of 5 was used, and activation was allowed to spread in the target as it does during the learning trials.

As is seen in biology, the axonal arbors become more narrow over time, and the final receptive fields are strongest when input stimulation is at the center of the receptive field, and taper off in strength as input stimulation moves away from their center [31].

## 4.5 The Role of Target Activity

In constructing this simulation, we have considerable latitude in modelling the target activity pattern,  $o_i(t)$ . In the adult animal, patterns of activity tend to follow a characteristic “mexican hat” pattern, with short-range excitatory and mid-range inhibitory interactions between inputs. This has led many researchers to hypothesize a pattern of direct lateral connections which are excitatory at close range and inhibitory at slightly longer ranges. However, this pattern of activity may be due to factors other than lateral synaptic connections, and interactions between inputs during development may be quite different than in adults.

However, the nature of lateral interactions in the target is very important in controlling the outcome of map formation. Lateral connections determine the target response to a given input stimulus, and the relationship between patterns of activity in the source and target maps determines the strength of the synaptic connections when map formation reaches an equilibrium state. If input activity is uniformly distributed, the dynamics of the system have a fixed point at

$$w_{ij,eq} \propto \sum_{p \in P_j} o_{i,eq}(p) \quad (4.2)$$

where  $P_j$  is the set of all input activity patterns in which source node  $j$  is active, and  $o_i(p)$  is the target response to input pattern  $p$ .<sup>5</sup> That is, the shape of the arbor for a given source node at equilibrium is proportional to the sum of the target responses to all input activity patterns in which that node is active. The form of the target activity patterns determines the final outcome.

This raises the question of what kind of activity is most useful for map formation. The next two sections look at this issue in more detail.

### 4.5.1 Noise Reduction

Map refinement can be thought of as a process of noise reduction. The location of the initial arbors provide a rough estimate of the desired target location (i.e. they are localized to a neighborhood around it, with some position error); near neighbors to a source neuron provide similarly rough estimates of nearby target locations.

When several source neurons fire in a cluster, their projections can be averaged to obtain a more accurate estimate of the correct target location than we could obtain

---

<sup>5</sup>This result is derived in Section 5.3.3.

from any single projection. When this process is repeated with different overlapping clusters, the estimate continues to improve. If we simply summed the target activity from the source layer, with no lateral connections, this is what we would get. However, although the centroid of the arbor converges to the correct location (in a map with full connectivity), the distribution of synaptic strength will spread out over time, until in the limit the strength is constant over the entire arbor.<sup>6</sup> To compensate for this effect, some kind of mechanism is needed to selectively enhance the target response in the center of the region activated by an input activity cluster.

A purely excitatory pattern of lateral connections was chosen because it is ideal for producing this type of activity. The only constraints on the source activity are that it be sufficient to initiate firing in the target over much of the extent of the axonal arbors, and that there be no large gaps in connectivity within an arbor. If these constraints are met, and the strength of lateral connections is such that neurons in the center of an active region continue to fire, while neurons bordering an active region cease firing, this will produce an activity pattern that is strongly enhanced in the center of the active region, with decreasing activity enhancement at greater distances from its center.

This kind of activity pattern is very difficult to obtain if a “mexican hat” pattern of lateral interactions is used. This pattern of connections tends to produce stable activity within a region whose breadth is determined by the extent of lateral excitation, and inhibit activity outside that region. Periodic activity can also be obtained with a mexican hat pattern. This kind of target activity pattern most naturally produces a discontinuous map; for example, the patterns of connections found in ocular dominance columns could be produced in this way.

Researchers using this pattern of lateral connections have utilized a variety of tricks to ensure a continuous final map. The neighborhood functions used with Kohonen maps [36] are initially very broad, and are manually reduced in size over the course of map formation. Synaptic arbors are in this way focussed very slowly into the correct region as map formation proceeds, which reduces the difficulty of maintaining map continuity.

Willshaw and von der Malsburg [68] also use a mexican hat pattern of lateral connections. In their model, continuity is ensured by the use of a nucleation region. A small part of the map is topographically organized as an initial condition, and synaptic strengths within this region are much stronger than in the surrounding tissue. This ensures that target activity is sufficient to induce learning only at the borders of the organized region, which prevents the formation of partial maps that might otherwise stabilize and form discontinuous sub-maps.

Because of the difficulty of maintaining map continuity in the presence of lateral inhibition, these results predict that map topography is largely determined before the development of an inhibitory surround. It is fairly well established that excita-

---

<sup>6</sup>See Section 5.3.4 for a derivation of this result.

tion predates inhibition in the developing nervous system [18, 40], so this seems a reasonable assumption.

In particular, experimental results on neurotransmitter metabolism in cat visual cortex during development [58, 14] were checked for compatibility with this hypothesis. The observed levels of glutamate metabolism during the stage of development in which map formation occurs are much higher than in adult animals, and GABA metabolism is still almost nonexistent. As glutamate is the most common excitatory transmitter in the cortex, and GABA is a well-known inhibitory transmitter, at least in the adult, this result supports the hypothesis that large amounts of excitatory activity are involved in map formation, and rules out one possible mechanism for lateral inhibition. However, as it is not actually known whether lateral inhibition in the adult is mediated by GABA, nor even whether GABA is inhibitory during development, this result is inconclusive.

Looking at the process as one of noise reduction also explains why the algorithm runs into problems with small cluster sizes and large position errors. The smaller the cluster size, the less information is available to each step of the noise reduction process, because there are fewer “samples” to average over. This means it will converge more slowly. However, as the arbors get narrower, due to the enhancement of activity in the center of the active region, their position becomes fixed. If this occurs before the noise reduction process produces an accurate estimate of the desired location, the map will remain somewhat disordered. This problem can be solved by increasing the size of the activity clusters. Another prediction of this model, then, is that activity clusters must be larger in early stages of map formation than they are later in development.

### 4.5.2 Convergence Properties

Another important effect of the target activity pattern is on the convergence properties of the learning algorithm. Erwin, Obermayer, and Schulten [13] have, in the case of Kohonen nets on a one-dimensional input space, determined the optimal target activity pattern<sup>7</sup> for ensuring a rapid convergence rate and for preventing the formation of map discontinuities. Although their results have not been demonstrated to generalize to this model, they nonetheless provide criteria that are useful for its analysis.

Two requirements are defined that are sufficient to ensure that the final map is continuous, and two more to ensure a rapid convergence rate. For a continuous final map, the first requirement is that the breadth of the activity pattern be greater than the uncertainty in position (in their model, this initially corresponds to the entire breadth of the map). The second is that it be “convex”, a term they define to include a slightly larger class of functions than the usual meaning of the term. For rapid

---

<sup>7</sup>The target activity pattern in this model corresponds to the “neighborhood function” used with Kohonen maps.

convergence, the requirements are that the breadth of the activity pattern be as narrow as possible without violating the continuity constraint, and that it be sloped toward the center, so that neighboring neurons have maximally differing activity levels.

Since the breadth of the target response in this model is determined directly by the breadth of the arbors, which is greater than their positional uncertainty, the first requirement is easily met. Also, as the arbors narrow down around their correct location, the breadth of the response also narrows, which not only meets the breadth constraint for rapid convergence, but also tailors itself over the course of learning to the current optimum, by narrowing as the position error narrows.

The shape of the response is a sum of direct activation from the source layer, which is (probabilistically) gaussian over the surface of the map, and the response due to spreading activation through the lateral connections, which is triangular except for some rounding at its peak. The gaussian function is convex within a finite region about its center, and the rounded triangular function is convex over its entire nonzero region; the target activity is also (probabilistically) convex. The triangular component of this activity pattern also gives it a slope that meets the second criterion for rapid convergence.

The activity pattern which arises naturally from intercellular interactions in this model thus meets all the requirements given in [13] for obtaining a continuous final map with an optimal convergence rate.

## 4.6 Extensions to the Model

### 4.6.1 Biological Mechanisms for Competition

The competitive mechanism used in this simulation is a form of input normalization, where the total input to a given target neuron is held at a fixed value. Increases in synaptic strength due to the Hebbian learning mechanism are offset by decreases in the strength of other synapses. Some form of competition is necessary to limit the total arbor size, and to explain map expansion and compression in response to lesions or changes in the level of input stimulation.

However, although input normalization is commonly used as a competitive mechanism in topographic map models, it requires information which is not locally available at the synapse, and for this reason it would be very difficult to implement in biology. It is therefore unsatisfactory for a model in which biological plausibility is an important consideration.

Oja [52] showed that vector input normalization can be approximated (in the limit where  $\alpha$  is small) by an activity-dependent decay, given the assumption that there are no lateral connections in the target map. This means that vector input normalization can be achieved, if there are no lateral connections, by decreasing the synaptic strengths at a rate which depends only on the target activity.

Activity-dependent decay suggests a biological mechanism whereby all synapses decrease in strength at a rate which is controlled by target depolarization. For example, a voltage-dependent process that affects the turnover rate of postsynaptic receptors might have this effect.

If we follow Oja's derivation, using the form of competition used in this model (which normalizes over the summed input strength instead of the vector magnitude), we obtain the following rule:

$$w_{ij}(T + 1) \approx w_{ij}(T) + \alpha A_{ij}(T) o_i(T) a_j(T) - w_{ij}(T) o_i(T) \frac{\alpha N_i(T)}{K} \quad (4.3)$$

where

$$N_i(T) = \sum_{j=0}^{m-1} A_{ij}(T) a_j(T) \quad (4.4)$$

$N_i(T)$  is constant if we assume a constant input cluster size and full connectivity between source and target maps, and in this case the decay term becomes a pure activity-dependent decay. Its behavior in situations which violate this assumption is discussed in more detail in Section 5.2.

## 4.6.2 Map Expansion and Compression

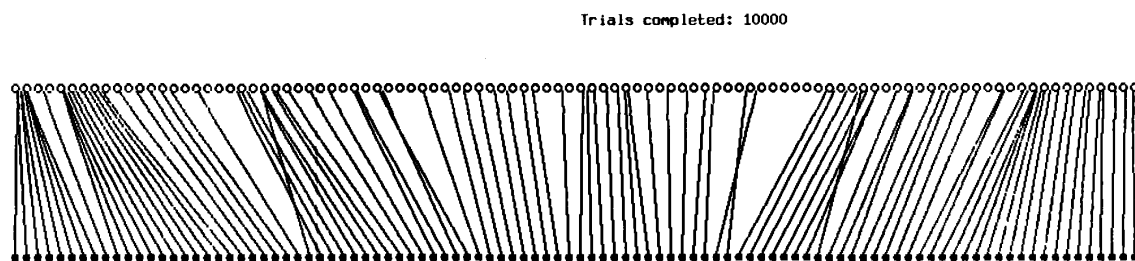
A final set of tests was run to replicate biological experiments showing map expansion and compression. There are two ways to get these effects: one is to stimulate a localized input area very heavily (or, conversely, deprive an area of input), and the other is to introduce a lesion into the source (or target) map, and later observe the pattern of connections formed by the remaining tissue [26].

### Usage-Dependent Changes

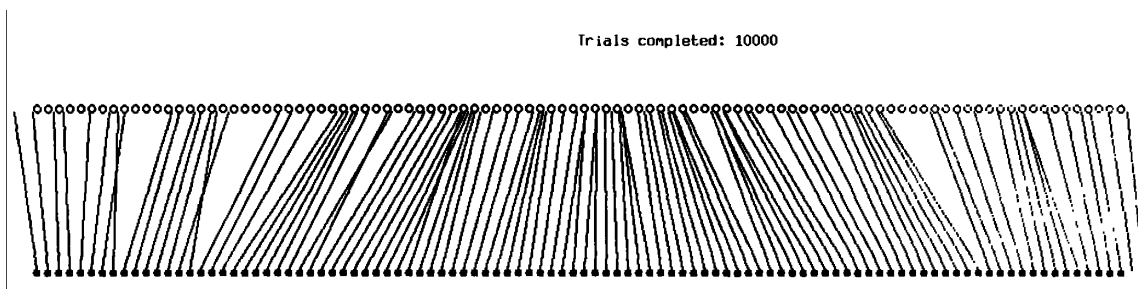
The stimulation-dependent experiments were run simply by changing the probability of occurrence of a source stimulus in different regions of the map. Results are shown in Figure 4-7.

In normal cortical maps (where there have been no experimental manipulations), the size of the receptive field varies inversely with map magnification [31]. Properties of receptive fields within the expanded and compressed regions of the final maps were tested to determine how well they match this property of biological maps.

Receptive field properties were averaged over a set of 20 nodes in the center of the compressed region, and 40 nodes in the center of the expanded region. The receptive field strength for each source location was determined by stimulating a cluster of 5



(a)



(b)

**Figure 4-7:** Final results for map expansion and compression after 10,000 stimulus presentations. (a) The central half of the input map was stimulated twice as often as the surround. (b) The center was stimulated half as often as the surround.

	Expanded	Compressed	Ratio
Magnification	1.4	0.65	2.2
Receptive Field Size	30	44	0.68
Mean Response Strength	15	8.5	1.8
Proportion Above Mean	0.47	0.48	0.98

**Table 4.1:** Map magnification and receptive field properties for expanded and compressed maps.

source neurons centered at that location,<sup>8</sup> and allowing activation to spread laterally in the target. Four properties of the final maps were measured:

1. The average spacing between nodes was used as a measure of map magnification.
2. The average number of source locations to which a target node responds was used as a measure of its receptive field size.
3. The mean response strength to locations within the receptive field was measured separately for each target node, and these values were averaged to determine the average mean response strength.
4. The proportion of source locations for which the response strength was greater than the mean response strength for that target was used as a rough measure of receptive field shape.

Results are shown in Table 4.1. This data indicates that the general shape of the receptive fields is unchanged by usage-dependent map expansion and compression; however, their size and average strength are strongly affected. The strength of the receptive fields increases as the map expands, and the receptive field size decreases. These properties are similar to biological results in that map magnification and receptive field size change in opposite directions. However, the proportional difference in receptive field size is considerably smaller than the magnification difference.

This may, in part, reflect a difference between properties of normal cortical maps and properties of experimentally manipulated maps. Magnification of normal cortical maps varies in proportion to the receptor density in the corresponding source region [31]. In the experimental situation, the usage of a source region is modified, but there is no corresponding change in receptor density. This could affect the relative change in receptive field size as the map expands or compresses. Receptive field sizes may also be affected by adaptive changes in the lateral connections, as modelled in [61].

---

<sup>8</sup>This is the same size that was used to drive map formation.

### Lesion Studies

Another change is necessary to run lesion studies. Up to this point, the formation of new synapses has not been included in this model. Because of this, it is necessary to ensure that the location of the initial arbor overlaps the desired final location. However, if some part of the source or target structure is lesioned, the desired final location of some arbors is quite far from their initial location, so it is necessary to include some form of synapse formation. An extremely simple mechanism for synapse formation is used, on the assumption that if it is sufficient, any more realistic model is also likely to work. The scheme used is to add new connections, with initially random weights, from active source neurons to the immediate neighbors of active target neurons. This pattern of synapse formation might result if the source axon were to “sprout” new terminals in the vicinity of a synapse that is being strengthened; these terminals could then make connections with nearby dendrites of neighboring cells.<sup>9</sup>

This scheme, though extremely simplistic, is sufficient to allow map expansion and migration into unused tissue after a source lesion, and map compression after a target lesion (see Figures 4-8 and 4-9).

## 4.7 Discussion and Summary

Map formation in this simulation is accurate and robust, and provides a good match to experimental data, despite the use of an extremely simple neuron model. It may be that developmental phenomena such as map formation are relatively insensitive to detailed properties of the cell, either because their success is so important to the organism, or because these properties are in such flux during development. It is likely that modelling of more complex neural behaviors will require the inclusion of higher-order effects that appear not to be critical for topographic map formation.

Chemoaffinity, in this model, is assumed to create a rough initial map that is refined by an activity-based mechanism. An LTP-like learning process uses this rough map, together with correlations in source activity, to focus the axonal arbors into localized regions matching the detailed topography of the source map. The accuracy of the initial map is surprisingly unimportant in achieving an accurate final map, as long as the axonal projections of neighboring source neurons overlap. Competitive mechanisms produce activity-dependent map expansion.

The pattern of activity in the target cell layer is critical in determining the result of the map formation process. The biological process described in this paper results in an activity pattern that is ideal for producing rapid convergence to a detailed map.

---

<sup>9</sup>The model described in [49], for example, uses a similar form of synaptic sprouting as an integral part of its learning mechanism. In the optic tectum in the frog, new synapse formation has been hypothesized as a primary mechanism for the map development [11].

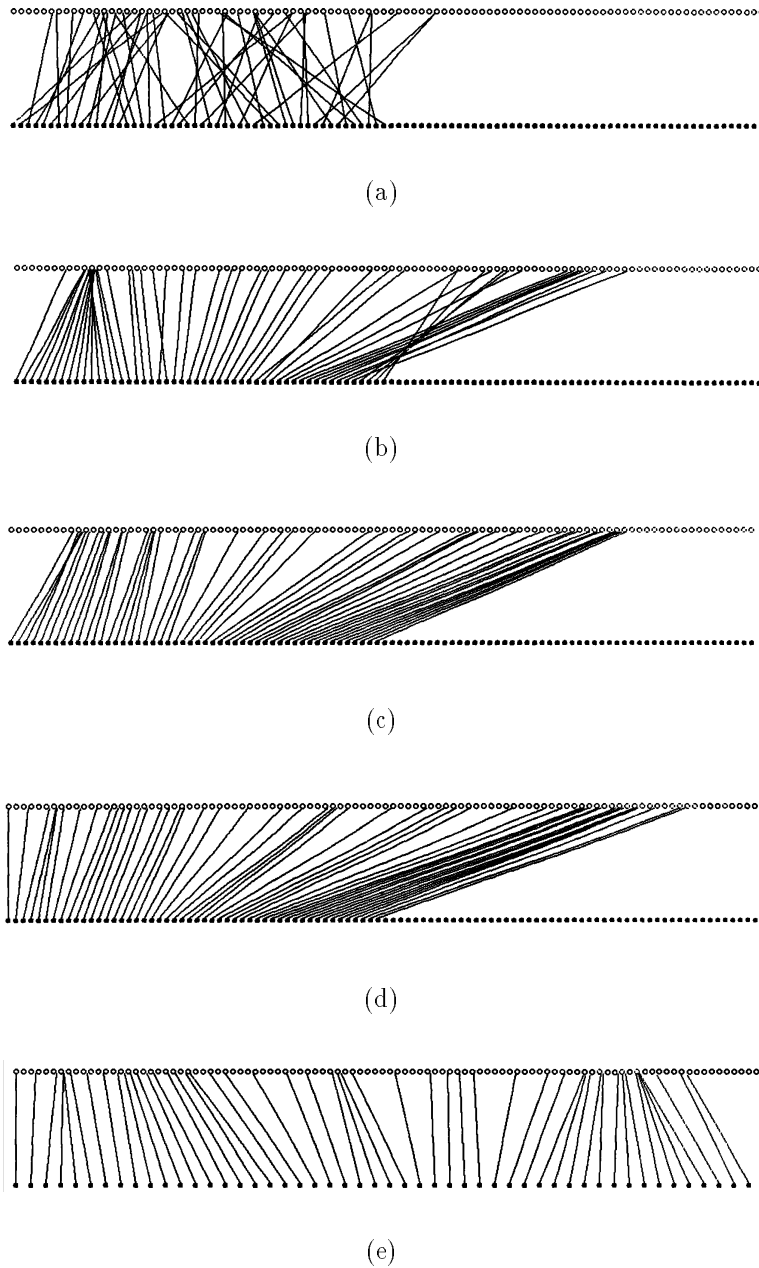
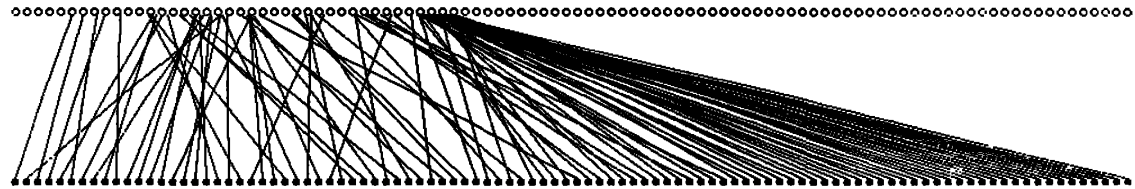
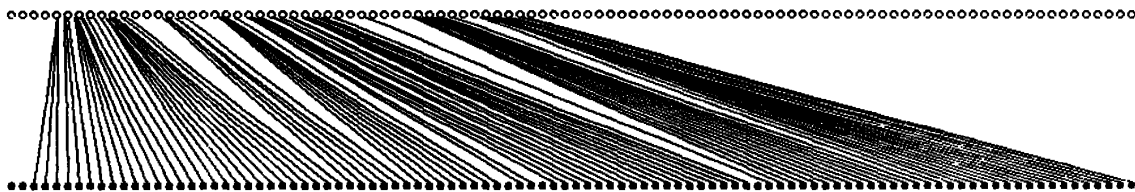


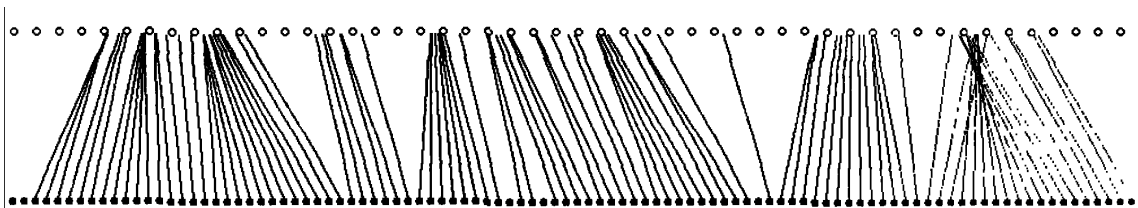
**Figure 4-8:** Map expansion following a lesion which removes the right half of the source map. Results are shown after (a) 0, (b) 100, (c) 1000, and (d) 10000 trials. (e) Same as (d), but with the remaining source neurons spaced apart to full breadth of the map.



(a)



(b)



(c)

**Figure 4-9:** Map compression following a lesion which removes the right half of the target map. Axons which would normally connect to the missing portion of the target are initially bunched up along the edge of the lesion. Results are shown after (a) 0 and (b) 10000 trials. (c) Same as (b), but with the remaining target neurons spaced apart to full breadth of the map.

# Chapter 5

## Mathematical Analysis of Map Formation

Chapter 4 presents a simulation of topographic map formation, along with experimental results of running that simulation in a variety of test conditions. In this chapter, the underlying mathematics are described in detail and analyzed.

The first section presents detailed equations describing the simulation, and gives constraints on the parameter values that ensure it will behave according to plan.

The second section derives a new learning rule which uses an activity-dependent decay as a competitive mechanism, and whose behavior is similar to that of input normalization given certain simplifying assumptions. Simulation results are presented which demonstrate that the new rule works well for map formation.

The third section addresses the question of the nature and stability of equilibrium states for the map formation process. An equation is derived showing the relationship between the final weights and the final target activity patterns. For the simple case with full connectivity between source and target and no lateral connections in the target, it is shown that the system is stable about an equilibrium point where all weights have the same value:  $\forall_{i,j} w_{ij} = K/m$ .

### 5.1 Description of Simulation

The network has a one-dimensional input layer with  $m$  nodes, which projects to a one-dimensional output layer with  $n$  nodes. At trial  $T$ , an input activity pattern  $[a_0(T)..a_{m-1}(T)]$  is presented, and a target response (target activity pattern)  $[o_0(T)..o_{n-1}(T)]$  is computed by simulating the spreading of activation via lateral connections in the target. The strength of the synaptic connection  $w_{ij}(T)$  from input node  $j$  to target node  $i$  is then updated by a Hebbian learning rule (in the numerator) combined with a competitive mechanism (in the denominator).

$$w_{ij}(T+1) = \frac{w_{ij}(T) + \alpha A_{ij}(T) o_i(T) a_j(T)}{\frac{1}{K} \sum_{j=0}^{m-1} (w_{ij}(T) + \alpha A_{ij}(T) o_i(T) a_j(T))} \quad (5.1)$$

In this equation,  $\alpha$  is the learning rate,  $A_{ij}(T) = 1$  if there is a synapse from  $j$  to  $i$  and 0 otherwise, and  $K$  is the maximum synaptic input to a target node. The synaptic strengths  $w_{ij}$  are strictly excitatory; that is,  $\forall_{i,j} w_{ij} \geq 0$ .

Initial conditions for the synaptic connectivity  $A_{ij}(0)$  and weights  $w_{ij}(0)$  are determined using two control parameters,  $r$  and  $\epsilon$ .  $r$  is the radius of the axonal arbor, and  $\epsilon$  is the maximum position error. For each input node  $j$ , the topographically corresponding target location is  $i = \text{round}[jn/m]$ . An error  $\epsilon_j$  for that projection is chosen randomly in a uniform distribution over the range  $[-\epsilon, \epsilon]$ . The initial connectivity is:<sup>1</sup>

$$A_{ij}(0) = \begin{cases} 1 & \text{if } j + \epsilon_j - r \leq i \leq j + \epsilon_j + r \\ 0 & \text{otherwise} \end{cases} \quad (5.2)$$

Synapses are removed if their strength goes below a minimum value, to prevent floating-point underflow errors in the simulation.

$$A_{ij}(T+1) = \begin{cases} 1 & \text{if } A_{ij}(T) = 1 \wedge w_{ij}(T) > \epsilon \\ 0 & \text{otherwise} \end{cases} \quad (5.3)$$

In lesion tests, where synapse formation is included, it takes a very simple form. The initial weight of a new synapse,  $w_{ij}(T+1)$ , is set to a random value. A new synapse is formed between a source node  $j$  and a target node to which it is not already connected when the synapse from  $j$  to a neighboring target node is strengthened:

$$A_{ij}(T+1) = \begin{cases} 1 & \text{if } (A_{ij}(T) = 1 \wedge w_{ij}(T) > \epsilon) \\ & \vee \Delta w_{(i-1)j}(T) > 0 \\ & \vee \Delta w_{(i+1)j}(T) > 0 \\ 0 & \text{otherwise} \end{cases} \quad (5.4)$$

Initial weights  $w_{ij}(0)$  are set to random values where  $A_{ij}(0) = 1$ , and 0.0 otherwise. The weights are then normalized using the competitive mechanism from the learning rule. This mechanism ensures that the summed synaptic strength of all connections from the source layer to a given target node is constant, that is,

$$\sum_{k=0}^{m-1} w_{ik}(T) = K \quad (5.5)$$

When  $K = 1.0$ , the competitive mechanism is known as “input normalization.” The input activity  $a_j(T)$  for a given trial consists of a contiguous activity cluster,

---

<sup>1</sup>Differences are calculated mod  $n$  for wraparound.

containing  $c(T)$  active nodes. The location of this cluster is chosen randomly. For most test runs,  $c(T)$  is a constant, and the cluster location is chosen using a uniform distribution across the source map.

$$a_j(T) = \begin{cases} 1.0 & \text{if node } j \text{ is active} \\ 0.0 & \text{otherwise} \end{cases} \quad (5.6)$$

The target activity  $o_i(T)$  for a given trial is determined by the time course of target activation within that trial. This time course is simulated by stepping the system through the trial with an intra-trial time step  $t$ , which is much shorter than the inter-trial step  $T$ . To get the total target activity for a trial, the activation at time  $t$  is summed over a time window of length  $\tau$ , beginning at the stimulus presentation for that trial.

$$o_i(T) = \sum_{t=t_0}^{t_0+\tau} \phi_i(t) \quad (5.7)$$

$$\phi_i(t) = \begin{cases} \sum_{j=0}^{m-1} w_{ij}(T) A_{ij}(T) a_j(T) & t = t_0 \\ \sum_{j=0}^{n-1} \lambda_{ij} f_j(t-1) & t_0 < t \leq t_0 + \tau \end{cases} \quad (5.8)$$

$$f_j(t) = \begin{cases} 1.0 & \text{if } \phi_j(t) > \theta \\ 0.0 & \text{otherwise} \end{cases} \quad (5.9)$$

In these equations,  $\phi_i(t)$  is the target activation at time step  $t$  within trial  $T$ ,  $\lambda_{ij}$  is the lateral connection strength between target nodes  $j$  and  $i$ , and  $\theta$  is the firing threshold for the target nodes.

The lateral connections  $\lambda_{ij}$  in the target are defined to be a symmetrical triangular ramp of radius  $\rho$ .<sup>2</sup>

$$\lambda_{ij} = \begin{cases} \Lambda \cdot \left(1 - \frac{|i-j|-1}{\rho}\right) & \text{if } 0 < |i-j| \leq \rho \\ 0.0 & \text{otherwise} \end{cases} \quad (5.10)$$

The constant  $\Lambda$  is the summed connection strength of all lateral inputs to a single target node.

$$\Lambda = \Lambda_i = \sum_{j=0}^{n-1} \lambda_{ij} \quad (5.11)$$

---

<sup>2</sup>Differences are calculated mod  $n$  for wraparound.

### 5.1.1 Parameter Constraints

There are a large number of parameters in the system, which might at first glance make it look like a connectionist's nightmare. However, an analysis of these parameters gives rise to a simple set of constraints on their values, within which the simulation will behave according to plan. The basic parameters are:

- $m$  (number of source nodes)
- $n$  (number of target nodes)
- $\alpha$  (learning rate)
- $K$  (competition limit)
- $\tau$  (length of time window for Hebbian learning)
- $\theta$  (firing threshold)
- $\Lambda$  (summed lateral connection strength)
- $\rho$  (radius of lateral connections)

#### Map Configuration

The map configuration was set at  $m = n = 100$ , with the ends wrapped to reduce edge effects, using one-dimensional maps. Using a one-dimensional map makes it possible to study effects over a longer distance in the map without the computation time becoming prohibitive.

#### Learning Parameters

The competition limit  $K$  is the sum of incoming synaptic strengths to a given target node. This limit must be set high enough to allow the target to fire in response to the source activity, or learning will not occur.

In the tests which use a uniform input activity cluster size, the competition limit is set relative to the cluster size to ensure that initial synaptic strengths are sufficient to induce firing in the target. The average initial projection strength is  $K/2r$ . For an activity cluster of size  $c$ , the maximum target activation at time  $t_0$  is therefore  $cK/2r$ , to initiate target firing we require the following condition:

$$\frac{cK}{2r} > \theta \tag{5.12}$$

In these tests, an intermediate  $K$  value is used that requires, in the initial state, input projections from roughly half the source nodes to initiate firing in a target node.

$$K = \frac{4r\theta}{c} \quad (5.13)$$

The target activity function is designed to die out naturally within a small number of time steps, and the time window  $\tau$  for Hebbian learning is to be longer than the maximum duration of the target activity.

The Hebb learning rate,  $\alpha$ , must be set low enough to ensure convergence, but otherwise we want it as large as possible so that it will converge quickly.

The derivation in Section 5.2 assumes that incremental changes are very small. One concrete constraint on the learning rate, required if we are to accurately approximate the competition term with an activity-dependent decay, is

$$\frac{\alpha c_{max} o_{i max}}{K} \ll 1.0 \quad (5.14)$$

or

$$\alpha \ll \frac{4r\theta}{c^2 o_{i max}} \quad (5.15)$$

For example, if  $c = 10$  and  $r = 30$ , assuming a maximum target activity of 50,

$$\alpha \ll \frac{4 \cdot 30 \cdot 1.0}{100 \cdot 50} = 0.024 \quad (5.16)$$

### Parameters Affecting Target Activity

The firing threshold is normalized to 1.0, and other activity-related parameters are set in proportion to it.

The desired target activity will die out naturally over time, but persist longer toward the center of the projection than at its edges. Therefore, if all nodes within the lateral activation range are firing, a node should continue to fire, while nodes along the borders of an active region should cease firing. In the center of an active region, the activation is  $\phi_i = \Lambda$ .

The activation of a node at the edge of an active region (all nodes on one side firing, all nodes on the other quiet), on the other hand, should fall below threshold. This activation is  $\phi_i = \Lambda/2$ .

If we want target activity to die out from the edges, persisting longest in the center, the bounds for the lateral connection strengths are therefore

$$\theta < \Lambda < 2\theta \quad (5.17)$$

An intermediate value for  $\Lambda$ , 1.5, was used.

of the summed target activity pattern given different

The radius of the lateral activation curve,  $\rho$ , is less critical. The primary effect of this parameter is to smooth over variations in the input activity — a longer radius

increases the ability to recover if individual nodes within an active region do not initially reach firing threshold. It also smooths out the summed activity pattern, making it more similar to a gaussian, while shorter values of  $\rho$  make the activity curve more triangular.

The value used in the simulation was  $\rho = 5$ .

### Test Conditions

A number of parameters were varied to create different situations for testing. These include

- $r$  (radius of initial axonal arbors)
- $\epsilon$  (maximum initial position error)
- $c(T)$  (size of input activity clusters)
- distribution of locations of input activity clusters

The first set of tests was designed to test the robustness of the learning algorithm. The accuracy of the chemical markers and the source activity pattern was varied to create different learning conditions.

The initial radius of the distribution was set at a breadth that would ensure overlap with the goal location, to avoid the need to model new synapse formation. The corresponding constraint is  $r > \epsilon$ .

In a map that wraps around on itself, we also need to ensure that the initial position error is not large enough for the axonal arbors to wrap around on themselves, as the wraparound is intended to simulate a very large map, not a circular one. To prevent this problem, we need the following constraint:

$$2(r + \epsilon) < n \tag{5.18}$$

To test  $\epsilon$  values between 0 and 20, the projection radius  $r$  was set at 30. It would be necessary to increase the map size in order to test larger position errors.

The size and distribution of input activity clusters was tested at constant levels between  $c = 2$  and  $c = 10$ . The simulation was also tested using input activity cluster sizes that varied randomly within that range. The distribution of input activity cluster locations was uniform in the initial tests, which should result in a map with uniform spacing. Tests of map expansion and contraction used non-uniform distributions.

## 5.2 Derivation of Activity-Dependent Decay

This section shows how input normalization can be approximated by an activity-dependent decay term. Although no biological process observed to date is known

to produce an activity-dependent decay, it nonetheless allows for a simple biological implementation, due to the local availability at the synapse of information about the target activity.

Oja [52] showed that vector input normalization can be approximated (in the limit where  $\alpha$  is small) by an activity-dependent decay, given the assumption that there are no lateral connections in the target map.

The analysis presented here shows that the decay term for input normalization cannot be made completely independent of input activity in the presence of lateral connections. However, if we allow the normalization constant  $K$  to vary slowly over time and across the surface of the target map, we can derive a new learning rule which is similar to our old rule but which uses an activity-dependent decay. This new rule is simulated to demonstrate that it does produce reasonable competitive behavior, and that the summed input strengths, although variable, nonetheless remain close to  $K$ .

Our original learning rule is

$$w_{ij}(T+1) = \frac{w_{ij}(T) + \alpha A_{ij}(T) o_i(T) a_j(T)}{\frac{1}{K} \sum_{j=0}^{m-1} (w_{ij}(T) + \alpha A_{ij}(T) o_i(T) a_j(T))} \quad (5.19)$$

Because of the input normalization,

$$\sum_{j=0}^{m-1} w_{ij}(T) = K \quad (5.20)$$

which means we can convert our learning rule to

$$w_{ij}(T+1) = \frac{w_{ij}(T) + \alpha A_{ij}(T) o_i(T) a_j(T)}{1 + \frac{\alpha o_i(T)}{K} \sum_{j=0}^{m-1} A_{ij}(T) a_j(T)} \quad (5.21)$$

All terms in

$$\frac{\alpha o_i(T)}{K} \sum_{j=0}^{m-1} A_{ij}(T) a_j(T) \quad (5.22)$$

are finite, so this term can be made arbitrarily small by a suitable choice of  $\alpha$ . In this case, we can make the following series expansion:

$$\frac{1}{1 + \frac{\alpha o_i(T)}{K} \sum_{j=0}^{m-1} A_{ij}(T) a_j(T)} = 1 - \frac{\alpha o_i(T)}{K} \sum_{j=0}^{m-1} A_{ij}(T) a_j(T) + O[\alpha^2] \quad (5.23)$$

This transforms our learning rule to

$$\begin{aligned}
& w_{ij}(T+1) \\
&= (w_{ij}(T) + \alpha A_{ij}(T) o_i(T) a_j(T)) \left( 1 - \frac{\alpha o_i(T)}{K} \sum_{j=0}^{m-1} A_{ij}(T) a_j(T) + O[\alpha^2] \right) \\
&= w_{ij}(T) + \alpha A_{ij}(T) o_i(T) a_j(T) - w_{ij}(T) \frac{\alpha o_i(T)}{K} \sum_{j=0}^{m-1} A_{ij}(T) a_j(T) + O[\alpha^2] \\
&\approx w_{ij}(T) + \alpha A_{ij}(T) o_i(T) a_j(T) - w_{ij}(T) o_i(T) \frac{\alpha N_i(T)}{K} \tag{5.24}
\end{aligned}$$

where

$$N_i(T) = \sum_{j=0}^{m-1} A_{ij}(T) a_j(T) \tag{5.25}$$

The real appeal of an activity-dependent decay term is that it is dependent *only* on target activity, and therefore has a superior claim to biological plausibility. If we assume a constant input cluster size and full connectivity between source and target maps, then  $N_i(T)$  is constant, and in this case the decay term becomes a pure activity-dependent decay.

In more realistic situations, however,  $N_i(T)$  will vary due to variations in the size of the input activity cluster and the connectivity between the two maps.

Up to this point, our derivation is quite similar to the one presented in [52], but this is as far as Oja takes us. In Oja's derivation, the decay term was made independent from the input activities by assuming that the output is simply the weighted sum of the inputs; that is,

$$o_i(T) = \sum_{j=0}^{m-1} w_{ij}(T) a_j(T) \tag{5.26}$$

which is only the case if there are no lateral connections. Because of the presence of lateral connections in this simulation, we cannot make this simplification.

If we average the effect of the decay term over many time steps, our learning rule can be further approximated as:

$$w_{ij}(T+1) \approx w_{ij}(T) + \alpha A_{ij}(T) o_i(T) a_j(T) - w_{ij}(T) \frac{\alpha}{K} \langle o_i(T) N_i(T) \rangle \tag{5.27}$$

where

$$\langle o_i(T) N_i(T) \rangle = \langle o_i(T) \rangle \langle N_i(T) \rangle + \text{Cov} [o_i(T), N_i(T)] \tag{5.28}$$

The angle brackets  $\langle \rangle$  denote expected value, and  $\text{Cov}[x, y]$  is the covariance of  $x$  and  $y$ . Substituting back in to our learning rule, and replacing  $\langle o_i(T) \rangle$  with  $o_i(T)$ , we obtain

$$w_{ij}(T + 1) \approx w_{ij}(T) + \alpha A_{ij}(T) o_i(T) a_j(T) - w_{ij}(T) o_i(T) \frac{\alpha N'_i(T)}{K} \quad (5.29)$$

where

$$N'_i(T) = \langle N_i(T) \rangle + \frac{\text{Cov}[o_i(T), N_i(T)]}{\langle o_i(T) \rangle} \quad (5.30)$$

with the averages taken over a large time window around  $T$ .

If we average  $N'_i(T)$  over both  $i$  and  $T$  and replace it by a constant  $N' = \langle N'_i(T) \rangle$ , we obtain a new learning rule with a pure activity-dependent decay.

$$w_{ij}(T + 1) = w_{ij}(T) + \alpha A_{ij}(T) o_i(T) a_j(T) - w_{ij}(T) o_i(T) \frac{\alpha N'}{K} \quad (5.31)$$

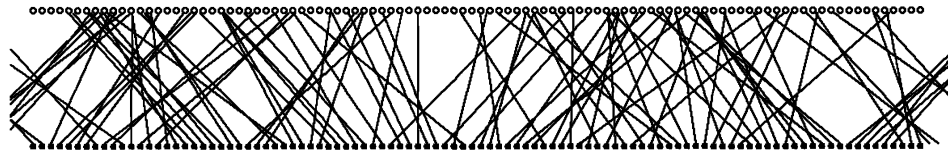
The behavior of the new learning rule is approximately equivalent to the old rule if the learning rate is small and if  $N'_i(T)$  does not vary over time or across the surface of the map.

However, the summed strength of the inputs to a single target node is no longer explicitly normalized to  $K$ , so if the actual value of  $N'_i(T)$  differs from our assumed value  $N'$ , the summed input strength will converge to a new value,

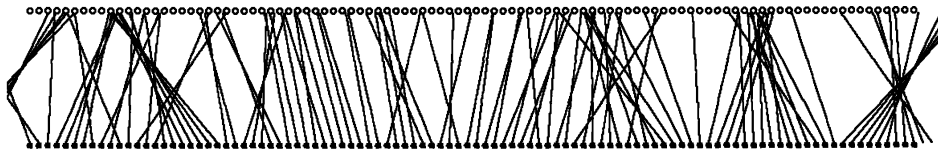
$$K_i(T) = K \frac{N'_i(T)}{N'} \quad (5.32)$$

This gives us a learning rule in which the summed input strength to a target node  $i$  is maintained at a value which may vary across the surface of the map, or which may change slowly over time.

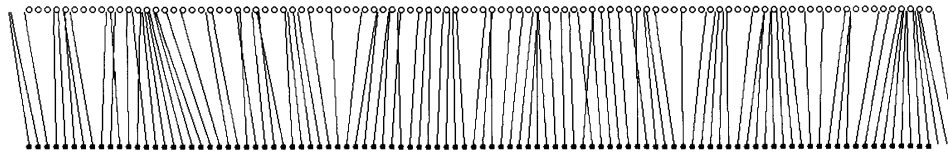
Two questions are of interest for evaluating this new learning rule. One obvious question is how similar it is to input normalization, which is known to work well as a competitive mechanism. But other competitive processes which do not normalize the inputs to a target node may work equally well. So we must ask, as a separate question, how well this activity-dependent decay term works as a competitive mechanism. Figure 5-1 shows the results of a map formation test using an activity-dependent decay in the place of input normalization. Figure 5-2 shows a graph of  $K_i(t)$  across the target map at four different times during map formation. These results indicate that activity-dependent decay works well for map formation, and although the values of  $K_i$  do spread out somewhat, they appear to remain within a relatively narrow range around a stable mean value.



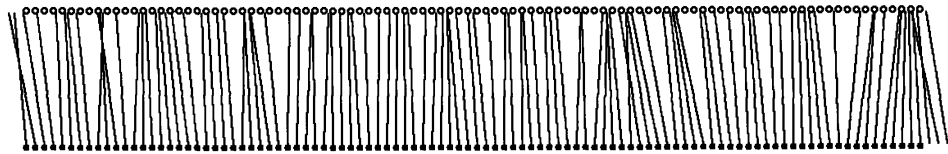
(a)



(b)



(c)



(d)

**Figure 5-1:** Map formation using activity-dependent decay as a competitive mechanism, with an initial error of  $\pm 20$  and an activity cluster size of 5. Results are shown after (a) 0, (b) 100, (c) 1000, and (d) 10000 trials.

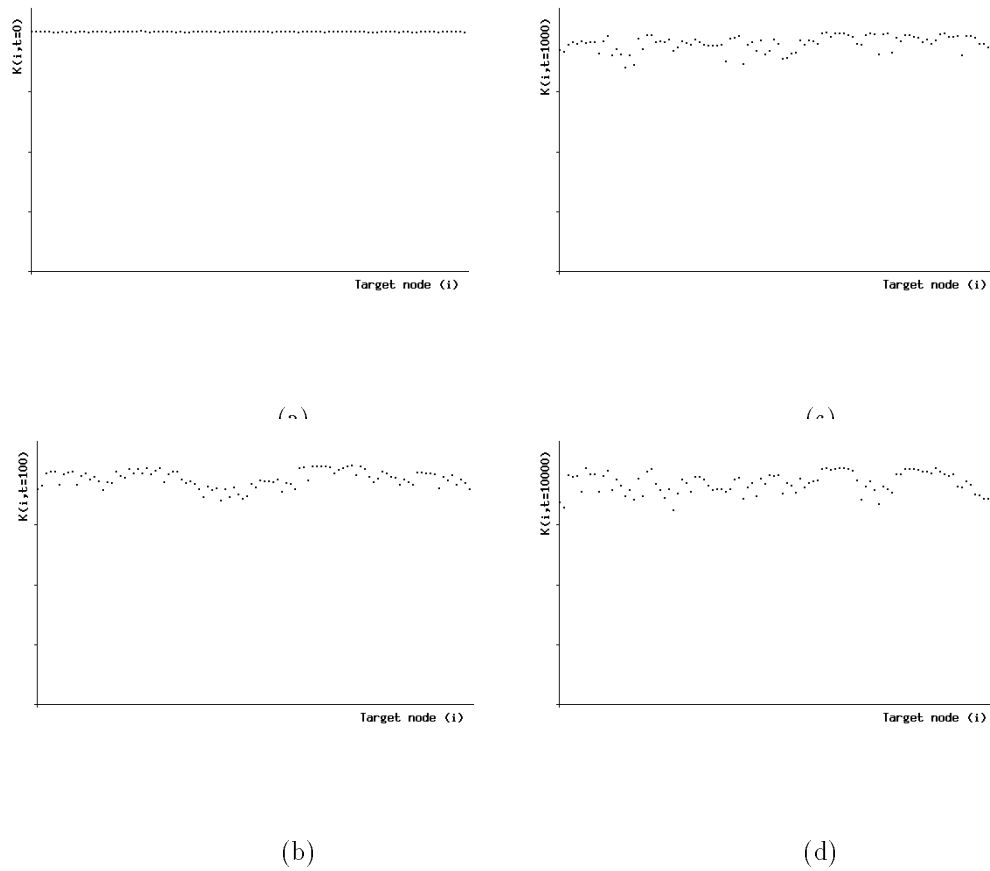


**Figure 5-2:** Variations in  $K_i(T)$  across the target map after (a) 0, (b) 100, (c) 1000, and (d) 10000 trials.

### 5.3 Equilibrium Solutions and Stability

This section derives equations describing the dynamic behavior of the weight vectors over the course of a learning simulation. General solutions are given for the equilibrium solutions, and an equation is given which can be used to determine the stability of a known equilibrium solution.

In the case of uniform input activity and full connectivity, it is shown that the weights  $w_{ij}$  have an equilibrium solution where their values are proportional to the sum of the target  $i$ 's response to all input activity patterns in which the node  $j$  is active, weighted by the probability of that input activity pattern. This means that the process which generates the target activity pattern also determines the shape (breadth and distribution of synaptic weights) of the final axonal arbors.

It is also shown that, for the case where there is uniform input activity, full connectivity, and no lateral connections, the map formation process will converge to a solution where all weights are equal.

#### 5.3.1 Equilibrium Solution

If we assume that incremental changes are very small, and sum a large number of time steps  $t$  into a single epoch  $E$ , we can approximate the system as follows:

$$\begin{aligned}
 w_{ij}(E+1) &\approx \frac{w_{ij}(E) + \alpha \sum_{p \in P} \mathbf{P}[p] A_{ij}(E) o_i(p, E) a_j(p)}{\frac{1}{K} \sum_{p \in P} \mathbf{P}[p] \left( w_{ij}(E) + \alpha o_i(p, E) \sum_{k=0}^{m-1} A_{ik}(E) a_k(p) \right)} \\
 &= \frac{w_{ij}(E) + \alpha \sum_{p \in P} \mathbf{P}[p] A_{ij}(E) o_i(p, E) a_j(p)}{1 + \frac{\alpha}{K} \cdot \sum_{p \in P} \mathbf{P}[p] o_i(p, E) \sum_{k=0}^{m-1} A_{ik}(E) a_k(p)} \tag{5.33}
 \end{aligned}$$

where  $P$  is the set of all possible input patterns,  $a_j(p)$  and  $o_i(p)$  are the source and target activities for pattern  $p$ , and  $\mathbf{P}[\cdot]$  denotes ‘‘probability of’’.

We can define functions to represent the Hebbian and Competition terms in this equation as follows:

$$H_{ij}(E) = \alpha \sum_{p \in P} \mathbf{P}[p] A_{ij}(E) o_i(p, E) a_j(p) \tag{5.34}$$

$$C_i(E) = \frac{\alpha}{K} \sum_{p \in P} \mathbf{P}[p] o_i(p, E) \sum_{k=0}^{m-1} A_{ik}(E) a_k(p) \tag{5.35}$$

$$w_{ij}(E+1) \approx \frac{w_{ij}(E) + H_{ij}(E)}{1 + C_i(E)} \quad (5.36)$$

Now we can determine the equilibrium states, in terms of  $H_{ij}(E)$  and  $C_i(E)$ , by setting  $w_{ij,eq} = w_{ij}(E+1) = w_{ij}(E)$ . This gives us the following:

$$w_{ij,eq} = \frac{H_{ij,eq}}{C_{i,eq}} \quad (5.37)$$

$$H_{ij,eq} = \alpha \sum_{p \in P} \mathbf{P}[p] A_{ij,eq} o_{i,eq}(p) a_j(p) \quad (5.38)$$

$$C_{i,eq} = \frac{\alpha}{K} \sum_{p \in P} \mathbf{P}[p] o_{i,eq}(p) \sum_{k=0}^{m-1} A_{ik,eq} a_k(p) \quad (5.39)$$

### 5.3.2 Stability of Equilibrium Solutions

To determine stability, we must look at the value of  $\Delta w_{ij}(E) = w_{ij}(E+1) - w_{ij}(E)$  in the neighborhood of the equilibrium solutions. Liapunov's method can then be used to determine the stability of a known equilibrium solution. To apply this method, we linearize the equation for  $\Delta w_{ij}(E)$  around around a known equilibrium solution, then solve for the characteristic roots of the variance matrix. If all real components of those roots are negative, then it is possible to construct a Liapunov function for the solution, and the state is stable.

Our variational equation is

$$\begin{aligned} \Delta w_{ij}(E) &= w_{ij}(E+1) - w_{ij}(E) \\ &= \frac{w_{ij}(E) + H_{ij}(E)}{1 + C_i(E)} - w_{ij}(E) \\ &= \frac{H_{ij}(E)}{1 + C_i(E)} - \frac{C_i(E)}{1 + C_i(E)} w_{ij}(E) \end{aligned} \quad (5.40)$$

The stability of this system cannot be determined in the general case, as the target activity, on which both  $H_{ij}(E)$  and  $C_i(E)$  depend, cannot be found in general except by simulation. However, we can determine stability for certain special cases. An example is given in Section 5.3.4.

### 5.3.3 Equilibrium Solution with Uniform Input Activity

In this section we solve for the equilibrium solutions in a simplified case, where the the input activity cluster size is a constant  $c$ , and the input activity is uniformly

distributed across the source map. In this case, for a map with its ends wrapped, there are  $m$  possible input patterns which contain  $c$  contiguous active nodes. Each of these patterns occurs with probability  $\mathbf{P}[p] = 1/m$ . These are the conditions under which the first set of tests was run.

Under these conditions, the equations simplify to

$$\begin{aligned} H_{ij}(E) &= \frac{\alpha}{m} \sum_{p \in P} A_{ij}(E) o_i(p, E) a_j(p) \\ &= \frac{\alpha}{m} \sum_{p \in P_j} A_{ij}(E) o_i(p, E) \end{aligned} \quad (5.41)$$

$$C_i(E) = \frac{\alpha}{K m} \sum_{p \in P} o_i(p, E) \sum_{k=0}^{m-1} A_{ik}(E) a_k(p) \quad (5.42)$$

$$w_{ij}(E+1) = \frac{w_{ij}(E) + \frac{\alpha}{m} \sum_{p \in P_j} A_{ij}(E) o_i(p, E)}{1 + \frac{\alpha}{K m} \sum_{p \in P} o_i(p, E) \sum_{k=0}^{m-1} A_{ik}(E) a_k(p)} \quad (5.43)$$

and

$$H_{ij,eq} = \frac{\alpha}{m} \sum_{p \in P_j} A_{ij,eq} o_{i,eq}(p) \quad (5.44)$$

$$C_{i,eq} = \frac{\alpha}{K m} \sum_{p \in P} o_{i,eq}(p) \sum_{k=0}^{m-1} A_{ik,eq} a_k(p) \quad (5.45)$$

$$\begin{aligned} w_{ij,eq} &= \frac{H_{ij,eq}}{C_{i,eq}} \\ &= \frac{K \cdot \sum_{p \in P_j} A_{ij,eq} o_{i,eq}(p)}{\sum_{p \in P} o_{i,eq}(p) \sum_{k=0}^{m-1} A_{ik,eq} a_k(p)} \end{aligned} \quad (5.46)$$

where  $P_j$  is the set of all input patterns in which node  $j$  is active.

In addition, we will assume that we have full connectivity between the two layers,<sup>3</sup> so that  $A_{ij} = 1$ , giving us:

---

<sup>3</sup>A node with a limited synaptic arbor will behave as if it had full connectivity as long as its arbor overlaps the same region in the target as other simultaneously active source nodes.

$$H_{ij}(E) = \frac{\alpha}{m} \sum_{p \in P_j} o_i(p, E) \quad (5.47)$$

$$\begin{aligned} C_i(E) &= \frac{\alpha}{K m} \sum_{p \in P} o_i(p, E) \sum_{k=0}^{m-1} a_k(p) \\ &= \frac{\alpha c}{K m} \sum_{p \in P} o_i(p, E) \end{aligned} \quad (5.48)$$

$$w_{ij}(E+1) = \frac{w_{ij}(E) + \frac{\alpha}{m} \sum_{p \in P_j} o_i(p, E)}{1 + \frac{\alpha c}{K m} \sum_{p \in P} o_i(p, E)} \quad (5.49)$$

and

$$H_{ij,eq} = \frac{\alpha}{m} \sum_{p \in P_j} o_{i,eq}(p) \quad (5.50)$$

$$C_{i,eq} = \frac{\alpha c}{K m} \sum_{p \in P} o_{i,eq}(p) \quad (5.51)$$

$$w_{ij,eq} = \frac{K \sum_{p \in P_j} o_{i,eq}(p)}{c \sum_{p \in P} o_{i,eq}(p)} \quad (5.52)$$

The weight between any source node  $j$  and target node  $i$  at equilibrium will be proportional to the ratio between the expected activity at  $i$  when  $j$  is active and the average activity at  $i$ .

If we assume a uniform solution, where all arbors have the same shape, then the average activity at  $i$  is the same for all  $i$ , and our weight equation at equilibrium simplifies still further, to

$$w_{ij,eq} \propto \sum_{p \in P_j} o_{i,eq}(p) \quad (5.53)$$

Since  $o_{i,eq}(p)$  is itself dependent on the  $w_{ij,eq}$ 's, this equation can be expanded to give a solution purely in terms of the weights and the target activity function.

$$\vec{o}_{eq}(p) = \vec{F}[W_{eq} \vec{a}(p)] \quad (5.54)$$

$$\begin{aligned}
W_{eq} &\propto \begin{bmatrix} \sum_{p \in P_0} \vec{o}_{eq}(p)^T \\ \vdots \\ \sum_{p \in P_{m-1}} \vec{o}_{eq}(p)^T \end{bmatrix} \\
&= \begin{bmatrix} \sum_{p \in P_0} \vec{F}[W_{eq} \vec{a}(p)]^T \\ \vdots \\ \sum_{p \in P_{m-1}} \vec{F}[W_{eq} \vec{a}(p)]^T \end{bmatrix} \tag{5.55}
\end{aligned}$$

where  $\vec{o}_{eq}(p)$  is the equilibrium target activity (in vector form) for pattern  $p$ ,  $\vec{F}[\vec{x}]$  is a function which returns the summed target activity given an initial activation of  $\vec{x}$ , and  $W_{eq}$  is the weight matrix.

Given a particular target activation function  $\vec{F}$ , we can calculate  $W_{eq}$  for the uniform solution, and determine its dependency on the ratio of the competition limit  $K$  and the cluster size  $c$ .

### 5.3.4 Equilibrium Solution with No Lateral Connections

In this section, we will consider the case where we have no lateral connections. Now each target node operates independently, so we only need to consider one target node, with inputs  $\vec{a}(p) = [a_0(p) \ a_1(p) \ \cdots \ a_{m-1}(p)]$ , weights  $\vec{w}(E) = [w_0(E) \ w_1(E) \ \cdots \ w_{m-1}(E)]$ , and output activity

$$o(p, E) = \sum_0^{m-1} w_j(E) a_j(E) = \vec{w}(E)^T \vec{a}(p) \tag{5.56}$$

Our learning rule, in this case, simplifies to

$$\begin{aligned}
\vec{H}(E) &= \alpha \sum_{p \in P} \mathbf{P}[p] \vec{w}(E)^T \vec{a}(p) \Lambda(E) \vec{a}(p) \\
&= \alpha \Lambda(E) \left( \sum_{p \in P} \mathbf{P}[p] \vec{a}(p) \vec{a}(p)^T \right) \vec{w}(E) \\
&= \alpha \Lambda(E) \mathbf{M} \vec{w}(E) \tag{5.57} \\
C(E) &= \frac{\alpha}{K} \sum_{p \in P} \mathbf{P}[p] \vec{w}(E)^T \vec{a}(p) \vec{A}(E)^T \vec{a}(p) \\
&= \frac{\alpha}{K} \vec{A}(E)^T \left( \sum_{p \in P} \mathbf{P}[p] \vec{a}(p) \vec{a}(p)^T \right) \vec{w}(E)
\end{aligned}$$

$$= \frac{\alpha}{K} \vec{A}(E)^T M \vec{w}(E) \quad (5.58)$$

$$\begin{aligned} \vec{w}(E+1) &\approx \frac{\vec{w}(E) + \vec{H}(E)}{1 + C(E)} \\ &= \frac{\vec{w}(E) + \alpha A(E) M \vec{w}(E)}{1 + \frac{\alpha}{K} \vec{A}(E)^T M \vec{w}(E)} \end{aligned} \quad (5.59)$$

where  $A(E)$  is an  $m$  by  $m$  matrix, with entries

$$A_{ij}(E) = \begin{cases} A_j(E) & \text{if } i = j \\ 0 & \text{otherwise} \end{cases} \quad (5.60)$$

and

$$M = \sum_{p \in P} \mathbf{P}[p] \vec{a}(p) \vec{a}(p)^T \quad (5.61)$$

Solving for the equilibrium states, we get

$$\vec{H}_{eq} = \alpha A_{eq} M \vec{w}_{eq} \quad (5.62)$$

$$C_{eq} = \frac{\alpha}{K} \vec{A}_{eq}^T M \vec{w}_{eq} \quad (5.63)$$

$$\vec{w}_{eq} = \frac{K A_{eq} M \vec{w}_{eq}}{\vec{A}_{eq}^T M \vec{w}_{eq}} \quad (5.64)$$

This system is linear, and we can write its equilibrium solution as

$$A_{eq} M \vec{w}_{eq} = \frac{\vec{A}_{eq}^T M \vec{w}_{eq}}{K} \vec{w}_{eq} \quad (5.65)$$

where

$$\frac{\vec{A}_{eq}^T M \vec{w}_{eq}}{K} = \frac{C_{eq}}{\alpha} \quad (5.66)$$

is an eigenvalue of the matrix  $A_{eq} M$ , and  $\vec{w}_{eq}$  is the corresponding eigenvector.

### Stability with Uniform Input Activity

If we assume a constant input activity cluster size  $c$ , full connectivity, and a uniform input activity distribution, we can solve for  $C(E)$ . In this case,

$$\mathbf{M} = \frac{1}{m} \sum_{p \in P} \vec{a}(p) \vec{a}(p)^T \quad (5.67)$$

$$\vec{A}(E) = \vec{n} \quad (5.68)$$

$$\mathbf{A}(E) = \mathbf{I} \quad (5.69)$$

where  $\vec{n}$  is a vector of all ones, and

$$\begin{aligned} C(E) &= \frac{\alpha}{K} \vec{A}(E)^T \mathbf{M} \vec{w}(E) \\ &= \frac{\alpha}{Km} \sum_{p \in P} \vec{n}^T \vec{a}(p) \vec{a}(p)^T \vec{w}(E) \end{aligned} \quad (5.70)$$

We can make the following substitutions in this equation:

$$\vec{n}^T \vec{a}(p) = c \quad (5.71)$$

$$\sum_{p \in P} \vec{a}(p)^T = c \vec{n}^T \quad (5.72)$$

$$\vec{n}^T \vec{w}(E) = K \quad (5.73)$$

at which point  $C(E)$  can be seen to be a constant:

$$C(E) = \frac{\alpha c^2}{m} \quad (5.74)$$

$\vec{H}(E)$ , similarly, can be simplified as follows:

$$\begin{aligned} \vec{H}(E) &= \frac{\alpha}{m} \left( \sum_{p \in P} \vec{a}(p) \vec{a}(p)^T \right) \vec{w}(E) \\ &= \frac{\alpha}{m} \mathbf{M}' \vec{w}(E) \end{aligned} \quad (5.75)$$

where

$$\mathbf{M}' = \sum_{p \in P} \vec{a}(p) \vec{a}(p)^T \quad (5.76)$$

The eigenvalue in this case is just

$$\frac{C_{eq}}{\alpha} = \frac{c^2}{m} \quad (5.77)$$

To determine stability, we want to look at the variation in  $\Delta\vec{w}$  in the neighborhood of the equilibrium states. In this case the system is linear, so we can solve for  $\Delta\vec{w}$  in general, as follows:

$$\begin{aligned} \Delta\vec{w}(E) &= \frac{\vec{H}(E)}{1 + C(E)} - \frac{C(E)}{1 + C(E)}\vec{w}(E) \\ &= \frac{\frac{\alpha}{m} M' \vec{w}(E)}{1 + \frac{\alpha c^2}{m}} - \frac{\frac{\alpha c^2}{m}}{1 + \frac{\alpha c^2}{m}}\vec{w}(E) \\ &= \frac{\frac{\alpha}{m}}{1 + \frac{\alpha c^2}{m}} (M' - c^2\mathbf{I}) \vec{w}(E) \end{aligned} \quad (5.78)$$

The stability of the equilibrium points can be determined by examining the eigenvalues of the matrix  $M' - c^2\mathbf{I}$ . This matrix is symmetric, therefore all its eigenvalues are real. It is stable if all its eigenvalues are less than or equal to zero.

If we set  $m = 5$  and  $c = 2$ , we find that the matrix  $M$  is

$$M = \frac{1}{m} \begin{bmatrix} 2 & 1 & 0 & 0 & 1 \\ 1 & 2 & 1 & 0 & 0 \\ 0 & 1 & 2 & 1 & 0 \\ 0 & 0 & 1 & 2 & 1 \\ 1 & 0 & 0 & 1 & 2 \end{bmatrix}$$

The eigenvalue in this case is  $c^2/m = 4/5$ , and the corresponding eigenvector is  $\vec{w} = (K/5)\vec{n}$ . That is to say, all weights are the same at equilibrium. Now, we consider the variational matrix to determine stability.

$$M' - c^2\mathbf{I} = \begin{bmatrix} -2 & 1 & 0 & 0 & 1 \\ 1 & -2 & 1 & 0 & 0 \\ 0 & 1 & -2 & 1 & 0 \\ 0 & 0 & 1 & -2 & 1 \\ 1 & 0 & 0 & 1 & -2 \end{bmatrix}$$

This matrix is negative semidefinite, so the system is stable, but not asymptotically stable.

### Evolution of the Weight Vector

An interesting property of map formation in this system can be seen by looking at the evolution of the weight vector over time. Combining Equations 5.36, 5.47, and 5.74 and considering only a single target node, we find

$$w_j(E+1) = \frac{w_j(E) + \frac{\alpha}{m} \sum_{p \in P} \vec{w}(E)^T \vec{a}(p)}{1 + \frac{\alpha c^2}{m}} \quad (5.79)$$

If we set  $c = 2$ , this equation becomes

$$\begin{aligned} w_j(E+1) &= \frac{w_j(E) + \frac{\alpha}{m}(w_{j-1}(E) + 2w_j(E) + w_{j+1}(E))}{1 + \frac{4\alpha}{m}} \\ &= \frac{1 + \frac{2\alpha}{m}}{1 + \frac{4\alpha}{m}} w_j(E) + \frac{\frac{\alpha}{m}}{1 + \frac{4\alpha}{m}} (w_{j-1}(E) + w_{j+1}(E)) \end{aligned} \quad (5.80)$$

What this means is that each of the weights  $w_j$  is continuously being averaged with its neighbors. This results in a gradual spreading out of the arbor over time, until it reaches the equilibrium state where all weights are the same.

# Chapter 6

## Summary and Conclusions

Most computational models of neurons have assumed that their electrical characteristics are of paramount importance. However, as the examples in this document show, chemical as well as electrical mechanisms play important computational roles in neurons. Many different mechanisms, both electrical and chemical (and, in some cases, mechanical) interact to allow the nervous system to respond to the environment in an “intelligent” manner. To adequately model the computational behavior of neurons, it is therefore necessary to consider chemical properties as well as electrical ones.

The processes underlying different aspects of classical conditioning utilize a variety of electrical and chemical processes. A functional division can also be made between short-term and long-term forms of these learning phenomena. Initial responses to conditioning experiments are short-term, but long-term mechanisms gradually come into play if learning trials are repeated over an extended time period.

The *Aplysia* circuit has been extensively studied, and is unusually well understood. The results demonstrate that biological learning is complex and many-faceted, rather than working via a single general-purpose mechanism. Even what appears as a single mechanism, in a high-level description, is made up of many component processes. These processes act at different time scales to modulate a neuron’s responses to electrical stimulation, working together to regulate the process so that it is stable and robust and produces consistent, meaningful behavior.

Chemical components of learning can be localized within a single synapse, which provides neurons with a very fine-grained control over its internal state and, as a result, over its electrical responses. These internal “state variables” have a natural time period over which they affect the cell’s function, and different processes in the cell have different temporal properties. Their effects can be controlled by interactions between inputs of different types (e.g. utilizing different neurotransmitters), as well as by individual inputs.

The observed high-level learning and behavioral effects may depend on the dynamics of underlying chemical reactions.

Because they allow the possibility of responding to changes in short-term internal

state, the presence of these chemical mechanisms means that a neuron's computational properties may resemble those of a finite state machine more than a combinational logic unit. This is in stark contrast to current computational models of neurons, which have little or no internal state outside the permanent state changes modelled in long-term learning processes. Some models include very short-term effects such as those which are caused by the membrane capacitance, but these generally provide little more than a capacity for short-term temporal integration.

Individual neurons are therefore much more complex than is traditionally assumed, and have the capacity to implement complex computational functions. These computations are specialized for different purposes in different regions of the brain.

In addition to mediating short-term and long-term changes in a cell's electrical behavior, chemical processes play important roles in creating the brain's anatomical structure during development. In the developing visual system, activity correlation and chemical markers cooperate to create a topographic mapping between different structures in the visual input pathway: neither mechanism alone is sufficient. Without the initial establishment of a rough topology, activity-dependent mechanisms fall prey to a variety of problems and instabilities, and the chemical processes alone cannot easily provide the precision necessary for the final map.

The pre-existing structure of a neural network, such as that specified by chemical markers in the visual system, thus directs learning in ways that vastly increase its efficiency. The network's structure, conversely, is determined in part by its inputs and the learning mechanisms that act within it. The behavior of a neural system over time results from a complex interaction between the environment, the network structure, and the nature of the learning mechanisms.

# Appendix A

## Modelling of Neurons

Neurons play a crucial role in the processing of sensory signals and production of behavioral responses. It is generally assumed that these functions are mediated by their electrical activity, which is described in this appendix. There are many types of neurons, and their properties vary considerably, but they all share the same basic structure. This appendix is mostly about what neurons have in common, but I also discuss some of the simpler variations. See [27] for a more comprehensive discussion of this topic.

### A.1 Theme

#### A.1.1 Basic Electrical Properties

The first neuron studied in detail was the squid giant axon, which is a popular experimental preparation due to its large size (it is visible to the naked eye). This meant it was possible to do intracellular recordings from this neuron, even when using 1930's electrode technology. Our basic understanding of the electrical properties of neurons is derived from this example.

A neuron, like all cells, consists of a lipid membrane which separates the salt water in our bodies into intracellular and extracellular compartments. Ions (charged particles, such as sodium ( $\text{Na}^+$ ) and potassium ( $\text{K}^+$ )) diffuse freely in water, but the lipid acts as an insulator, and prevents ions from flowing between the two compartments. Electrically, therefore, the cell membrane behaves as a capacitor, as structurally it consists of a thin layer of insulating material sandwiched between two conductive layers.

Ions are able to flow across the cell membrane through ion channels, which are proteins that span the membrane and create channels that are often specific to a particular type of ion. These channels act as variable resistors, where the channel resistance is controlled by such things as the voltage across the cell membrane or the presence of substances such as neurotransmitters. In addition to the ion channels,

the cell has ion pumps, which actively maintain a concentration gradient of particular types of ions across the cell membrane.

When an ion channel is “open”, that is, permeable to a particular ion type, there are two forces which control the flux of that ion across the membrane. Diffusion causes ions to flow down their concentration gradient, and the voltage across the membrane attracts positively charged ions toward the negative side and negatively charged ions toward the positive side of the membrane. Because of the ion pumps, which maintain the concentration gradient at a near-constant level (the ion fluxes are very small compared to their total concentration), each type of ion therefore has an equilibrium voltage, called the *reversal potential*, at which the diffusion force exactly counters the electrical force. An open ion channel behaves, electrically, as if its resistance is connected to a battery set at the reversal potential for the ions it is permeable to.

These basic properties of the cell membrane, ion channels, and ion pumps give the neuron a great deal of control over its internal electrical state. Electrical communication between neurons, on the other hand, is more often mediated by neurotransmitters, chemicals which are released by one cell to diffuse through the extracellular fluid and bind to proteins on another cell’s surface. If these receptor proteins open or close ion channels in the receiving cell, the extracellular chemical “message” will be transduced into an intracellular electrical one.

There are a number of different neurotransmitters, but each neuron only produces a single neurotransmitter. Their effects may be excitatory (that is, they have a depolarizing effect on the receiving cell) or inhibitory (hyperpolarizing the receiving cell.)

### A.1.2 Anatomical and Functional Structure

Understanding how information is processed and transferred within and between neurons requires a basic understanding of their anatomical structure. The general anatomy of a neuron can be seen in Figure A-1.

Within a single neuron, there are four basic functional parts:

- The *postsynaptic terminals*, most often located in the dendrites and surface of the cell body (soma), contain receptors that transduce chemical signals from other neurons into electrical currents across the cell membrane. These changes can be excitatory (depolarizing) or inhibitory (hyperpolarizing).<sup>1</sup> A cell may have hundreds to hundreds of thousands of postsynaptic terminals.
- The *trigger zone*, of which there is usually only one, is located in the initial segment of the axon near the soma. Action potentials are initiated in the trigger zone (that is, it causes the neuron to “fire,” producing a brief voltage spike) when the electrical potential exceeds a threshold value.

---

<sup>1</sup>In its resting state, a neuron is polarized, with the intracellular fluid carrying a negative charge relative to the extracellular fluid.

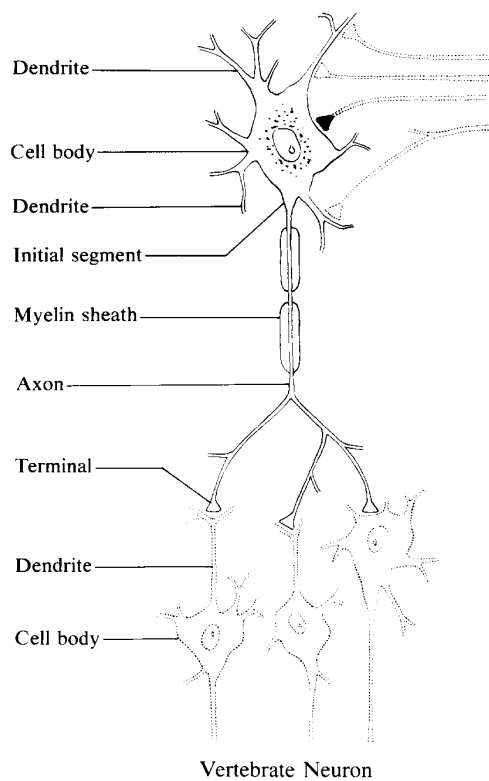


Figure A-1: What a neuron looks like (from [27, page 97]).

- The *axon*, which acts as an active transmission line, carries the voltage spike of the action potential to its presynaptic terminals.
- The *presynaptic terminals*, located on branches of the cell's axon, transduce the action potential into a chemical signal for intercellular communication. A neurotransmitter substance is released into the extracellular fluid, and diffuses through this fluid to bind to receptors on another cell, thus completing the circuit. Like postsynaptic terminals, a single neuron may have hundreds to thousands of presynaptic terminals.

A *synapse* is a very important functional unit involving two cells: it consists of a presynaptic terminal from one cell and a postsynaptic terminal from the other. These terminals are paired, with a narrow gap called the *synaptic cleft* between them.

The dendrites are assumed to be the major “input” region of the cell, where signals from other cells are received and processed. Electrical signals travel along these long thin processes<sup>2</sup> until they reach the cell body, where they are integrated to produce a single electrical signal. If the cell is sufficiently depolarized by its inputs, it will fire, producing an all-or-nothing output signal which is transmitted down the axon to the presynaptic terminals. This is considered to be the source of a cell's “outputs.”

### A.1.3 Mechanisms of Action Potential Generation

In its resting state, the intracellular fluid carries a negative charge relative to the extracellular fluid. The resting potential of a cell is generally around -70 mV. During an action potential, this voltage is briefly reversed.

Two major ion types participate in the generation of action potentials, sodium ( $\text{Na}^+$ ) and potassium ( $\text{K}^+$ ).  $\text{Na}^+$  is normally highly concentrated in the extracellular fluid, so when  $\text{Na}^+$  channels open, both the concentration gradient and the electrical gradient tend to draw ions into the cell. This has a depolarizing action, with a reversal potential at around +55 mV.

$\text{K}^+$  on the other hand, is highly concentrated inside the cell, so when  $\text{K}^+$  channels are open the ions generally flow out of the cell, which has a hyperpolarizing action. The reversal potential for  $\text{K}^+$  is around -75 mV.

There are several different ion channels for each of these two important ions, each of which opens and closes under different circumstances. A highly conductive type of  $\text{Na}^+$  channel, located along the axon, is voltage-sensitive and transient, opening briefly when the potential depolarizes to some threshold value.  $\text{Na}^+$  channel opening initiates a positive feedback process whereby  $\text{Na}^+$  influx further depolarizes the cell and activates more  $\text{Na}^+$  channels. This process causes the rapid depolarization that

---

<sup>2</sup>A process, as defined in Webster's Dictionary, is “a prominent or projecting part of an organism or organic structure.”

characterizes the start of an action potential, and the effect spreads in a fast traveling wave down the cell's axon.

Voltage-activated  $K^+$  channels then open, with a slight delay, which repolarizes the cell as the  $Na^+$  channels close. This produces the rapid falling edge at the end of an action potential. The  $K^+$  channels remain open somewhat longer, causing an "after-hyperpolarization" of the cell which limits the maximum frequency at which it can fire. Ion pumps restore the resting concentration of  $Na^+$  and  $K^+$  between action potentials.

The voltage spike at each region along the axon brings the next region above threshold, so the action potential propagates. However, because the waveform at each point results from the local properties of ion channels, local changes in its shape can be caused by locally introducing chemicals that affect those channels. For example, in the presynaptic terminals of *Aplysia*'s sensory neurons, a type of  $K^+$  channel is partially inactivated during sensitization, which lengthens the action potential's duration. The effect of this local manipulation of the action potential waveform is discussed in Section 3.1.3.

When an action potential arrives at a presynaptic terminal, a class of voltage-sensitive calcium ( $Ca^{++}$ ) channel opens.  $Ca^{++}$  is normally maintained at high concentrations outside the cell, so this causes  $Ca^{++}$  to flow into the cell.  $Ca^{++}$  influx mediates neurotransmitter release from the presynaptic terminals.

The neurotransmitter in a presynaptic terminal is contained in *vesicles*, which are tiny "bubbles" of lipid membrane. When  $Ca^{++}$  is present in the terminal, it binds to these vesicles and catalyzes a reaction by which they are attached to release sites and emptied into the synaptic gap. Active mechanisms remove free  $Ca^{++}$  from the terminal very rapidly after an action potential has passed through, so neurotransmitter is released in a brief pulse.

After their release, neurotransmitter chemicals are removed from the synaptic cleft by reuptake mechanisms which gather them back into the presynaptic terminal, or by enzymes which metabolize them, breaking them down into substances which are inert with respect to intercellular communication.

## A.2 Variations

### A.2.1 on the synapse

A synapse consists of a paired presynaptic and postsynaptic terminal. In addition to *axodendritic* (that is, from the axon to the dendrite) and *axosomatic* (from the axon to the cell body) synapses, described above, some cells have *axoaxonal* synapses, where the postsynaptic terminal is on the axon of a cell, rather than on the dendrites. This has the effect of modulating a neuron's output directly, instead of through the process of signal integration in the soma. One functional implication of this is that it is a much finer-grained type of control over a neuron's behavior, as it can affect individual

synaptic outputs independently. An example of this can be seen in dopamine release in the striatum [55, 10], where local interactions at the presynaptic terminals can cause neurotransmitter release that is completely independent of the neuron's electrical response at the soma. This release can occur after the cell's axon is cut, at which point it no longer even has a soma.

Invertebrates have long been known to have direct electrical coupling between neurons, through a type of synapse called a *gap junction*. These junctions are comprised of coupled ion channels which span the gap between two cells, forming a direct connection between their intracellular compartments. Electrically, gap junctions create a simple resistance between the voltages of the two cells. It was long believed that gap junctions did not exist in vertebrates, but evidence has recently been found for their presence in mammals during development [53].

### A.2.2 on the inputs

In sensory neurons, specialized input regions transduce sensory signals into electrical potential changes. For example, in the retina of the eye, neurons have specialized processes called *photoreceptors*, which detect impinging photons and emit electrical signals in response. Touch sensors convert pressure and vibration into electrical signals, and proprioceptive sensors in muscles detect and signal in response to muscle tension, stretch and velocity. The firing frequency of these neurons is usually proportional to either the strength of the input or the time derivative of input strength.

In simple models of neurons, it is assumed that inputs are simply integrated in the soma to produce an electrical depolarization proportional to their sum. However, the positioning of postsynaptic terminals along the dendrites may have functional effects. For example, an inhibitory synapse may have a shunting effect on excitatory signals, which will inhibit an excitatory signal much more effectively if it is located along the section of dendrite which lies between the excitatory synapse and the soma. This may result in a neuronal response which is proportional to a product of inputs, or some combination of sums and products, instead of a simple integration [35].

In addition to *ionotropic* neurotransmitter receptors, which open and close ion channels in response to inputs, there is also a class of receptors whose action is *metabotropic*. These receptors initiate chemical processes inside the cell, instead of acting through electrical currents. The actions of neurotransmitter receptors are discussed in more detail in Appendix B.

### A.2.3 on the Outputs

In addition to electrical currents caused by synaptic inputs, many neurons have intrinsic currents that cause them to fire spontaneously even in the absence of input activity [3]. These autoactive neurons show four basic firing patterns: silent (not autoactive), regular pulses at some frequency, regular bursts of pulses at some fre-

quency, and irregular pulses. This kind of periodic activity in thalamic neurons is responsible for the brain waves seen in EEG recordings [24].

In the basic neuron model, it is assumed that action potentials propagate globally to all presynaptic terminals. However, a model has been proposed [54] where branch points in the axon may selectively block action potentials based on the interpulse interval, thus performing a more complex output function.

## A.3 Recapitulation

This appendix describes the basic properties of neurons. Electrical activity within neurons and chemical signalling between neurons are generally assumed to be the mediators of a neuron's functional properties.

Although most neurons have the same basic functional components, the details of their structure and behavior vary considerably, and neurons in different brain regions can be highly specialized.

Several aspects of cellular and neural behavior are discussed in more detail in other appendices.



# Appendix B

## Neurotransmitter Receptors

Neurotransmitter receptors fall into two major classes, ionotropic receptors and metabotropic receptors. There are also receptors such as the NMDA receptor (described below) which have both ionotropic and metabotropic effects.

Many of the examples discussed in this appendix are glutamate receptors, as different receptors for glutamate exhibit the full range of receptor types. Glutamate is the primary excitatory neurotransmitter in the mammalian cortex, and the synapses which exhibit long-term potentiation are glutamatergic. A review can be found in [48].

### B.1 Ionotropic Receptors

The best-known and most well-understood neurotransmitter receptors are ionotropic. Ionotropic receptors are ion channel proteins whose activation is regulated by a neurotransmitter binding site. Ionotropic receptors respond to specific neurotransmitters, such as glutamate, by either opening or closing their ion channels. The postsynaptic effect of ionotropic receptor activation is a rapid and brief change in the electrical currents entering or leaving the cell.

The glutamatergic AMPA receptor is a highly-conductive  $\text{Na}^+$  channel which opens in response to the application of glutamate. It is the primary mediator of the depolarizing effects of this excitatory neurotransmitter. Postsynaptic terminals in which AMPA receptors are present usually also have other glutamate receptors, which mediate other postsynaptic effects.

### B.2 Metabotropic Receptors

Metabotropic receptors have no direct effect on ion channels or membrane potential. Instead, they are coupled to metabolic processes which have indirect effects both on ion channel activity and on a variety of other cellular functions. Examples are the metabotropic serotonin receptor, described in Chapter 3, the dopamine D1 and D2

receptors, which play an important role in motor control [32, 45], and the recently discovered metabotropic glutamate receptor [57], whose activation in the hippocampus may act to filter incoming signals through selective inhibition or enhancement of the cell's electrical response. It has been hypothesized to play a role in regulating attention, and in the control of long-term potentiation.

Many metabotropic receptors are coupled to members of a family of GTP-dependent proteins (G proteins). When the receptor is activated, the associated G protein complex breaks apart into independent subunits which go on to catalyze reactions in the cell. These subunits may in some cases act directly on ion channels, producing electrical changes in the cell that persist somewhat longer than those of ionotropic receptors. However, they also regulate the cell's activity via second messenger systems, activating enzymes such as adenylate cyclase.

G protein activation of adenylate cyclase stimulates the production of cyclic AMP, which controls cellular processes by activating a cyclic AMP-dependent protein kinase. Protein kinases regulate the activity of a variety of substrate proteins through phosphorylation (described in Appendix D.)

Metabotropic receptors act on a much slower time scale than ionotropic receptors, due to the complex cascade of chemical events that mediate their effects. This cascade also acts to amplify the incoming signal. For example, a small amount of activated G protein can produce a large increase in the cyclic AMP concentration through activation of adenylate cyclase. The effects of metabotropic receptors may also persist over an extended time period, in part through the catalytic action of protein kinases.

Activation of metabotropic receptors can have persistent and far-reaching effects, ranging from short-lived changes in the sensitivity of other receptors or ion channels to large-scale morphological change.

### B.3 The NMDA Receptor

Some receptor types, such as the glutamatergic NMDA receptor, have both ionotropic and metabotropic actions. NMDA receptor activation is necessary for the induction of long-term potentiation, a form of synaptic change that requires coactivation of presynaptic and postsynaptic cells.

NMDA receptors contain an ion channel that is primarily permeable to calcium ions.  $\text{Ca}^{++}$  influx has both a direct, rapid electrical effect on the cell, and a range of indirect metabolic effects.<sup>1</sup>

If glutamate binds to an NMDA receptor when the cell is near its resting potential, the ion channel is blocked by magnesium ions ( $\text{Mg}^+$ ), which, like  $\text{Ca}^{++}$  are present in high concentrations outside the cell. Magnesium, however, is unable to fit through this channel and enter the cell. When the cell depolarizes,  $\text{Mg}^+$  loses its affinity to

---

<sup>1</sup> $\text{Ca}^{++}$  is extremely important in regulating many aspects of neuronal function. It plays some role in all of the processes discussed in these appendices.

the channel, and it is freed up for use by  $\text{Ca}^{++}$  ions. Maximum channel activation occurs around -20 to -30 mV. Less  $\text{Ca}^{++}$  influx is seen at higher voltages because they are nearer its reversal potential, and less influx is seen at lower voltages due to the  $\text{Mg}^+$  block.

The effect of the NMDA receptor is therefore highly nonlinear. They exhibit almost no activity at low voltage, but as the cell is sufficiently excited by other receptors (for example, the AMPA receptor, which is usually present in the same postsynaptic terminals), it will “turn on”, enhancing the depolarizing effect of strong input signals, and initiating longer-term processes in the cell. This dependence on presynaptic activity coupled with postsynaptic depolarization, combined with its ability to produce long-term changes through the second-messenger effects of  $\text{Ca}^{++}$  ions, give the NMDA receptor a unique and important role in neuronal functioning.



# Appendix C

## The Importance of Calcium in Neurons

Calcium mediates many important intracellular processes. As a charged ion, the flux of  $\text{Ca}^{++}$  ions across the cell membrane has a direct electrical effect, acting to depolarize the cell. However, unlike  $\text{Na}^+$  and  $\text{K}^+$  ions, whose primary effects appear to be electrical,  $\text{Ca}^{++}$  also mediates many important metabolic processes inside the cell.  $\text{Ca}^{++}$  ions are necessary to induce transmitter release from vesicles at presynaptic terminals. The  $\text{Ca}^{++}$ -calmodulin complex, an important cellular second messenger, activates a class of calcium-dependent protein kinases.  $\text{Ca}^{++}$  ions have also received attention for their role in the induction of long-term potentiation. Some of these processes are discussed in more detail in Appendices D and E.

### C.1 Sources of Calcium

A knowledge of the sources of  $\text{Ca}^{++}$  in the cell is important for understanding the control of  $\text{Ca}^{++}$ -dependent processes.<sup>1</sup>

The steady-state intracellular calcium concentration is around  $10^{-7}$  M. Most ion channels are inactivated at concentrations above  $10^{-6}$  M, which defines a physiological range of concentrations at which biologically meaningful events occur.

There are two major sources of intracellular calcium: influx through ion channels in the cell membrane, and release from internal calcium stores in the endoplasmic reticulum or other locations.

#### C.1.1 Voltage-dependent Calcium Channels

There are four major types of calcium channels that operate in a voltage-dependent manner, opening in response to cell depolarization. The activity of ion channels is

---

<sup>1</sup>The information in this section is taken from a number of sources, including [4, 39, 64].

defined in terms of their conductance, their location in the cell membrane, and the conditions under which they open and close. Two voltage-activated calcium channels, the T-type (transient) and L-type (long-lasting) channels, are discussed here.

T-type calcium channels are low-voltage-activated and transient. These channels decay rapidly to an inactive state when cell depolarization is prolonged, and become insensitive to further changes in voltage until the cell repolarizes to a level that is outside their inactivation range, at which point they return to a resting (closed) state. They are believed to be important in producing the spontaneous oscillatory activity that underlies periodic bursting in the thalamus. T-type calcium channels may also play a role in mossy fiber LTP.

The L-type calcium channel is one of several high-voltage-activated channels. It, too, inactivates under sustained depolarization, but its time constant is extremely long, so under most conditions it can be considered a purely voltage-dependent channel. The L-type channel is activated in response to large changes in membrane potential, such as occur during action potentials. It is widely distributed in the central nervous system and tends to be concentrated in cell bodies and proximal dendrites, especially at the base of the major dendrites. As such, it is believed to play a role in action potential generation.

The L-type channel must be phosphorylated before it can open; this process can be mediated by a cyclic AMP-dependent protein kinase. There is evidence to indicate that its activation may be actively modulated by endogenous substances.<sup>2</sup> The mechanism for  $\text{Ca}^{++}$  channel modulation is likely to involve neurotransmitters or peptides whose receptors are coupled to G proteins. These proteins may affect the channel directly or act via an intracellular second messenger such as cyclic AMP.<sup>3</sup>

### C.1.2 NMDA Receptors

The NMDA (for n-methyl-d-aspartate, a drug which activates it) receptor is a neurotransmitter receptor which has a voltage-dependent  $\text{Ca}^{++}$  channel. Unlike the T-type and L-type channels, the NMDA receptor requires the presence of glutamate, an excitatory neurotransmitter, for its activation. This receptor is described in Appendix B.

### C.1.3 Calcium Release from Internal Stores

Increases in calcium concentration in the cell generally last only a few milliseconds. Calcium is rapidly removed from the cell, bound up in protein complexes such as  $\text{Ca}^{++}$ -calmodulin, or taken up into internal stores, which may be in mitochondria, in the endoplasmic reticulum, or in calciosomes.

---

<sup>2</sup>Endogenous substances are those which occur naturally in the body.

<sup>3</sup>See Appendices B and D for more information on G proteins, second messengers, and protein phosphorylation.

Calcium release from internal stores can be induced by caffeine. The function of this release may be to induce oscillatory activity in the cell; it is probably not involved in transmitter release.

Calcium release from the endoplasmic reticulum is also induced by a chemical called inositol 1,4,5-triphosphate (InsP<sub>3</sub>). The intracellular concentration of InsP<sub>3</sub> increases in response to the activation of phospholipase C from cell receptors. This is a relatively recently discovered form of cellular second messenger, and its action is not well understood. It may be the mechanism by which caffeine acts.

## C.2 Calcium Actions

The particular changes mediated by Ca<sup>++</sup> influx may vary from cell to cell, and may also be modulated by other substances. This section describes a few of the known actions of Ca<sup>++</sup> in neural cells.

Its second-messenger effects and role in long-term potentiation are discussed in other appendices, so this section will focus on electrical effects and on the role of Ca<sup>++</sup> in transmitter release.

### C.2.1 Electrical Effects

Many of Ca<sup>++</sup>'s actions in cells are initiated by Ca<sup>++</sup> influx through ion channels in the cell membrane. Because it is a positively charged ion, this influx results in a voltage change in the cell. There is some controversy over the relative importance of electrical and metabolic Ca<sup>++</sup> effects.

One of the more striking properties of voltage-activated Ca<sup>++</sup> channels is that, like the Na<sup>+</sup> channels which mediate the depolarizing phase of action potentials, their opening produces a positive feedback response, which can produce Ca<sup>++</sup> spikes in the cell. Ca<sup>++</sup> spikes can occur, for example, in a cell's dendrites in response to input-mediated depolarization. They are much slower and smaller in amplitude than Na<sup>+</sup> spikes.

In addition to calcium spiking due to voltage-activated Ca<sup>++</sup> channels, the voltage-sensitivity of NMDA channels can result in a nonlinear dendritic response to synaptic inputs.

Dendrites have traditionally been considered to be passive electrical cables whose primary role was the transport of electrical signals into the cell body for integration in the trigger zone, but the presence of depolarization-induced dendritic Ca<sup>++</sup> spikes indicates that they may play a more active role in information processing than has been traditionally hypothesized. The properties of active dendrites have been modelled and found to have a significant effect on the cell's response to patterns of synaptic input with differing spatial distributions [44, 43].

Low-voltage-activated Ca<sup>++</sup> channels also play a role in generating periodic oscillations in spontaneously active cells. The low activation threshold of these channels

produces a small “leak” current, which slowly depolarizes the cell. As it depolarizes, more  $\text{Ca}^{++}$  channels are activated, which brings the cell to its firing threshold, at which point the  $\text{Na}^+$  channels take over and an action potential is generated. These  $\text{Ca}^{++}$  channels are transient, but the hyperpolarization of the cell due to  $\text{K}^+$  channel opening at the end of an action potential re-activates them, and the process repeats at some characteristic frequency.

Periodic oscillations in cells are important in a class of neural circuits called *central pattern generators*, which control periodic motor responses such as walking, chewing, and wing-flapping [3].

### C.2.2 The Role of Calcium in Neurotransmitter Release

The presynaptic terminals of neurons are populated with voltage-activated  $\text{Ca}^{++}$  channels. When these channels open during an action potential,  $\text{Ca}^{++}$  flows rapidly into the terminal. It is removed from the terminal equally rapidly after the channels close at the end of an action potential, either by being bound to calmodulin or by a variety of other uptake mechanisms. However, during that brief period, the presence of free  $\text{Ca}^{++}$  in the terminal causes the release of neurotransmitter into the synaptic cleft [33].

$\text{Ca}^{++}$  catalyzes a reaction between vesicles of neurotransmitter and release sites on the cell membrane. It requires four  $\text{Ca}^{++}$  ions to catalyze the release of a single vesicle of transmitter [27], through a process called *exocytosis*. Vesicles are small free-floating bubbles inside the presynaptic terminals, with neurotransmitter on the inside and a lipid membrane on the outside, made of the same substance as the cell membrane. In exocytosis,  $\text{Ca}^{++}$  ions increase the affinity between vesicles and release sites, where the lipid membrane of the vesicle can merge with the cell membrane, dumping its contents outside the cell.

# Appendix D

## Protein Phosphorylation

Essentially everything that happens inside a cell is mediated by proteins. The structure of proteins is what is encoded in the DNA, and the particular proteins present in a cell determine its behavior, its morphology, and its function in the body. The obvious differences between a skin cell, a muscle cell, and a nerve cell, for example, are caused by differences in which particular proteins are present and active in those cells.

The activity of many proteins can be up- or down-regulated by protein phosphorylation, an important mechanism by which extracellular messengers, such as neurotransmitters and hormones, influence what happens inside a cell. This appendix describes the basic mechanisms involved in protein phosphorylation. Much of this information was taken from [50].

### D.1 First and Second Messengers

Chemical *first messengers* travel in extracellular space and bind to receptors on cell surfaces, but they do not themselves carry messages into the cell (though they may originate in and be released from cells.) Instead, their message is relayed by *second messengers*, which are produced in response to receptor activation, and which mediate the cell's response to the extracellular signal.

The time course of second messenger effects may be quite long, and they can control a wide variety of intracellular processes. Their effects can range from indirect opening or closing of ion channels, to up- or down-regulation of the activity of a variety of proteins in the cell, to modifications in gene transcription, which may result in large-scale changes in cell morphology. Many of these results are accomplished through protein phosphorylation.

## D.2 What is Protein Phosphorylation?

A class of proteins, called *protein kinases*, act as catalysts for protein phosphorylation reactions. The basic reaction is the binding of a phosphate molecule to a phosphorylation site on a protein, which results in a conformational change in the protein. Many proteins respond to phosphorylation by changes in their activity. The reaction, therefore, can be seen as turning the protein “on” or “off”, or increasing or decreasing the rate at which it acts.

Each of protein kinase is capable of phosphorylating a specific set of *substrate proteins*, with different affinities for each. A protein kinase may phosphorylate a wide range of proteins, or it may be specific to one or a very few.

The complementary reaction is protein dephosphorylation, which is catalyzed by a class of proteins called *protein phosphatases*. Each protein phosphatase also acts on some set of substrate proteins, but their substrate specificity is generally not complementary to any particular protein kinase.

## D.3 What does it Do?

1. A number of ion channels can be activated or inactivated by protein phosphorylation. An example of this is the  $K^+$  channel discussed in Section 3.1.3. This channel is inactivated by phosphorylation, which affects the duration of action potentials in the cell, and indirectly affects synaptic strength due to the relationship between action potential duration and transmitter release. The L-type  $Ca^{++}$  channel, in contrast, is active only when phosphorylated [4].
2. The intermediate-term maintenance of long-term synaptic potentiation in the hippocampus (over a period lasting 3-6 hours after induction of LTP) is blocked by protein kinase inhibitors, which indicates the importance of protein phosphorylation in mediating this process. LTP discussed in detail in Appendix E.
3. DNA transcription factors may act as substrate proteins in phosphorylation reactions [12]. These proteins bind to particular DNA sequences and activate or inhibit transcription of the associated genes. The role of cyclic AMP in regulating long-term synaptic potentiation in *Aplysia*'s sensory neurons, described in Section 3.1.3, is an example of this use of protein phosphorylation.
4. Protein kinases can regulate their own actions through autophosphorylation. In the case of cyclic AMP-dependent protein kinase RII, autophosphorylation decreases the rate at which the kinase is deactivated, and thus prolongs its period of activity. Other possible actions of autophosphorylation are to change the affinity of the protein kinase for its substrate proteins, or to maintain its activity independent of the continued presence of a second messenger.

Phosphorylation of a protein kinase by some other protein kinase could provide a mechanism by which the presence of one second messenger might modulate the cell's response to another second messenger.

5. The activity of proteins can also be indirectly regulated by regulating protein phosphatases. Several protein kinases have been found that inhibit protein phosphatase activity. This will result in prolonged phosphorylation of the substrate proteins that the phosphatase acts on (which may be distinct from those affected directly by the protein kinase.) This provides another mechanism by which the action of one second messenger can indirectly control the cell's response to other second messengers.
6. The activity of many hormone and neurotransmitter receptors and other proteins that regulate the production of second messengers is also affected by protein phosphorylation. This is yet another mechanism by which second messengers can modulate their own activity or the activity of other second messengers.

## D.4 How is it Controlled?

There are many substances which regulate protein kinase activity. Among the best-known of these are cyclic AMP, cyclic GMP, and the compounds  $\text{Ca}^{++}$ -calmodulin and  $\text{Ca}^{++}$ -phosphatidylserine. Each of these is a cellular second messenger, whose concentration in the cell is regulated in part by first messengers such as neurotransmitters and hormones.

Cyclic AMP is produced by adenylate cyclase, and is metabolized (broken down) by phosphodiesterase. Cyclic GMP is produced by guanylate cyclase, and is also metabolized by phosphodiesterase. Each of these enzymes can itself undergo phosphorylation. Adenylate cyclase and guanylate cyclase are activated by G proteins coupled to receptors in the cell membrane. This process is described in Appendix B. The concentration of these second messengers may remain elevated for minutes to hours after the initial stimulus initiating their production.

The calcium compounds  $\text{Ca}^{++}$ -calmodulin and  $\text{Ca}^{++}$ -phosphatidylserine are formed, along with a number of less well-known second messenger compounds, whenever  $\text{Ca}^{++}$  ions are present in the intracellular fluid. This can come about either by the opening of calcium-permeable ion channels in the cell membrane or by release of calcium from internal stores.<sup>1</sup>  $\text{Ca}^{++}$  bonds decay rapidly, and free  $\text{Ca}^{++}$  ions are actively removed from the cell, so the concentration of these compounds peaks and decays rapidly after the influx of  $\text{Ca}^{++}$  ends.

---

<sup>1</sup>See Appendix C for details.



# Appendix E

## Long-Term Potentiation

### E.1 Neural Plasticity and Learning

Learning in neurons is generally assumed to be mediated by changes in synaptic efficacy. These can result from changes in the signal transmitted by an existing synapse or morphological changes in which new synapses are formed or existing synapses grow or atrophy. Outside of early development, learning is usually assumed to take place primarily in previously existing synapses.

This learning can, in theory, take place either in the presynaptic terminal, which would result in changes in the amount of transmitter released per action potential, or in the postsynaptic terminal, which would result in changes in the response for a given amount of transmitter [6], or both.

Presynaptic mechanisms can be very specific, involving a single or small group of connections, as individual presynaptic terminals tend to be isolated both electrically and chemically. On the other hand, postsynaptic mechanisms can more easily affect large populations of synapses [38].

### E.2 Long-Term Potentiation

Long-term potentiation (LTP), first studied in the hippocampus, is a persistent increase in the synaptic efficacy of glutamatergic synapses in response to coactivation of presynaptic and postsynaptic cells. It has been observed in many regions in the brain, and is believed to be an important mechanism for learning.

Long-term potentiation can be induced either by a burst of activity in an input pathway or by input activity coupled with excitation of the target cell from another source. The behavior of this kind of LTP is similar to the classic Hebb learning rule, where the weight of a synaptic link is enhanced after paired activity in the source and target neuron. Because of its Hebbian properties, long-term potentiation has generated a great deal of interest in the neuroscience community. As a result, our understanding of the mechanisms underlying LTP is changing rapidly. A recent

review can be found in [5].

### E.2.1 Stages in LTP induction and maintenance

Like the forms of learning seen in *Aplysia*, long-term potentiation has several stages, ranging from short-term potentiation which lasts about an hour, through three different stages of long-term potentiation, which depend on different types of cellular mechanisms.

Short-term potentiation, lasting 30-60 minutes, is likely to be presynaptic, and is independent of protein kinase activity.

The first phase of LTP, in contrast, requires the activity of protein kinases. This implies that protein phosphorylation is required to make the transition from short-term to long-term forms of learning in this system. In particular,  $\text{Ca}^{++}$ -phospholipid-dependent protein kinases have been implicated in the initial phase of LTP, which lasts only a couple of hours.

The second phase of LTP, lasting up to 6 hours, requires protein synthesis. The third, and longest-lasting, phase of LTP requires changes in gene transcription.

### E.2.2 Properties of LTP

LTP is characterized by three basic properties. It is *cooperative*, meaning that it responds to the co-activation of multiple inputs. Low activation levels may induce short-term synaptic potentiation, but cooperative activation is needed for long-term potentiation. It is *associative*, in the sense that a weak input may be potentiated by coactivation with a strong input. And it is *input-specific*; that is, potentiation acts at the level of individual synapses.

### E.2.3 Induction of LTP

These properties are believed to be mediated by the response properties of NMDA receptors, which require paired presynaptic activity and postsynaptic depolarization for activation. Strong evidence has been found for the role of NMDA receptor activation in the induction of LTP. However, NMDA alone is not usually sufficient, and, in fact, NMDA receptors have been shown to inhibit as well as enhance LTP in different situations. It has been hypothesized that coactivation of NMDA and metabotropic glutamate receptors may be necessary for LTP induction.

Both these receptors increase intracellular  $\text{Ca}^{++}$  levels, but they act in different ways. NMDA receptor activation causes  $\text{Ca}^{++}$  influx through its ion channel, whereas metabotropic glutamate receptors may affect  $\text{Ca}^{++}$  levels by increasing  $\text{Ca}^{++}$  release from internal stores. This effect is most likely mediated by the second messenger inositol 1,4,5-triphosphate ( $\text{InsP}_3$ ).

### E.2.4 Maintenance of LTP

The maintenance of LTP requires persistent changes in synaptic efficacy. The locus of these changes is not known, but both presynaptic and postsynaptic modifications have been implicated. Different stages of LTP may occur in different locations.

In the postsynaptic cell, possible mechanisms of action include sensitization of the AMPA receptors by phosphorylation in the initial phase, and possibly the synthesis of more sensitive subtypes of AMPA receptors in later phases. NMDA receptors may also be affected by phosphorylation, reducing the effectiveness of the  $Mg^+$  block, or they may be affected by agonists such as arachidonic acid or  $InsP_3$ .

Because the induction of LTP occurs in the postsynaptic terminal, presynaptic changes require the release of a retrograde messenger to communicate this activation to the presynaptic terminal. The nature of the retrograde messenger is not known, although both arachidonic acid and nitrous oxide (NO) have been hypothesized.

The mechanism for presynaptic changes is also unknown, although changes in  $Ca^{++}$  levels or in the process of transmitter release have been hypothesized. Presynaptic metabotropic glutamate receptors have been hypothesized as a possible mediator of presynaptic changes. However, which presynaptic mechanisms are most likely to be involved depends in part on the (currently unknown) identity of the retrograde messenger.

## E.3 Summary

What is currently known about LTP in the mammalian nervous system implies that it acts through metabolic pathways that are very similar to the mechanisms of action of classical conditioning in *Aplysia*. These mechanisms, namely, protein phosphorylation, protein synthesis, and gene transcription, are basic metabolic processes in the cell, and the regulation of these processes by neurotransmitters provides a powerful mechanism for information processing and the control of neuronal and behavioral responses. These responses can be separated into short-term and long-term components, which can be induced or blocked separately and which utilize different metabolic pathways. The interaction between multiple mechanisms and pathways, and the synapse specificity of the responses, provides the neuron with a very fine-grained degree of control over its responsiveness to different input patterns.



# Bibliography

- [1] Thomas W. Abrams. Cellular studies of an associative mechanism for classical conditioning in aplysia: Activity-dependent presynaptic facilitation. In Allen I. Selverston, editor, *Model Neural Networks and Behavior*. Plenum Press, 1985.
- [2] Andrew G. Barto, Richard S. Sutton, and Charles W. Anderson. Neuronlike adaptive elements that can solve difficult learning control problems. *IEEE Transactions on Systems, Man, and Cybernetics*, SMC-13(5), 1983.
- [3] Randall Dean Beer. *Intelligence as Adaptive Behavior: an Experiment in Computational Neuroethology*. PhD thesis, Case Western Reserve University, 1989.
- [4] Mariella Bertolino and Rodolfo R. Llinás. The central role of voltage-activated and receptor-operated calcium channels in neuronal cells. *Annual Reviews of Pharmacology and Toxicology*, 32, 1992.
- [5] T. V. P. Bliss and G. L. Collingridge. A synaptic model of memory: long-term potentiation in the hippocampus. *Nature*, 361, 1993.
- [6] T.V.P. Bliss and A.C. Dolphin. Where is the locus of long-term potentiation? In Lynch, McGaugh, and Weinberger, editors, *Neurobiology of Learning and Memory*. The Guilford Press, 1984.
- [7] Thomas H. Brown, Anthony M. Zador, Zachary F. Mainen, and Brenda J. Clai-borne. Hebbian modifications in hippocampal neurons. In Michel Baudry and Joel L. Davis, editors, *Long-Term Potentiation*. MIT Press, 1982.
- [8] John H. Byrne and Kevin J. Gingrich. Mathematical model of cellular and molecular processes contributing to associative and nonassociative learning in aplysia. In John H. Byrne and William O. Berry, editors, *Neural Models of Plasticity: Experimental and Theoretical Approaches*, pages 58–73. Academic Press, 1989.
- [9] Douglas K. Candland. *Psychology: The Experimental Approach*. McGraw-Hill Book Company, 1968.

- [10] A. Chéramy, R. Romo, G. Godeheu, P. Baruch, and J. Glowinski. *In Vivo* presynaptic control of dopamine release in the cat caudate nucleus — ii. facilitatory or inhibitory influence of l-glutamate. *Neuroscience*, 19(4), 1986.
- [11] Holly T. Cline. Activity-dependent plasticity in the visual systems of frogs and fish. *Trends in Neuroscience*, 14(3), 1991.
- [12] Pramod K. Dash, Binyamin Hochner, and Eric R. Kandel. Injection of the camp-responsive element into the nucleus of *aplysia* sensory neurons blocks long-term facilitation. *Nature*, 345, 1990.
- [13] E. Erwin, K. Obermayer, and K. Schulten. Self-organizing maps: Stationary states, metastability and convergence rate. *Biological Cybernetics*, 67, 1992.
- [14] Viggo M. Fosse, Paul Heggelund, and Frode Fonnum. Postnatal development of glutamatergic, GABAergic, and cholinergic neurotransmitter phenotypes in the visual cortex, lateral geniculate nucleus, pulvinar, and superior colliculus in cats. *The Journal Of Neuroscience*, 9(2), 1989.
- [15] Lucia Galli and Lamberto Maffei. Spontaneous impulse activity of rat retinal ganglion cells in prenatal life. *Science*, 242, 1988.
- [16] Alan Gelperin, J. J. Hopfield, and D. W. Tank. The logic of limax learning. In Allen I. Selverston, editor, *Model Neural Networks and Behavior*. Plenum Press, 1985.
- [17] David L. Glanzman, Eric R. Kandel, and Samuel Schacher. Target-dependent structural changes accompanying long-term synaptic facilitation in *aplysia* sensory neurons. *Science*, 249, 1990.
- [18] Y. Hata, T. Tsumoto, H. Sato, K. Hagihara, and H. Tamura. Development of local horizontal interactions in cat visual cortex studied by cross-correlation analysis. *Journal of Neurophysiology*, 69(1), 1993.
- [19] R. D. Hawkins, V. F. Castellucci, and E. R. Kandel. Interneurons involved in mediation and modulation of gill-withdrawal reflex in *aplysia*. i. identification and characterization. *Journal of Neurophysiology*, 45(2):304–314, 1981.
- [20] Robert D. Hawkins. A simple circuit model for higher-order features of classical conditioning. In John H. Byrne and William O. Berry, editors, *Neural Models of Plasticity: Experimental and Theoretical Approaches*, pages 74–93. Academic Press, 1989.
- [21] Robert D. Hawkins and Eric R. Kandel. Steps toward a cell-biological alphabet for elementary forms of learning. In Lynch, McGaugh, and Weinberger, editors, *Neurobiology of Learning and Memory*, pages 385–404. The Guilford Press, 1984.

- [22] Binyamin Hochner and Eric R. Kandel. Modulation of a transient  $k^+$  current in the pleural sensory neurons of *aplysia* by serotonin and camp: Implications for spike broadening. *Proceedings of the National Academy of Sciences USA*, 89, 1992.
- [23] J. W. Johnson and P. Ascher. Glycine potentiates the nmda response in cultured mouse brain neurons. *Nature*, 325, 1987.
- [24] Edward G. Jones. *The Thalamus*. Plenum Press, 1985.
- [25] Richard A. Y. Jones. *Physical and Mechanistic Organic Chemistry*. Cambridge University Press, 1984.
- [26] Jon H. Kaas, M. M. Merzenich, and H. P. Killackey. The reorganization of somatosensory cortex following peripheral nerve damage in adult and developing mammals. *Annual Reviews of Neuroscience*, 6, 1983.
- [27] Eric R. Kandel. *Cellular Basis of Behavior*. W. H. Freeman and Company, 1976.
- [28] Eric R. Kandel. *A Cell-Biological Approach to Learning*. Society for Neuroscience, 1978.
- [29] Eric R. Kandel and Thomas J. O'Dell. Are adult learning mechanisms also used for development? *Science*, 258, 1992.
- [30] Eric R. Kandel and James H. Schwartz. Molecular biology of learning: Modulation of transmitter release. *Science*, 218:433–443, 1982.
- [31] Eric R. Kandel and James H. Schwartz. *Principles of Neural Science*. Elsevier, 1985.
- [32] Eamonn Kelly and Stefan R. Nahorski. Specific inhibition of dopamine d-1-mediated cyclic amp formation by dopamine d-2, muscarinic cholinergic, and opiate receptor stimulation in rat striatal slices. *Journal of Neurochemistry*, 47(5), 1986.
- [33] Regis B. Kelly, James W. Deutsch, Steven S. Carlson, and John A. Wagner. Biochemistry of neurotransmitter release. *Annual Reviews of Neuroscience*, 2, 1979.
- [34] Mary B. Kennedy. Regulation of synaptic transmission in the central nervous system: Long-term potentiation. *Cell*, 59, 1989.
- [35] Christof Koch, Tomaso Poggio, and Vincent Torre. Computations in the vertebrate retina: Gain enhancement, differentiation and motion discrimination. A. I. Memo 914, MIT Artificial Intelligence Laboratory, 1986.

- [36] Teuvo Kohonen. Self-organized formation of topologically correct feature maps. *Biological Cybernetics*, 43, 1982.
- [37] Teuvo Kohonen. *Self-Organization and Associative Memory*. Springer-Verlag, 1988.
- [38] Benjamin Libet. Heterosynaptic interaction at a sympathetic neuron as a model for induction and storage of a postsynaptic memory trace. In Lynch, McGaugh, and Weinberger, editors, *Neurobiology of Learning and Memory*. The Guilford Press, 1984.
- [39] Rodolfo R. Llinás. The intrinsic electrophysiological properties of mammalian neurons: Insights into central nervous system function. *Science*, 242, 1988.
- [40] H. J. Luhmann and D. A. Prince. Postnatal maturation of the gabaergic system in rat neocortex. *Journal of Neurophysiology*, 65(2), 1991.
- [41] Lamberto Maffei and Lucia Galli-Resta. Correlation in the discharges of neighboring rat retinal ganglion cells during prenatal life. *Proceedings of the National Academy of Sciences USA*, 87, 1990.
- [42] Markus Meister, Rachel O. L. Wong, Denis A. Baylor, and Carla J. Shatz. Synchronous bursts of action potentials in ganglion cells of the developing mammalian retina. *Science*, 252, 1991.
- [43] Bartlett W. Mel. Information processing in an excitable dendritic tree. CNS Memo 17, California Institute of Technology, 1992.
- [44] Bartlett W. Mel. Nmda-based pattern discrimination in a modeled cortical neuron. *Neural Computation*, 4, 1992.
- [45] S. El Mestikawy and M. Hamon. Is dopamine-induced inhibition of adenylate cyclase involved in the autoreceptor-mediated negative control of tyrosine hydroxylase in striatal dopaminergic terminals? *Journal of Neurochemistry*, 47(5), 1986.
- [46] Christopher Miller. How ion channel proteins work. In Leonard K. Kaczmarek and Irwin B. Levitan, editors, *Neuromodulation: the biochemical control of neuronal excitability*, pages 39–63. Oxford University Press, 1987.
- [47] Ken Miller. Ocular dominance column development: Analysis and simulation. *Science*, 245, 1989.
- [48] Daniel T. Monaghan, Richard J. Bridges, and Carl W. Cotman. The excitatory amino acid receptors: Their classes, pharmacology, and distinct properties in the function of the central nervous system. *Annual Reviews of Pharmacology and Toxicology*, 29, 1989.

- [49] P. R. Montague, J. A. Gally, and G. M. Edelman. Spatial signalling in the development and function of neural connections. *Cerebral Cortex*, 1, 1991.
- [50] Eric J. Nestler and Paul Greengard. *Protein Phosphorylation in the Nervous System*. John Wiley and Sons, 1984.
- [51] K. Obermayer, H. Ritter, and K. Schulten. A principle for the formation of the spatial structure of cortical feature maps. *Proceedings of the National Academy of Sciences USA*, 87, 1990.
- [52] Erkki Oja. A simplified neuron model as a principal component analyzer. *Journal of Mathematical Biology*, 15, 1982.
- [53] A. Peinado, R. Yuste, and L. C. Katz. Extensive dye coupling between rat neocortical neurons during the period of circuit formation. *Neuron*, 10(1), 1993.
- [54] Gill Andrews Pratt. *Pulse Computation*. PhD thesis, MIT, 1990.
- [55] R. Romo, A. Chéramy, G. Godeheu, and J. Glowinski. *In Vivo* presynaptic control of dopamine release in the cat caudate nucleus — i. opposite changes in neuronal activity and release evoked from thalamic motor nuclei. *Neuroscience*, 19(4), 1986.
- [56] Christie Sahley, Jerry W. Rudy, and Alan Gelperin. An analysis of associative learning in a terrestrial mollusk. *Journal of Comparative Physiology*, 144:1–8, 1981.
- [57] Darryle D. Schoepp and P. Jeffrey Conn. Metabotropic glutamate receptors in brain function and pathology. *Trends in Pharmacological Sciences*, 14, 1993.
- [58] Carla J. Shatz and Marla B. Luskin. The relationship between the geniculocortical afferents and their cortical target cells during development of the cat's primary visual cortex. *The Journal Of Neuroscience*, 6(12), 1986.
- [59] Carla J. Shatz and David W. Sretavan. Interactions between retinal ganglion cells during the development of the mammalian visual system. *Annual Reviews of Neuroscience*, 9, 1986.
- [60] Carla J. Shatz and Michael P. Stryker. Prenatal tetrodotoxin infusion blocks segregation of retinogeniculate afferents. *Science*, 242, 1988.
- [61] Joseph Sirosh and Risto Miikkulainen. How lateral interaction develops in a self-organizing feature map. In *Proceedings of the IEEE International Conference on Neural Networks*, 1993.
- [62] Richard S. Sutton. Learning to predict by the methods of temporal differences. *Machine Learning*, 3:9–44, 1988.

- [63] Richard S. Sutton and Andrew G. Barto. Time-derivative models of pavlovian reinforcement. In Michael Gabriel and John Moore, editors, *Learning and Computational Neuroscience: Foundations of Adaptive Networks*, pages 497–537. MIT Press, 1990.
- [64] D. Swandulla, E. Carbone, and H. D. Lux. Do calcium channel classifications account for neuronal calcium channel diversity? *Trends in Neuroscience*, 14(2), 1991.
- [65] J. David Sweatt and Eric R. Kandel. Persistent and transcriptionally-dependent increase in protein phosphorylation in long-term facilitation of *aplysia* sensory neurons. *Nature*, 339, 1989.
- [66] Susan B. Udin and James W. Fawcett. Formation of topographic maps. *Annual Reviews of Neuroscience*, 11, 1988.
- [67] Ch. von der Malsburg and D. J. Willshaw. How to label nerve cells so that they can interconnect in an ordered fashion. *Proceedings of the National Academy of Sciences USA*, 74(11), 1977.
- [68] D. J. Willshaw and C. von der Malsburg. How patterned neural connections can be set up by self-organization. *Proceedings of the Royal Society of London, Series B*, 194, 1976.